Radon Exposure in Canadian Residences: Predictive Models, Low-Cost Sensor Evaluation, and Multi-Family Building Assessments

by

Amanda Giang

A thesis

presented to the University of Waterloo

in fulfillment of the

thesis requirement for the degree of

Master of Applied Science

in

Civil Engineering

Waterloo, Ontario, Canada, 2025

© Amanda Giang 2025

Author's Declaration

I hereby declare that I am the sole author of this thesis. This is a true copy of the thesis, including any required final revisions, as accepted by my examiners.

I understand that my thesis may be made electronically available to the public.

Abstract

Radon gas is a naturally occurring carcinogen that infiltrates homes and buildings, where it can accumulate to dangerous levels. Although it is the second leading cause of lung cancer in Canada, public testing and mitigation remain limited. Modern changes to residential construction, particularly the move toward airtight designs, have inadvertently contributed to increased radon levels in Canada. Alongside geological variations and the emergence of new radon detection tools, the interplay of all these factors needs to be further explored.

This thesis examines the residential radon exposure across Canada through three key research objectives: 1) the development of predictive models for radon risk; 2) the evaluation of low-cost electronic radon monitors (ERMs); and 3) the characterization of radon patterns in Canadian high-rise multi-family buildings. To address the first objective, random forest regression models were developed using national and regional datasets from Health Canada (HC) and the British Columbia Radon Data Repository (BCRDR), respectively. These models integrated spatial, seasonal, and building-specific variables to estimate residential radon levels. The BCRDR model explained up to 47% of the variance in radon concentrations, whereas the HC model was lower at 27%, with forward sortation area ranking consistently as the most influential predictor across both models. However, limited cross-dataset performance using the BCRDR model on the HC model highlights the ongoing challenge in the transferability of models from one region to another.

The second objective involved short- and long-term colocation tests of several low-cost ERMs with reference-grade instruments in residential settings. Results show that while a few ERMs achieved an acceptable agreement with reference values (within 10% relative percent error), most demonstrated substantial variability, even among sensors of the same model. Some issues included delayed response times and wide limits of agreement. These findings emphasize the limitations of deploying ERMs for consumer or research use without regulatory supervision.

For the third objective, radon levels were monitored in a 12-storey, multi-family student residence building at the University of Waterloo. Average radon concentrations were relatively

low (3.7 – 8.9 Bq/m^3); however, concentrations exceeding 50 Bq/m^3 were recorded during periods of reduced ventilation on all floors. Notably, the conventional assumption that radon concentrations decrease with building height was challenged by the observation of the highest average concentration on the 12th floor, albeit with low absolute values.

Collectively, these results provide insights into the limitations of predictive modelling for substitution in real-world testing, the performance of low-cost ERMs and reliability for use for testing, and the complex nature of indoor radon distribution, particularly in multi-family buildings. A coordinated strategy integrating predictive risk mapping, validated ERMs, and targeted testing can inform evidence-based policies and ensure that radon risk is addressed across all housing types and Canadian regions.

Acknowledgements

I would like to express my deepest gratitude to my supervisor, Dr. Amy Li, whose unwavering support, patience, and encouragement have been central to this thesis. From the very beginning of my research journey to the very end, Dr. Li has been a constant source of insight, inspiration, and guidance. Her thoughtful mentorship has not only shaped the quality of my work but has made this experience truly meaningful and empowering. I cannot thank her enough for the weekly meetings, countless edits, and calm reassurance throughout this journey. Her constant belief in my abilities and her capacity to both challenge and support me have made me incredibly fortunate to have such an exceptional supervisor. Thank you for taking a chance on me and giving me this opportunity. I will forever be grateful and proud to be Dr. Li's first graduate student!

I would also like to thank the team at Health Canada and the British Columbia Centre for Disease Control for allowing me access to their data and sensors. Special thanks to the University of Waterloo Campus Housing Facilities Team and the participants of Claudette Millar Hall.

Lastly, I would like to thank my wonderful friends and family who allowed me to use their homes for radon testing while supplying me with endless amounts of laughter and love, motivating me throughout my thesis. A very special thanks to Jillian Martin for letting me use her house twice and deploying 45 sensors in her basement for three months. None of this work would have been possible without this community of people helping me. Thank you so much!

Table of Contents

Author's Declaration ii
Abstract iii
Acknowledgements v
List of Figures ix
List of Tables xii
List of Abbreviations xiv
List of Equations xv
Chapter 1 – Introduction 1
1.1 Background & Motivation 1
1.2 Research Gaps & Objectives 2
1.3 Thesis Organization 4
Chapter 2 – Literature Review 6
2.1 Overview of Radon 6
2.2 Radon's Impact on Human Health 8
2.3 Sources of Radon in the Built Environment 9
2.3.1 Ground Sources 9
2.3.2 Building Materials 10
2.4 Factors Influencing Radon in the Built Environment 11
2.4.1 Environmental Factors 12
2.4.2 Building Design Factors 14
2.5 Predictive Modelling 21
2.6 Radon Measurement Strategies 23
2.6.1 Passive Detectors 23
2.6.2 Electronic Radon Monitors (ERMs) 24
2.7 Radon Mitigation Strategies 29
2.8 Global Regulations, Standards, and Guidelines 32
2.8.1 European Countries 32
2.8.2 North America and Other Countries 33
2.9 Summary of Literature Review 35

Chapter 3 – Methodology 36
3.1 Predictive Modelling 36
3.1.1 Health Canada (HC) Dataset Description 37
3.1.2 British Columbia Radon Data Repository (BCRDR) Dataset Description 38
3.1.3 Dataset Preprocessing 38
3.1.4 Statistical Analysis 41
3.1.5 Random Forest (RF) Regression Model Development 42
3.2 Evaluation of Low-Cost ERMs 46
3.2.1 Experimental Set-up 46
3.2.2 Devices Evaluated 50
3.2.3 Performance Evaluation Metrics 55
3.2.4 Environmental and Meteorological Analysis 59
3.3 Multi-Family Buildings 60
3.3.1 Preliminary Screening 60
3.3.2 Sensor Selection and Calibration 61
3.3.3 Long-term Field Measurement 62
3.3.4 Differences in Concentrations 65
3.3.5 Environmental and Meteorological Analysis 65
Chapter 4 – Results 66
4.1 Predictive Modelling Results 66
4.1.1 Factors Influencing Radon from the BCRDR Dataset 66
4.1.2 Random Forest (RF) Regression 75
4.1.3 Cross-Dataset Model Training 79
4.2 Collocation Test Results 80
4.2.1 Short-Term Test 80
4.2.2 Long-Term Test 88
4.2.3 Comparison of Short-Term & Long-Term Tests 101
4.3 High-Rise Multi-Family Building Results 104
4.3.1 Preliminary Screening 104
4.3.2 Claudette Millar Hall (CMH) 107

Chapter 5 – Discussion 114
5.1 Predictive Modelling of Radon Exposure in Canadian Residences 114
5.2 Performance of Electronic Radon Monitors (ERMs) 116
5.3 Policy, Technology, and Future of Radon Testing in Canada 118
Chapter 6 – Conclusions 123
6.1 Summary & Conclusions 123
6.2 Recommendations for Future Work 124
6.3 Summary of Contributions and Publications 125
References 127
Appendix A 142

List of Figures

Figure 1: Weighted average of radon concentrations by region in multi- vs. single-family dwellings from Giang & Li (2024) [23].....3
Figure 2: Percentage of radon concentrations in multi- vs. single-family dwellings from Giang & Li (2024) [23]. 3
Figure 3: Infographic of the Radon Decay Chain from the Cross-Canada Radon Survey 2024 [2]7
Figure 4: Radon entry points in buildings from Health Canada “Radon - What you need to know” factsheet [42].....10
Figure 5: Trend of radon concentrations by year of construction by country. The solid lines denote countries that reported radon concentration for specific years. The dashed lines denote countries that reported radon concentrations over a range of years, where the first year in the range was plotted. Geometric means, arithmetic means, or medians are shown based on the measurements reported in reference studies (Giang, Goodarzi, Li, *in prep*.). 17
Figure 6: Arithmetic means (AM) of radon concentrations by building type, grouped by country. Standard deviations reported by the study are represented by error bars. The sample size (n) for each building type is shown above each bar (Giang, Goodarzi, Li, *in prep*.). 20
Figure 7: Typical experimental set-up of collocated devices.....48
Figure 8: Experimental set-up of devices for long-term collocation test. 49
Figure 9: Original photo captured from time-lapse camera (left), processed photo for manual data extraction (right). 54
Figure 10: Experimental set-up for collocation test for calibration factors of RadonEyes. 62
Figure 11: (a) Sensors deployed in each unit, (b) typical dorm room, (c) typical dorm room with sensor placement, (d) typical lounge with sensor placement. 64
Figure 12: Radon concentrations in Canada for single-family vs. predicted concentrations for multi-family buildings by province or territory. In each box plot, the orange line represents the median concentration, while the bottom and top halves of the box indicate the second and third quartiles, representing the interquartile range. The whiskers extend to the most extreme data points within 1.5 times the interquartile range. Outliers are shown as individual points. ..70
Figure 13: Year of Construction vs. GM Radon Concentration 72

Figure 14: Ranked feature importances by increase in OOB error score for HC and BCRDR models. 77
Figure 15: Radon concentration at Site D by all devices from Giang & Li (2025) [188] 81
Figure 16: Radon concentration at Site A by all devices 81
Figure 17: Linear regression of RadonEye vs. RAD7, a) all concentrations (0 – 2,000 Bq/m^3), b) low concentration range (0 – 100 Bq/m^3), c) medium concentration range (101 – 300 Bq/m^3), d) high concentration range (> 301 Bq/m^3) from Giang & Li (2025) [188]. 83
Figure 18: Bland-Altman plots across all concentration ranges per low-cost ERM vs. RAD7, a) RadonEye, b) Inkbird, c) Spirit, and d) Wave from Giang & Li (2025) [188] 86
Figure 19: Radon concentration in the basement recorded by the AlphaGuard and the indoor and outdoor environmental conditions. 89
Figure 20: Linear regression of RE-4 vs. AlphaGuard 94
Figure 21: Linear regression of CRAD-4 vs. AlphaGuard 94
Figure 22: Percent Ratios of ERMs against AlphaGuard at matching sampling intervals. In each box plot, the orange line represents the median concentration, while the bottom and top halves of the box indicate the second and third quartiles, representing the interquartile range. The whiskers extend to the most extreme data points within 1.5 times the interquartile range. Outliers are shown as individual points. 95
Figure 23: Coefficient of variation of ERM. In each box plot, the orange line represents the median concentration, while the bottom and top halves of the box indicate the second and third quartiles, representing the interquartile range. The whiskers extend to the most extreme data points within 1.5 times the interquartile range. Outliers are shown as individual points. ..96
Figure 24: Bland-Altman plot for RE-4 vs. AlphaGuard....98
Figure 25: Bland-Altman plot for FK-4 vs. AlphaGuard....98
Figure 26: Bland-Altman plot for LB-4 vs. AlphaGuard....98
Figure 27: Time series of calibrated radon concentrations across all floors. 108
Figure 28: Arithmetic means of calibrated radon concentrations reported on top of 95% error bars, with ‘n’ representing the number of data points collected on each floor. 109

Figure 29: Box plot of radon concentration distributions by floor. In each box plot, the orange line represents the median concentration, while the bottom and top halves of the box indicate the second and third quartiles, representing the interquartile range. The whiskers extend to the most extreme data points within 1.5 times the interquartile range. Outliers are shown as individual points..... 110

List of Tables

Table 1: Summary of studies evaluating ERMs (Giang, Goodarzi, Li, *in prep.)* 26
Table 2: Summary of Data Points for Statistical Analysis of BCRDR Data 41
Table 3: Summary of Random Forest (RF) Model Parameters from Hyperparameter Tuning.....44
Table 4: Summary of Site Information.....47
Table 5: Summary of reference instruments 51
Table 6: Summary of ERMs evaluated for both short-term and long-term collocation tests.....52
Table 7: Summary of sampling frequency, total number of radon measurements, and percentage of available data for ERMs in long-term collocation test 55
Table 8: Performance Evaluation Metrics used in short-term test vs. long-term test.....56
Table 9: Radon distribution by residential building type.....67
Table 10: Summary of statistics for multi-family buildings vs. single-family buildings.....69
Table 11: Radon distribution by year of construction.....71
Table 12: Radon distribution by heating type 73
Table 13: Radon distribution by season 74
Table 14: Random Forest (RF) Model Evaluation Metrics 75
Table 15: Model Evaluation Metrics for Cross-Dataset Model Training 79
Table 16: Linear Regression, Spearman Rank Correlations (ρ), and RMSE Summary of all low-cost ERMs from Giang & Li (2025).....84
Table 17: Confusion Matrix of the Four Tested Sensors against RAD7 87
Table 18: Spearman Rank Correlation of Outdoor Environmental Parameters.....89
Table 19: Relative Percent Errors for Low-Cost ERMs with sensors within ±10% bolded 90
Table 20: Summary of linear regression, RMSE, and Spearman Rank Correlations for Long-term Test with Statistically Significant ERMs bolded 92
Table 21: Summary of Confusion Matrix for Long-Term Collocation Test.....99
Table 22: Summary of Preliminary Screening of Multi-Family Buildings.....104
Table 23: Calibrated Factors Applied to Radon Concentration by Floor 107
Table 24: Comparison of Mean Reported by Sensor vs. Alpha-Track Detector.....109
Table 25: Air Exchange Rate Analysis during April 15th, 2025 – May 7th, 2025.....111

Table 26: Sensitivity Analysis on Confusion Matrix Threshold Parameter for Short-Term Test using F1 Score.....117

List of Abbreviations

ERM	Electronic Radon Monitor
BCRDR	British Columbia Radon Data Repository
BCCDC	British Columbia Centre for Disease
HC	Health Canada
RF	Random Forest
WHO	World Health Organization
SSD	Sub-slab depressurization
HVAC	Heating, ventilation, air conditioning
US EPA/EPA	United States Environmental Protection Agency
C-NRPP	Canadian National Radon Proficiency Program

List of Equations

Equation (1) 56
Equation (2) 57
Equation (3) 57
Equation (4) 57
Equation (5) 57
Equation (6) 58
Equation (7) 58
Equation (8) 58
Equation (9) 58
Equation (10) 58
Equation (11) 58
Equation (12) 62

Chapter 1 – Introduction

1.1 Background & Motivation

Radon is a ubiquitous yet largely invisible health threat that is permeating into buildings across the Canadian landscape. For millions of Canadians, high-risk exposure to this naturally occurring radioactive gas is an everyday reality as radon migrates through soil and infiltrates buildings through cracks and joints in the foundation [1], [2]. Radon poses an alarming health danger to humans because it emits alpha radiation during radioactive decay [3]. The risk of exposure is heightened by the fact that radon is an odourless, tasteless, and colourless gas, leaving most individuals unaware of its presence, even when it exists at elevated levels.

Classified as a Group 1 human carcinogen by the World Health Organization (WHO), radon is surpassed only by tobacco smoking as the leading cause of lung cancer both nationally and worldwide. It is responsible for more than 3,000 lung cancer deaths in Canada each year [4]. The WHO recommends a national reference level of 100 Bq/m^3; however, if this is not feasible, the WHO has identified 300 Bq/m^3 as the upper limit for radon exposure before mitigation is strongly recommended [5]. Its dose-response relationship is linear, with every 100 Bq/m^3 increase in long-term radon exposure equating to an increase in lifetime risk of lung cancer by 16% [6]. Health Canada has set the national radon exposure reference level at 200 Bq/m^3, strongly encouraging remedial action for buildings that exceed this threshold [7].

Recent building developments have introduced additional complexity to Canada's radon landscape, with emerging evidence suggesting that indoor radon concentrations are increasing across the country. According to the 2024 Cross-Canada national survey, 17.8% of Canadians now reside in buildings with radon concentrations at or exceeding the national threshold, representing a 10.9% increase relative to findings reported in the 2012 Cross-Canada national survey [2], [8]. Research indicates that modern energy-efficient construction practices in Canada may inadvertently contribute to higher radon accumulation, likely due to the increase in airtightness [9], [10], [11], [12]. As the standardization of energy-efficient building practices becomes more widespread, the number of Canadians living in elevated radon levels may continue to increase [9]. Furthermore, public awareness and understanding of radon among

Canadians remain limited, while 55% of people report some awareness regarding radon, only 6% have undertaken residential testing [13], [14].

Despite the well-established health risks and the prevalence of rising indoor radon levels, a compelling need remains to deepen the understanding of radon dynamics in Canadian residences due to the danger it poses to public health. Advancing this knowledge is essential to more accurately identifying vulnerable populations, guiding the development of effective detection and mitigation strategies, and ultimately reducing radon-related health risks and preventing avoidable harm.

1.2 Research Gaps & Objectives

Residential radon exposure in Canada is influenced by a combination of factors, including underlying geology, seasonal variations, ventilation systems, building age, and building type. While advancements have been made in characterizing radon prevalence and risk, important research gaps persist regarding the prediction of radon levels, performance of new monitoring technologies, and assessment of risk in high-rise multi-family buildings. One key limitation of current radon risk assessment is the lack of comprehensive predictive models that can effectively incorporate geological and architectural factors. While previous studies have examined individual factors influencing radon, the development of integrative predictive models applicable to the diversity of Canadian housing remains limited. The inherent complexity of the interaction of factors governing radon levels has led to models that are often narrow in scope, constrained by regional data sets, specific building types, or simplified input parameters [15], [16], [17]. Consequently, the applicability of these models to various contexts, such as Canada's diverse geological landscape and residential building stock, is limited. To improve radon risk estimation, there is a need for predictive models in Canada that are capable of forecasting radon risk exposure in varied residential environments.

Another research gap pertains to the proliferation of unregulated, low-cost, consumer-grade electronic radon monitors (ERMs), which facilitate rapid, on-site measurement of indoor radon concentrations. In contrast to long-term passive detectors, which have been recommended by Health Canada and require extended deployment periods (90 days), ERMs provide real-time

results, often within an hour [18]. However, the rapid growth of consumer devices in the absence of standardized validation methods has raised concerns regarding their accuracy and reliability. Existing literature has predominantly evaluated the performance of low-cost ERMs under controlled laboratory conditions, offering limited insight into their performance across different building environments, radon concentrations, and prolonged exposure periods [19], [20], [21], [22].

Furthermore, the majority of radon research in Canada has historically focused on single-family detached homes, largely due to their prevalence and the perception that they are at greater risk of elevated radon due to building foundation typology [8]. Comparatively, multi-family and high-rise residential buildings have been understudied, often presumed to present lower risk based on findings from the literature. However, there has been emerging evidence in literature that challenges this presumption. Our recent rapid review comparing global studies reveals that, while single-family dwellings generally report higher average radon concentrations, there is substantial variability in the ratio of radon concentrations between dwelling types across different regions [23]. Figure 1 and Figure 2 show that the average radon concentrations in multi-family dwellings range from 37% - 92% of those in single-family dwellings within the same regions. In some cases, multi-family dwellings approached or even exceeded WHO thresholds, especially for ground-contacting units.

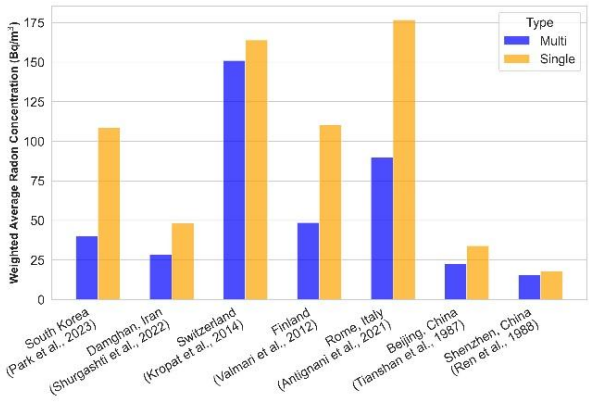


Figure 1: Weighted average of radon concentrations by region in multi- vs. single-family dwellings from Giang & Li (2024) [23].

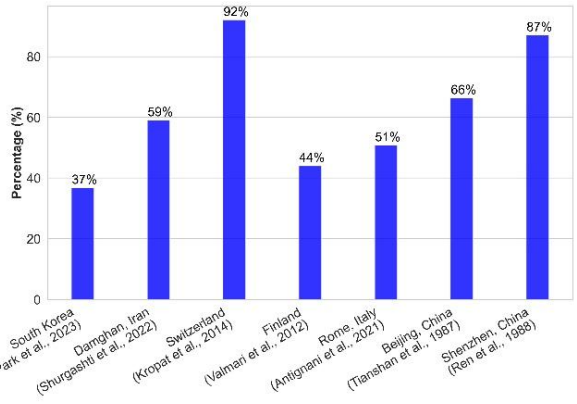


Figure 2: Percentage of radon concentrations in multi- vs. single-family dwellings from Giang & Li (2024) [23].

With multi-family residences comprising approximately 10.7% of Canada's residential building stock, the limited testing in these environments leaves a considerable number of occupants potentially at risk for radon exposure [24]. Thus, it is important to expand radon research and monitor initiatives to multi-family dwellings, ensuring that potentially high concentrations are not overlooked.

Motivated by these research gaps, this thesis seeks to address the following research objectives:

1) To develop and validate predictive models for residential radon concentrations in Canada that integrate geological, seasonal, and building-specific variables
2) To evaluate the performance of low-cost ERMs in real-world residences, through collocations with certified research-grade reference instruments and conventional passive samplers
3) To investigate the pattern of radon concentrations in high-rise multi-family buildings and the impact of building and environmental characteristics on radon concentrations in these environments

By addressing these objectives, this research will provide new predictive tools for identifying high-risk dwellings; inform the performance of low-cost ERMs and their best practices regarding the use of residential radon testing; and offer data-driven guidance on radon exposure risks in multi-family residences. Collectively, these contributions aim to generate actionable insights for policymakers and support incremental improvements in Canadian radon policy and public health interventions that better safeguard public health.

1.3 Thesis Organization

This thesis is structured around three major research topics: the development of a predictive model for residential radon concentrations using data provided by Health Canada and the British Columbia Centre for Diseases Control (BCCDC); a two-phase collocation assessment of low-cost ERMs; and a field campaign of radon concentration measurements in a high-rise multi-unit student residence on a university campus.

Chapter 1 introduces the research topic, outlines the background and motivation, and articulates the research gaps and objectives that guide this thesis. Chapter 2 provides a literature review on radon, covering topics from its health impacts, sources, and behaviour in the built environment, influencing factors, measuring and mitigation techniques, and relevant regulatory frameworks. Chapter 3 details the methodology for each of the three research topics. Chapter 4 presents the key results obtained from each topic. Chapter 5 discusses and synthesizes the findings in the context of existing literature and broader public health implications. Lastly, Chapter 6 offers conclusions and recommendations for future research and highlights other contributions by me to the field of indoor air quality.

Chapter 2 – Literature Review

In this chapter, a comprehensive review of the literature on residential radon is presented, framed to provide a clear understanding of both the scientific background and practical challenges of indoor radon risk. The chapter begins with a general overview of radon and its origins in the radioactive decay of uranium, explaining why it poses substantial health risks to humans. The primary sources of radon are examined, detailing how radon gas infiltrates building spaces through various pathways. The discussion then explores the range of environmental and building design factors that influence radon levels in the built environment. The review goes on to explore predictive modelling approaches, highlighting how advances in data integration are being used to estimate radon exposure across different regions. Subsequently, the chapter evaluates current measurement tools and mitigation strategies, emphasizing both established and emerging methods for managing indoor radon. An overview of global regulations, standards, and guidelines is provided.

2.1 Overview of Radon

Radon (Rn^{222}) is generated as part of the radioactive decay series of uranium (U^{238}), which is found in varying amounts in virtually all rocks, soils, and groundwater. As uranium decays, it forms the radionuclide radium-226 (Ra^{226}), which subsequently undergoes radioactive decay to produce radon gas. Among the radionuclides in its decay sequence, radon is distinctive as it is the only element that exists in a gaseous form, rendering it both chemically inert and highly mobile. This high mobility enables radon to travel through soil, water, and various building materials, eventually emanating into the outdoor environment or accumulating within enclosed structures [1].

In addition to radon, thoron (Rn^{220}) is another common isotope that emerges from the decay chain of thorium (Th^{232}). However, the relevance of thoron is limited by its short half-life of 55.8 seconds, which typically prevents it from escaping from subterranean sources unless thorium is located close to the surface [25]. The primary contributors to indoor thoron levels are building materials containing radium-224 (Ra^{224}), which possesses a longer half-life than thoron

but is shorter-lived compared to Ra^{226} in the uranium decay chain [26]. The migration rates of both radon and thoron are influenced by multiple variables, including soil permeability, pressure gradients, the presence of these elements in building materials, and the extent of structural cracks or openings.

Radon gas, with a half-life of 3.8 days, emits alpha particles as it decays into a series of radioactive progeny, collectively known as radon decay products (RDPs) or radon progeny. These progeny are heavy metal particulate matter, beginning with polonium-218 (Po^{218}) and continuing through intermediate particulates such as lead-214 (Pb^{214}) and polonium-214 (Po^{214}). Through a sequence of further decays, which may extend over decades, these radionuclides ultimately form stable lead-206 (Pb^{206}), emitting alpha and beta radiation in the process [27]. Figure 3 illustrates the radon decay chain and highlights its transformation from gas to particulate matter over time. The unique properties of radon gas and its progeny form the foundation for identifying its significant impact on human health.

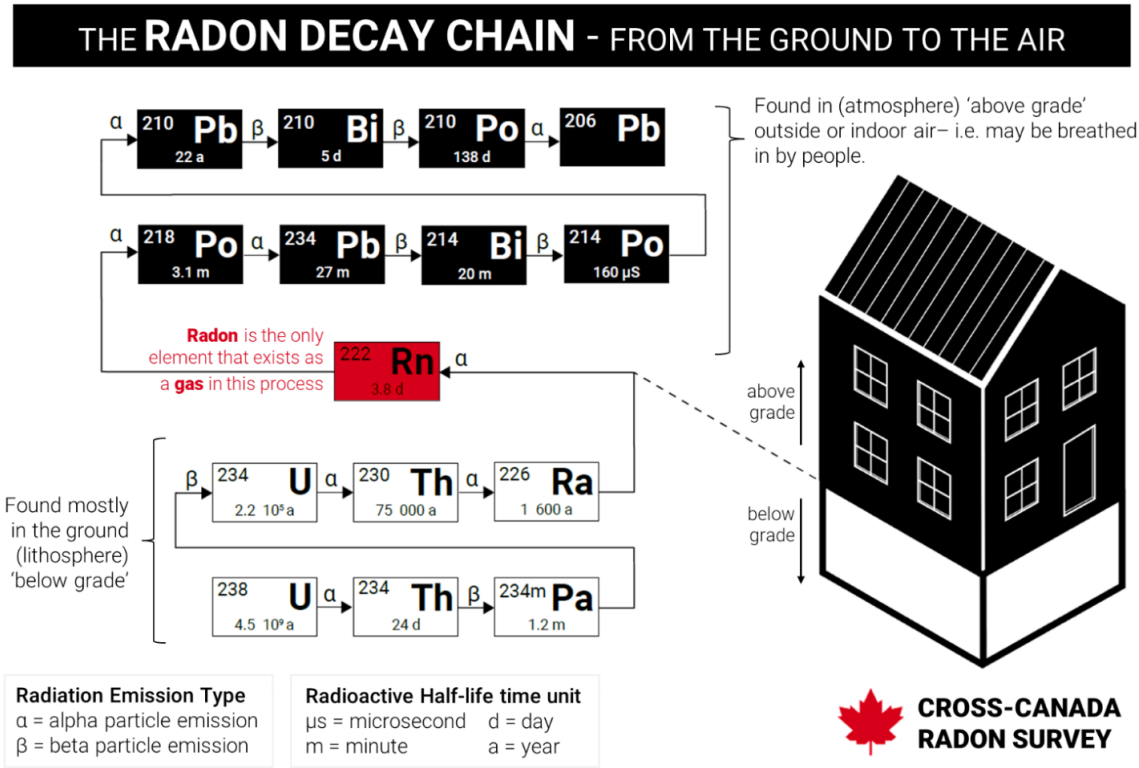


Figure 3: Infographic of the Radon Decay Chain from the Cross-Canada Radon Survey 2024 [2]

2.2 Radon's Impact on Human Health

As a radioactive gas, radon poses a significant health risk to humans, predominantly through the harmful effects of alpha radiation emitted by its decay products [28]. Although inhaled radon gas is largely exhaled, its progeny can deposit deep within the respiratory tract, where their solid property allows for extended retention and interaction with lung tissue. As a result, radon progeny, rather than radon gas itself, is the primary driver of radon's harmful health effects. These RDPs could be in free form or attached to fine particulate matter (particles less than or equal to 2.5 μm in diameter, also known as $PM_{2.5}$) in the air, facilitating their deposition in the lungs upon inhalation [29]. These particles are composed of a mixture of solid and liquid components containing metals and other organic compounds [30]. In particular, Po^{218} and Po^{214} are responsible for the majority of the damage to cells in the respiratory epithelium. Once lodged in the lung tissue, the radioactive particles continue to decay, emitting alpha radiation that can damage healthy cellular DNA. Notably, alpha particles lack the energy required to penetrate through external barriers, such as clothing or skin, as opposed to gamma rays or X-rays from background cosmic radiation or medical devices. Consequently, external exposure to radon is not concerning. However, once alpha-emitting particles enter the body, they are more dangerous than other types of radiation due to their dense ionization properties, resulting in more severe damage to surrounding cells [31]. Over time, this damage increases the likelihood of genetic mutations, potentially leading to the development of lung cancer [32].

The connection between radon exposure and lung cancer was first identified in large-scale epidemiological studies of uranium miners who were exposed to high radon concentrations in poorly ventilated conditions in the 1950s. These studies demonstrated a clear correlation between radon exposure and lung cancer incidence, providing evidence of increased risks for both smokers and non-smokers [33]. In 1988, the International Agency for Cancer Research (IACR) classified radon gas and its decay products as Group 1 carcinogens, indicating sufficient evidence of their risk to humans. Today, radon is recognized as the second leading cause of lung cancer worldwide, surpassed only by smoking. In the United States, the proportion of lung cancer cases among never-smokers rose from 8.9% in 1990 – 1995 to 17% from 2011 – 2013,

highlighting the increasing relevance of radon as a risk factor for lung cancer in non-smokers [34].

2.3 Sources of Radon in the Built Environment

When released outdoors, radon gas disperses rapidly in the atmosphere, resulting in relatively low concentrations that typically range from 5 Bq/m^3 to 15 Bq/m^3. In contrast, the presence of enclosed structures can inhibit this dispersion, leading to the accumulation of radon indoors at levels sufficient to pose significant health risks [5]. The primary source of indoor radon is soil gas from the ground beneath and surrounding structures, with building materials acting as a secondary source.

2.3.1 Ground Sources

The soil surrounding and underlying buildings constitutes the primary source of radon infiltration indoors. In the Canadian context, radon commonly enters residential structures through foundation cracks, unsealed construction joints, and various penetrations created for mechanical, electrical, and plumbing systems [35]. These pathways enable radon to migrate from the soil into living spaces, a process that is further intensified by pressure differentials between the indoor environment and the surrounding soil, known as the "stack effect." This phenomenon, which is driven by temperature gradients within a building, is particularly pronounced during colder months. As warm indoor air rises and escapes from upper portions of the structure, a negative pressure zone is created near ground level, drawing in outdoor air and hence radon gas from the soil [36].

Beyond typical entry points, radon intrusion can also stem from the proximity of buildings to subsurface structures, such as underground wells, which can provide direct pathways from deeper geological sources to surface soils and consequently indoor environments. Research in Alberta, Canada, for example, demonstrated that rural residents with groundwater wells experienced average radon exposures 31.2% higher than those in urban settings [37]. Similar trends have been noted internationally, with water treatment plant staff in Bavaria, Germany, receiving annual radon doses above acceptable limits due to groundwater well use [38] and a systematic review confirming the strong association between well depth and radon

concentrations [39]. Additionally, indoor radon may be augmented by direct water sources, including tap water [40]. Although such exposures are usually brief, they can meaningfully elevate total indoor radon levels. For instance, post-shower radon concentrations in bathrooms have been measured from 74 Bq/m^3 up to 4200 Bq/m^3, with elevated levels persisting for up to 20 minutes after water use [41]. As depicted in Figure 4, the pathways for radon entry are diverse and can lead to accumulation without occupants' awareness.

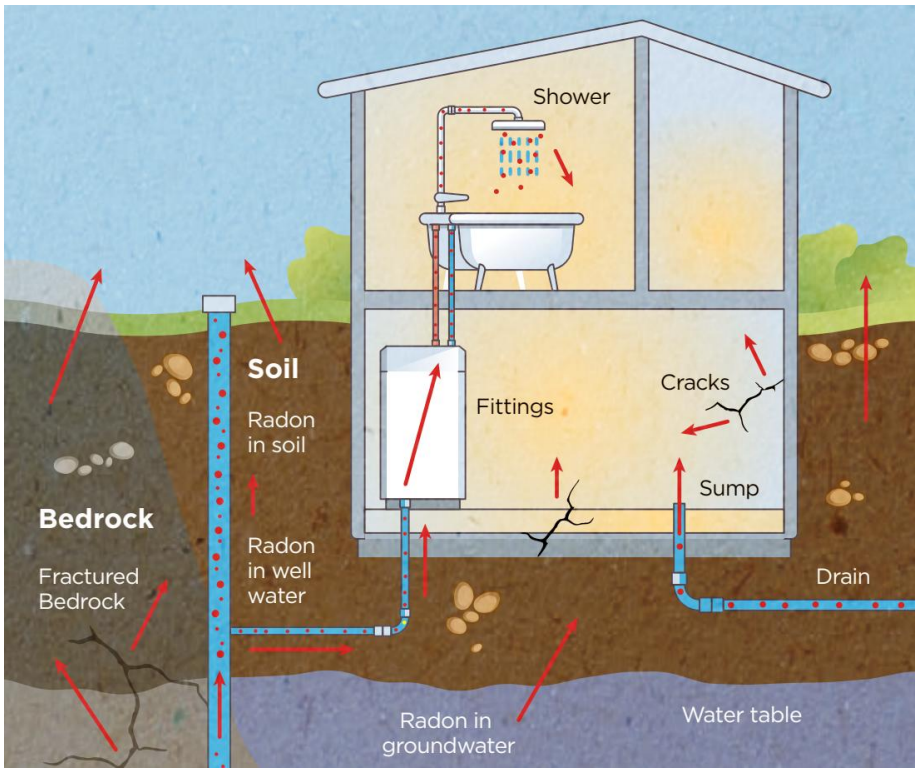


Figure 4: Radon entry points in buildings from Health Canada "Radon - What you need to know" factsheet [42]

2.3.2 Building Materials

Building materials, in addition to soil, can serve as notable contributors to indoor radon concentrations because of the presence of radium. While soil gas remains the predominant source of indoor radon, studies have shown that radon exhalation from certain building materials can be considerable in specific circumstances [43], [44]. In Sweden, for example, "blue concrete" was commonly produced from uranium-rich alum shale between 1929 and

1975. The high uranium content in this material has been linked to significant radon emissions, with indoor concentrations in affected buildings sometimes reaching up to 400 Bq/m^3 [45], [46]. Similarly, research by Bem et al. (2020) demonstrated that lightweight concrete containing ash additives, used in multi-family residences in Poland and Serbia, was associated with higher indoor radon levels [47]. Other factors, such as carbonation processes, can further affect the rate at which cement-based materials release radon into the indoor environment [48].

While multi-family residences, including high-rise buildings, typically register lower indoor radon concentrations compared to single-family dwellings, certain upper-level units may still experience elevated radon levels [49], [50], [51]. As units in high-rise structures are situated further from the ground, the potential contribution of building materials to indoor radon concentrations should be taken into consideration. For example, a predictive study of a newly constructed, unoccupied 18-storey building in Hong Kong employed concrete sample analysis and mass balance modelling to estimate radon exhalation rates. The study found that calculated radon concentrations arising from construction materials closely matched those measured within the building, with only a 3–6% variation, emphasizing the impact of building materials on radon levels at elevated floors [52]. Similarly, Valmari et al. (2012) observed that upper-floor apartments in Finnish multi-family buildings exhibited radon levels comparable to those in neighbouring low-rise structures, supporting the premise of ongoing radon discharge from construction materials [43], [53]. Health Canada has also assessed radon emanation from building materials used for decorative purposes and sub-slab aggregates in residential construction, concluding that while such materials generally contribute minimally to total indoor radon concentrations, they can still be a source of exposure under specific conditions [54].

2.4 Factors Influencing Radon in the Built Environment

The concentration of radon within a building is determined by a combination of environmental and building-related factors, which together produce variation in exposure risk. These influences include natural variables such as local geology, as well as diurnal and seasonal changes, in addition to a range of building-specific characteristics. Recent

advancements in construction practices and the adoption of sustainable building designs aimed at addressing climate change have further modified how particular building features impact indoor radon levels. As building stock, standards, and regulatory guidelines differ across countries and regions, the effects of these variables are not uniform, introducing additional complexity to the task of assessing radon risk in residential environments.

2.4.1 Environmental Factors

Underlying Geological Features

As mentioned previously, radon gas originates from the Earth's crust and is present throughout the environment, making it detectable in nearly all regions around the world. However, the concentration of radon varies substantially depending on local geological characteristics. Geology is commonly employed as a key predictor for radon mapping and risk assessment because of the established relationship between elevated indoor radon levels and uranium-rich rock formations.

For example, Nordic countries such as Finland, Sweden, and Norway rank among the highest globally in terms of radon concentrations, which is largely attributable to their geological profiles [55]. These areas feature high uranium content in bedrock and extensive glacial eskers. In contrast, Iceland, despite its similar geographic location and climate, exhibits very low radon concentrations due to its predominantly basaltic bedrock [56]. This difference illustrates how underlying geology is a critical factor in determining radon risk and highlights notable regional variability.

Numerous investigations have documented a strong relationship between geogenic factors and indoor radon concentrations [57], [58], [59], [60], [61]. For instance, a study conducted in Sweden revealed a clear association between radiometric uranium deposit maps and measured household radon levels [59]. Similarly, Borgoni et al. (2011) examined radon concentrations within the varied landscapes of Lombardy, Italy, and identified lithology as a key determinant of indoor radon [57]. In another example, research in Danyang-Gun, South Korea, found that elevation was the most influential variable for predicting radon levels, closely

followed by lithology. By integrating machine learning with radon sampling, the study classified more than 40% of the region as having high or very high radon potential [60]. Predictive radon models using certain parameters, such as geology, will be discussed in further detail in Section 2.5.

Interestingly, research from the Western Cape in South Africa showed that similar bedrock lithology does not always translate to comparable radon concentrations. Smit & Bezuidenhout (2021) compared radon values in two towns, both situated on granite bedrock approximately 100 km apart [62]. Despite their identical geological setting, the towns exhibited statistically significant differences in median indoor radon levels. The authors suggest that climate differences between the regions contributed to this disparity, indicating that geology alone is not sufficient to fully predict radon risk.

While geogenic mapping has proven valuable for identifying high-risk areas and guiding local building codes and policy, all of these studies highlight the limitations of relying exclusively on geological factors. Other environmental conditions, including outdoor temperature and seasonal changes, were consistently shown to also influence radon concentrations.

Diurnal and Seasonal Variations

Radon concentrations within buildings are not static; rather, they fluctuate over both diurnal and seasonal timescales. This variability is influenced by a combination of meteorological conditions and human activity patterns, and is well documented across the literature [63], [64], [65], [66], [67], [68], [69]. Diurnal changes in radon levels are mainly governed by atmospheric conditions, temperature differentials, and interior occupancy patterns. Typically, radon concentrations are elevated at night, peaking around dawn before decreasing during the daytime hours [70]. This daily cycle is attributed to stable atmospheric conditions and positive temperature gradients at night, which restrict vertical air mixing and cause radon to accumulate near the surface [69]. During the day, increased atmospheric instability and negative temperature gradients enhance the dispersion of radon, resulting in lower concentrations. Additionally, activities such as opening windows or using ventilation systems further reduce indoor radon concentrations during daylight hours [66], [67], [71]. Given these

daily fluctuations, long-term monitoring is generally recommended for accurately assessing average radon exposure, rather than relying solely on short-term spot measurements.

Seasonal variability exerts an even stronger influence on cumulative radon exposure and the associated radiation dose. In colder climates, indoor radon levels often rise during winter and decrease in the summer, a trend largely explained by the stack effect, which becomes more prominent with increasing temperature gradients between indoor and outdoor environments. Reduced ventilation during winter months also contributes to radon accumulation [63], [72].

The magnitude of seasonal variation has been quantified in literature. For instance, Pinel et al. (1995) developed a model for seasonal correction, finding that indoor radon levels could change by up to 35% over six months and by as much as 56% over three months [73]. For this reason, measuring radon concentrations during the winter is often recommended to obtain a representative mean value. To address this seasonal effect, countries such as Canada, the United Kingdom, France, Ireland, Poland, and South Korea have adopted correction factors for radon measurements taken outside a full 12-month period [68]. Nevertheless, these correction factors should be applied cautiously, as their appropriateness may vary with climate, geographic region, and local building practices.

Recent research has identified exceptions to these conventional patterns. Some studies have reported little to no seasonal variability, or even higher radon concentrations during summer in certain residences [74], [75]. In the Canadian Prairies, for example, nearly half of the surveyed homes exhibited steady radon levels across all seasons [11]. The increasing airtightness of modern buildings and greater use of air conditioning are thought to contribute, as they reduce dependence on natural ventilation even in warmer months. If such trends become more widespread, the applicability of the continued use of seasonal correction factors may be questioned and prompt a reconsideration of current radon risk assessment methods.

2.4.2 Building Design Factors

Building design characteristics play a significant role in determining indoor radon concentrations, often leading to notable differences between neighbouring structures. For example, homes situated in close proximity to one another may display markedly different

radon levels, which can be attributed to factors such as differences in types of ventilation systems, the building's age, or overall building type and height. Research conducted in Quebec examining the relative effects of geological and architectural factors found that geological variables explained up to 5% of the variation in basement and first-floor radon concentrations, whereas design-related factors accounted for as much as 18% [76]. Therefore, when assessing the radon potential of a building, it is important to consider design elements such as ventilation system type, year of construction, and the overall building type and height. These factors should be evaluated alongside the environmental variables previously discussed in Section 2.4.1 to provide a comprehensive estimation of radon risk.

Ventilation Type

Airtight construction practices, intended to reduce energy loss throughout a building, frequently create conditions that facilitate radon accumulation by limiting passive air exchange with the outdoors. Consequently, newer constructions that prioritize airtightness and energy efficiency have been associated with increasing indoor radon concentrations [77], [78].

Meyer (2019) investigated radon levels in buildings renovated for energy efficiency and observed that mean radon concentrations doubled in those that underwent refurbishment compared to non-refurbished counterparts [78]. A related study from Lithuania found mean radon levels rose from 34 Bq/m^3 to 44 Bq/m^3 following deep energy retrofits, a change attributed in part to reduced ventilation rates and enhanced airtightness [79]. In contrast, the same research assessed Finnish buildings before and after similar retrofits and found no statistically significant increase in radon, which the authors linked to more frequent installation of mechanical ventilation in Finnish buildings compared to the Lithuanian cases. This unintended increase in radon levels after airtight renovations has been documented in multiple countries, including Canada [9], Russia [80], Greece [81], and Ireland [82].

A consistent finding across the literature is the inverse relationship between ventilation rate and indoor radon concentration. Studies have shown that increasing the ventilation rate can significantly reduce radon levels, since enhanced air exchange more effectively dilutes and expels radon from indoor spaces [83], [84]. For instance, research in Korea demonstrated that

mechanical ventilation systems lowered radon concentrations in multi-family dwellings by facilitating greater air exchange from 0.5 ACH (legal requirement by the South Korean government) to 1.0 ACH or greater [85]. Similarly, a German study found that using radon sensors to control mechanical ventilation successfully reduced indoor radon up to 90%, highlighting this approach as a practical mitigation strategy [86]. These results indicate that buildings within the same region exhibiting lower air exchange rates may be more likely to present with elevated radon concentrations. In multi-family structures, particularly those with limited ventilation, radon concentrations on upper floors can also exceed recommended limits, a situation that can be exacerbated by radon diffusion from building materials, as described by Vasilyev et al. (2015) [80].

Year of Construction

The year a building is constructed has emerged as an important factor influencing indoor radon concentrations, reflecting changes in construction techniques for evolving requirements for energy efficiency, such as the use of continuous air barriers and the adoption of modern heating, ventilation, and air conditioning (HVAC) systems. For example, a study in Alberta, Canada, found that residences built after 1992 had radon levels that were, on average, 31.5% higher compared to older homes [11]. This increase has been linked to the early adoption of energy-efficient construction methods that enhanced the airtightness of buildings to reduce energy loss, but consequently decreased natural ventilation, allowing radon to accumulate indoors.

Similar patterns have been reported in other countries with a focus on energy-efficient building design. Research in Russia, for instance, demonstrated that multi-storey buildings constructed after 2000 consistently exhibited higher indoor radon concentrations than those built earlier [87]. As building practices continue to evolve in the direction of sustainable, passive design techniques, some countries have observed an increase in radon concentrations within newer residential buildings. This pattern suggests that younger occupants, who are more likely to occupy these modern, energy-efficient homes, may be at greater risk of elevated radon exposure in comparison to individuals residing in older, less airtight structures [12].

Figure 5 presents international data on indoor radon concentrations by construction year, drawing on ten studies published from 2010 to the most recent study in 2023. The figure illustrates diverse trends around the world, showing both increases and decreases in radon levels associated with changes in building age and construction standards. In some countries, newer homes exhibit higher radon concentrations, while in others, recent construction is associated with stable or declining levels.

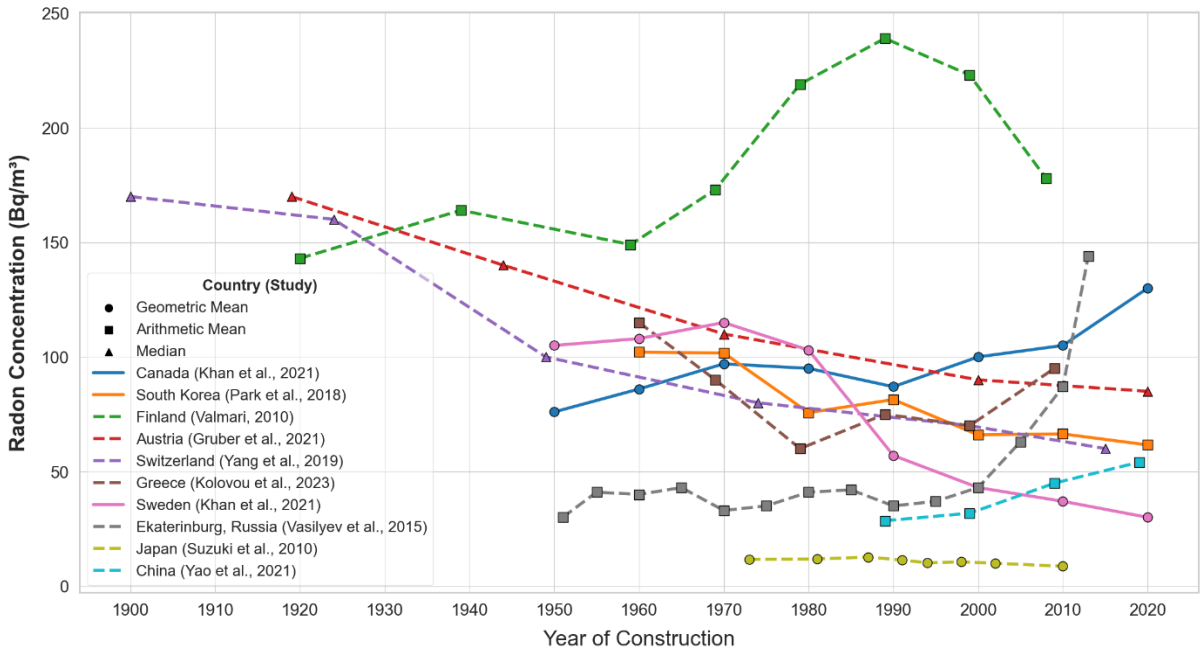


Figure 5: Trend of radon concentrations by year of construction by country. The solid lines denote countries that reported radon concentration for specific years. The dashed lines denote countries that reported radon concentrations over a range of years, where the first year in the range was plotted. Geometric means, arithmetic means, or medians are shown based on the measurements reported in reference studies (Giang, Goodarzi, Li, *in prep.*).

Notably, evidence from Sweden indicates a decline in radon concentrations in modern homes, even in areas characterized by high uranium content in the local geology [59]. Although Swedish building codes have not undergone major radon-specific updates, the overall construction approaches are similar to those in countries experiencing opposite trends. Khan et al. (2021) highlighted these contrasts, noting that the differences may be partly explained by HVAC systems. In Sweden, central district heating systems using radiant heat are common,

whereas in Canada, natural gas furnaces and forced-air ventilation are predominant, which can affect building pressure dynamics in ways that influence radon entry and concentration [9].

Comparable trends have also been documented in Austria and Switzerland, where newer residential buildings, especially those built after 1990, tend to have lower radon concentrations. Data from the Austrian national survey indicated that older dwellings (constructed before 1945) had higher radon levels, while those built after 1990 showed a negative linear trend in radon concentrations, likely due to changes in building materials and practices over time [88]. Many older structures were constructed with stone walls, which may have allowed greater radon infiltration compared to modern concrete walls [15], [50]. In Switzerland, more recent dwellings (2000–2015) demonstrated mean radon concentrations of 51 Bq/m^3, whereas dwellings built before 1900 and later renovated had concentrations as high as 150 Bq/m^3 [89]. The higher levels in renovated older buildings are thought to result from insufficient original sealing of lower floors and increased airtightness post-renovation, without corresponding improvements in ventilation.

Overall, while the push toward airtight, energy-efficient construction has often been associated with higher radon concentrations in some countries, this trend is not universal. Additional research is required to clarify the complicated relationship between building age, construction characteristics, and indoor radon levels.

Building Type and Height

Radon concentrations are also affected by the type of building. Single-family homes commonly have higher radon concentrations than other types of structures, such as high-rise multi-family residences [64]. Additional factors, including the presence of basements and similar underground foundation types, also play significant roles in increasing indoor radon levels. For example, in Finland, the national radon survey reported that houses with semi-basements or basements exhibited radon concentrations more than 50% greater than those with slab-on-grade foundations, largely due to their location below ground level [90]. The literature consistently points to a negative correlation between radon concentration and floor height [47], [91], [92]. Gallelli et al. [93] found that the lower floors of multi-family buildings

have much higher radon levels compared to upper floors [93]. Consequently, many national radon testing programs focus their efforts on single-family dwellings. This has, however, contributed to the misconception that radon risk is negligible on higher floors in multi-family buildings, offices, and institutional buildings, leaving a gap in monitoring and research for these types of structures.

Focusing on multi-family buildings, research in Hong Kong by Man & Yeung (1999) documented a consistent decrease in radon concentration with increasing floor level [52]. This decline in radon levels was matched by a corresponding increase in air exchange rates on higher floors. Notably, while the 18th floor registered a radon level of 95 Bq/m^3, about 100 Bq/m^3 less than the first floor, all floors except the top still exceeded the World Health Organization (WHO) recommended guideline of 100 Bq/m^3. This indicates that, although radon concentrations generally decrease with building height, upper floors may still present a risk, and safe levels are not guaranteed. Additionally, radon concentrations measured in ground-contact units of multi-family buildings are often similar to those found in low-rise single-family homes within the same geographic region, yet these units may be underrepresented in testing programs [43]. Studies from South Korea and Russia have shown that, despite the overall trend of lower radon in multi-family dwellings compared to single-family homes, specific apartments in urban areas, especially newer, energy-efficient buildings with low ventilation rates, can still exceed national reference levels [44], [94]. These observations demonstrate the need to broaden radon measurement and mitigation efforts to include multi-family residences and high-rise structures, as residents in these buildings can still face unsafe levels of exposure.

Figure 6 displays the arithmetic mean (AM) radon concentrations by building type and country. It is evident that single-family dwellings consistently report the highest mean radon concentrations, with Switzerland (164 Bq/m^3), Sweden (132 Bq/m^3), and Rome, Italy (129 Bq/m^3) leading among the countries studied [49], [50], [95]. Multi-family buildings, while generally lower in radon than single-family homes within the same country, still present noteworthy levels; for example, in Switzerland, multi-family dwellings averaged 152 Bq/m^3, which is higher than the single-family means in most other countries. Average radon concentrations for schools and public buildings, such as workplaces and institutes, are usually

lower than those for residences in the same regions, likely due to differences in building usage and design [96], [97], [98].

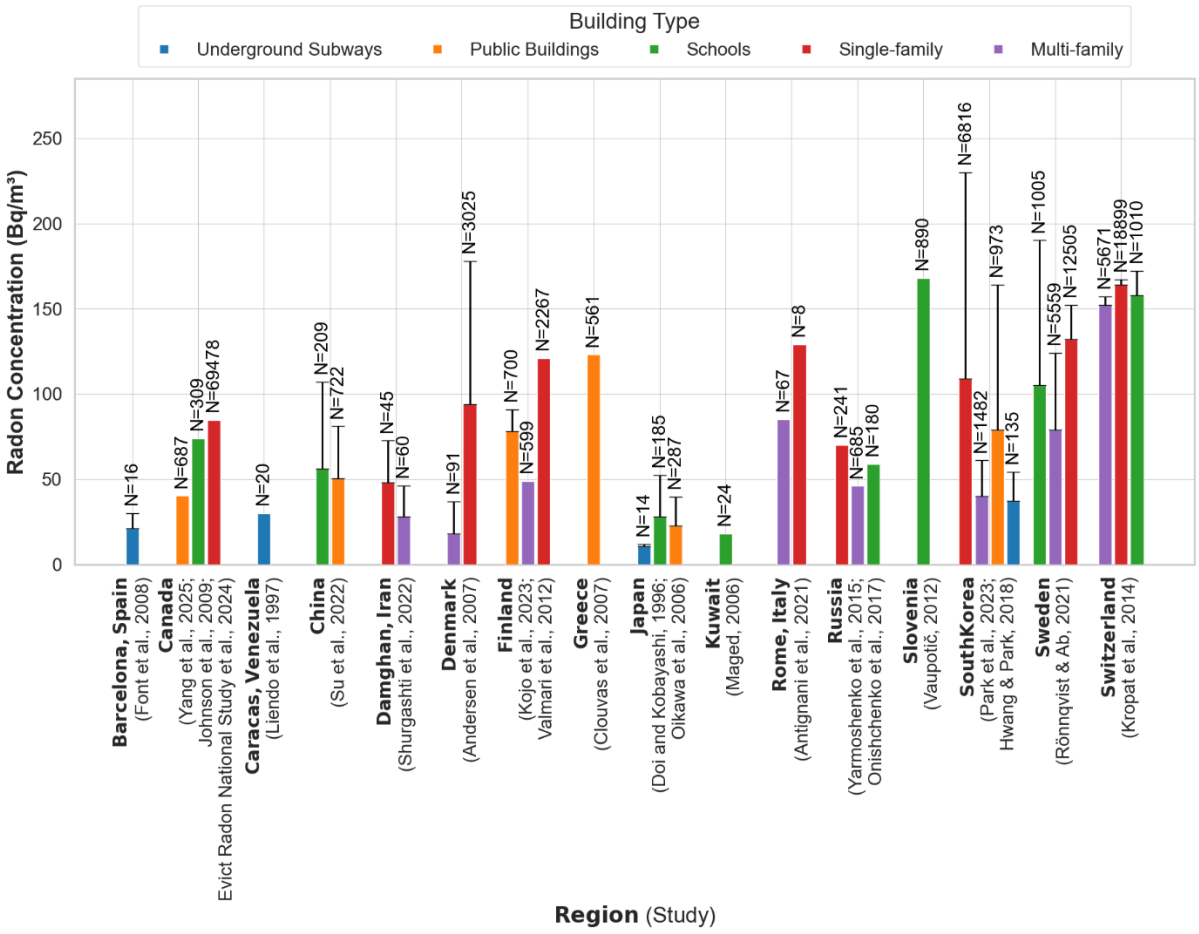


Figure 6: Arithmetic means (AM) of radon concentrations by building type, grouped by country. Standard deviations reported by the study are represented by error bars. The sample size (n) for each building type is shown above each bar (Giang, Goodarzi, Li, *in prep.*).

However, average radon values in schools in Switzerland and Slovenia have been reported above the WHO guideline of 100 Bq/m^3, at 158 Bq/m^3 and 168 Bq/m^3, respectively, posing a potential health risk to children, particularly in Slovenian kindergartens [50], [99]. Subway systems, examined in four studies, showed moderate radon concentrations relative to other building types, with South Korea reporting the highest at 37 Bq/m^3 [100]. Together, these findings indicate the necessity for approaches to radon risk assessment and mitigation that are

tailored to specific building types and regional characteristics, rather than depending on broad generalizations based solely on building typology or underlying geology.

2.5 Predictive Modelling

As understanding of indoor radon risk has advanced, there is increasing demand for the development of sophisticated national radon mapping systems that integrate both geological and building design factors to provide screening tools for residents and policymakers. Many countries have developed national radon maps using combinations of measured radon concentrations and their respective geological, as well as building characteristics, that enable residents to identify high-radon risk areas [101], [102], [103]. These mapping initiatives serve as crucial public health tools, with some regions making these commercially available to the public, such as the United Kingdom's purchasable radon potential maps [104]. The Italian national action plan for radon exemplifies this systematic approach, requiring regions to monitor indoor radon concentrations to identify radon-prone areas where radon concentrations exceed 300 Bq/m^3 in 15% of the monitored buildings [105]. Similarly, the British Columbia Centre for Disease Control (BCCDC) in Canada established the BC Radon Data Repository (BCRDR), which compiles indoor radon measurements from multiple sources to create an interactive online map that summarizes regional concentrations and raises awareness of associated health risks [106]. While these initiatives highlight the importance of integrating diverse data sources, rather than relying solely on geological factors, for effective radon risk assessment, as cautioned by the BCCDC, these maps alone cannot replace radon testing in residences.

Researchers have increasingly turned to machine learning algorithms to address the complex, non-linear relationships between various predictive factors and indoor radon concentrations. Random forest (RF) regression models have emerged as an effective tool for radon-related research due to their ability to capture intricate interactions between multiple environmental and building-specific variables [107], [108], [109], [110]. The traditional linear statistical analysis approaches often fail to accurately capture all influencing parameters, such as geology, diurnal and seasonal variations, and building characteristics and their relationships

[60]. RF models have been effectively applied at various scales, from national mapping efforts in Germany utilizing over 4400 field measurements of geogenic radon potential to state-level predictions in the northeastern and midwestern United States using over 2.8 million historical radon measurements [110], [111]. These studies consistently demonstrate that RF models outperform traditional statistical methods, with the German study showing that RF models exhibited the best performance (highest R^2 of 21.8%, and lowest RMSE of 52.76 Bq/m^3) when compared to other machine learning approaches [111].

The application of RF models has enabled researchers to adopt more holistic approaches to radon exposure assessment, incorporating different geological, meteorological, architectural, and socioeconomic factors as predictors to varying degrees of accuracy. Petermann et al. (2024) developed high-resolution indoor radon maps that were able to reproduce the observed distribution of radon concentrations across the validation dataset in Germany [112]. In the United States, Li et al. (2023) were able to achieve a coefficient of determination of $R^2 = 0.7$ for community-level predictions when sufficient measurement data was available. However, it is important to note that the study was conducted using a special variant of RF models (spatial RF) that can better account for spatially related variables over traditional RF models used by other studies [110]. A Swedish study has shown that RF models can explain 28% of the variance in multi-family homes and 21% in single-family homes, demonstrating the model's ability to account for complex geogenic and building factors, including uranium concentrations, ventilation systems, construction year, and basement type [113]. Furthermore, the applicability of these models between regions has also been investigated. For example, RF models trained on German data were able to predict geogenic radon potential in Belgium, though optimal model configurations vary between regions depending on local geological and climatic conditions [114]. In general, while studies report that RF models tend to outperform traditional statistical approaches, their overall predictive power can be weak to moderate, with R^2 values frequently less than 30% in the studies mentioned above. This suggests that, despite their advantages, current radon prediction models often face challenges and capture all sources of variability, further highlighting the need for continued refinement and the integration of additional, high-quality predictive data.

Overall, these developments highlight the opportunities of using integrated, data-focused approaches for radon risk prediction, demonstrating the value of predictive modelling methods in protecting public health and supporting targeted radon mitigation efforts worldwide.

2.6 Radon Measurement Strategies

As described previously, even with the advancement in predictive modelling, the combined influence of environmental conditions and building design leads to substantial variability in radon concentrations, making it difficult to rely on generalized assumptions for estimating radon exposure in individual buildings. Therefore, large-scale radon measurement is essential for identifying radon exposure and its associated health risks.

In Canada and many countries, the responsibility for measuring and mitigating radon exposure in private residences typically falls on homeowners or occupants [53]. Mandatory regulations versus recommended guidelines vary based on radon activity and legal governing frameworks at the provincial level in Canada. As a result, there are no legal protocols to measure radon at the national level, although Health Canada advises a minimum 90-day testing period at the lowest occupied level of a residence during the winter season [115]. In addition, the most commonly used and recommended measurement devices are passive detectors.

2.6.1 Passive Detectors

Long-term passive detectors have been extensively employed in both academic research and national surveys worldwide as a reliable approach for radon measurement [49], [116], [117], [118], [119]. In Canada, approved devices for long-term testing under the Canadian National Radon Proficiency Program (C-NRPP) include alpha track detectors and electret ion detectors, available for use by professionals and consumers alike [21]. Alpha track detectors function by recording the damage tracks produced when alpha particles from radon progeny strike a plastic film; after the testing period, the detector is sent to a laboratory where the tracks are counted to estimate the mean radon concentration. Electret ion detectors, meanwhile, utilize a charged plastic disk that detects ionization events caused by the decay of

radon progeny [18]. These long-term passive devices are relatively affordable compared to other radon sensors, with alpha track test kits available for approximately 50 CAD.

2.6.2 Electronic Radon Monitors (ERMs)

Electronic radon monitors (ERMs) have become increasingly popular among building occupants in recent years, offering the advantage of real-time radon monitoring [21]. Among these, professional-grade devices such as the RAD7 (Durridge) and AlphaGUARD (Bertin Technologies) are widely used, with the RAD7 being included on the C-NRPP's list of recommended professional instruments. The RAD7 operates as a solid-state alpha detector, while the AlphaGUARD makes use of a pulsed ionization chamber for detection [120], [121]. Both devices are known for their high sensitivity and reliable real-time measurements, though their considerable cost typically restricts their use to radon professionals rather than the general public.

Beyond these professional models, there are several consumer-grade ERMs available at a lower cost, generally in the range of 100 to 300 CAD, that have been approved by C-NRPP for residential use. These devices are attractive to consumers due to their rapid results and user-friendly interfaces, offering distinct advantages over passive detectors, which only provide an average value after a minimum three-month testing period and lab analysis. However, important limitations exist regarding the accuracy and relevance of short-term measurements and the overall performance of these consumer-grade sensors [122]. As mentioned earlier, because of the fluctuations in indoor radon concentrations, short monitoring periods may not accurately capture the long-term exposure risks faced by occupants. Additionally, considerable variation in accuracy, performance, and precision exists across available ERMs. Despite manufacturers' claims of the sensors employing similar detection mechanisms as professional instruments, such as pulsed ion chambers or passive diffusion chambers, the reliability of consumer-grade ERMs cannot be assumed. This concern is underscored by Health Canada's recall of an ERM that underreported radon levels by over 90% [123]. Without standardized calibration or large-scale field testing, poorly performing sensors may provide misleading results and fail to protect users from potential radon risks.

While some studies have compared the performance of popular consumer-grade ERMs with professional-grade monitors or passive detectors as reference standards, most research has been confined to controlled laboratory conditions. Table 1 summarizes research evaluating various ERMs under a range of test settings and highlights the analytical methodologies employed. Although study protocols differ, all seek to determine the accuracy and precision of ERMs to better inform their use for radon testing. Findings from these studies indicate that, while certain consumer-grade ERMs show promising correlation with professional devices, their performance can vary significantly depending on the specific device and testing conditions.

Table 1: Summary of studies evaluating ERMs (Giang, Goodarzi, Li, *in prep.)*

Study (Year) [Citation]	ERMs Tested	Reference Instrument (Manufacturer; Device No.)	Testing Location	Testing Duration (Days)	Concentration Range (Bq/m^3)	Additional Parameters	Analysis Method
Bahadori and Hanson (2024) [122]	8 unique devices; 5 units each; 40 total	AB-5 (Pylon, n = 2); Radon Eye Pro (Ecosense, n = 2)	66 m^3 Radon chamber	7	22; 474 - 574; 1025 - 10868	N/A	Individual percent error; Relative standard deviation
Beck et al. (2024) [22]	13 unique devices; 1 unit each; 13 total	AlphaGUARD (Bertin Technologies, n = 1)	0.3 m^3 Radon chamber	42	100 - 1000	Temperature; Air pressure; Relative humidity	Mean ratio; Relative standard deviation; Measurement percent error; Student's T-test; Weighted mean ratios; Linearity error; Durbin-Watson test; Response time
Daraktchieva et al. (2024) [124]	7 unique devices; 2 -10 units each; 27 total	Atmos 12 DPX (Gammadata Instruments AB, n = 1); AlphaGUARD P30 (Bertin Technologies, n = 1); Passive solid-state nuclear track detectors (UKHSA, n = 70)	43 m^3 Radon chamber	90	100 - 216; 3733 - 6000;	N/A	Relative percent error; Relative standard deviation; Measurement percent error; Calibration factor; Response time
Dimitrova et al. (2023) [125]	1 unique device; 36 units each; 36 total	AlphaGuard DF2000 (Saphymo, n = 1); RAD7 (Durridge, n = 1); AlphaE (Saphymo, n = 1)	0.2 m^3 Radon chamber	0.5 - 3	150 - 7000	N/A	Correction factor; Linear regression; Response time
Dimitrova et al. (2025) [126]	3 unique devices; 1 unit each; 102 total	Passive solid-state nuclear track detectors (UKHSA, n = 4)	Dwellings (n = 32), Workplaces (n = 2)	395	0 - 200; 1000 - 2000	N/A	Relative percent error; Z-scores
Fuente et al. (2018) [127]	4 unique devices; 1 - 2 units each; 5 total	Atmos 12 (Gammadata Instruments AB, n = 1); CR-39 (Radosys Ltd, n > 2)	1 m^3 Radon chamber	7	2648; 0 - 6441; 6441 - 2648	N/A	Relative percent error; Mean concentration; Response time

Gunning et al. (2016) [128]	6 unique devices; 1 - 2 units each, 7 total	Atmos 12 DPX (Gammadata Instruments AB, n = 1); CR-39 (Track Analysis System Ltd, n = 8)	Radon chamber, Dwelling (n = 1)	28	2560; 57	N/A	Mean concentration; Relative percent error
McGrath et al. (2022) [129]	1 unique device; 4 units per dwelling; 88 total	Alpha track-etch detectors (n = 56)	Dwellings (n = 22)	90	1-100, 100-200, >200	N/A	Linear regression
Rábago et al. (2024) [19]	7 unique devices; 1 unit each; 7 total	AlphaGUARD (Bertin Instruments, n = 1)	45 m^3 Room in laboratory	54	500 - 1500, 3000 - 15000	N/A	Relative percent error; Student's T-test; Pearson correlation; Response time
Rey et al. (2024) [130]	10 unique devices; 6 unique passive detectors; 1 unit each; 16 total	Radonmapper (TECHNAVIA SA, n = 1); AlphaGUARD (Bertin Technologies, n = 1)	144 m^3 Room in laboratory	2 - 3	300, 2000-3000	Household aerosols	Mean ratios; Relative standard deviation; Wilcoxon tests
Rey et al. (2024) [20]	10 unique devices; 6 unique passive detectors; 1 unit each; 16 total	Radonmapper (TECHNAVIA SA, n = 1); AlphaGUARD (Bertin Technologies, n = 1)	144 m^3 Room in laboratory	2 - 3	300, 2000-3000	N/A	Mean ratios; Absolute relative percent error; Pearson correlation
Stern et al. (2023) [131]	2 unique devices; 1 unit each; 2 units total	E-PERM (Rad Elec, n = 1); RAD7 (Durridge, n = 1)	Dwelling (n = 1)	286 - 507	0 - 500	N/A	Linear regression
Warkentin et al. (2020) [132]	6 unique devices; 3 units each; 18 total	AlphaGuard DF2000 (Saphymo, n = 1)	12 m^3 Radon chamber	7	200 - 1000	N/A	Relative percent error; Relative standard deviation; Measurement percent error

For instance, Warkentin et al. (2020) evaluated six electronic radon monitors (ERMs) produced by three different manufacturers within Canada's national radon chamber [132]. Across a range of radon concentrations from 200 Bq/m^3 to 1000 Bq/m^3, all devices demonstrated acceptable performance, with precision values spanning 2% to 15% and accuracy ranging from 1 – 24%. In a similar laboratory investigation, Rábago et al. (2024) assessed sensors from the same manufacturers and reported significant correlations among ERMs, with Pearson correlation coefficients between 0.63 and 0.90. This study also found no significant percentage difference between most ERMs and reference instruments, except for one monitor [19]. Both studies concluded that many ERMs show good agreement with professional-grade reference instruments, suggesting their potential suitability for radon testing. These findings are consistent with results reported in other studies [22], [122], [125], [127], [131]. Furthermore, McGrath et al. (2022) investigated real-world performance by deploying alpha track detectors alongside pre-installed ERMs in residential settings. Their analysis using linear regression revealed a strong correlation between the devices, supporting the viability of ERMs for use outside laboratory conditions [129].

Despite these encouraging results, researchers have highlighted several important limitations of ERMs. Daraktchieva et al. (2024) conducted a three-month study under controlled conditions at both low (166 Bq/m^3) and high (4,781 Bq/m^3) radon concentrations. The results indicated that while measurement error for all ERMs was less than 10% at high concentrations, it increased markedly at lower concentrations, ranging from 20 – 50%, and instances of overestimation reached up to 80% [124]. This trend is consistent with findings by Rey et al. (2024), who observed greater measurement errors and reduced correlation among ERMs at lower radon levels (300 Bq/m^3) [130]. Additionally, Daraktchieva et al. (2024) pointed out that most consumer-grade ERMs lack calibration, with devices exhibiting decreased performance often showing considerable shifts in their calibration factors over time [124]. This observation suggests that the accuracy and precision of ERMs may deteriorate with extended use and highlights the necessity of recalibration for reliable long-term measurement. It is important to consider that these limitations may partly result from the constraints of controlled laboratory environments and the relatively short duration of some studies. Therefore, further research involving longer-term, real-world testing and enhanced regulatory oversight from

organizations such as the C-NRPP and Health Canada is needed to ensure that consumers have access to reliable and effective radon monitoring devices.

2.7 Radon Mitigation Strategies

When radon concentrations in a residence exceed recommended safety thresholds, effective reduction techniques are essential to minimize health risks. In Canada, Health Canada sets the national threshold for indoor radon at 200 Bq/$m^{3,}$ with concentrations above this level warranting mitigation efforts to protect occupants' health. Mitigation approaches differ for new constructions and existing buildings. New homes can more easily incorporate radon-resistant features during the construction process. In contrast, retrofitting is necessary for existing residential buildings, which make up over 17 million dwellings in Canada, and this process can be more complicated and costly [133], [134]. The effectiveness and challenges of these mitigation strategies also depend on specific building characteristics and regional factors.

New Construction

Implementing radon prevention measures during the construction phase of new buildings is recognized as more cost-effective than installing mitigation systems in existing homes after construction is complete. Integrating radon-resistant construction techniques from the outset provides a proactive and economical approach to reducing radon risks [53]. A widely used preventive strategy is the installation of a radon impermeable membrane under the foundation slab. This type of membrane serves as a barrier that limits the entry of radon gas into the building. Although studies have found that these membranes can lower indoor radon concentrations, their effectiveness on their own is often not as great as more comprehensive solutions, such as sub-slab depressurization systems (SSD) [135]. Due to their low cost and ease of installation, membranes remain a popular choice in areas with low or moderate radon potential. In many jurisdictions, building codes require the use of radon barriers to ensure a minimum level of protection for occupants [56], [136], [137]. In locations identified as having higher radon risk, additional interventions are generally necessary to further reduce radon entry. For instance, the Canadian National Building Code requires the installation of a capped

rough-in pipe beneath the foundation slab. This pipe is not used immediately but can easily be converted to an active SSD system if elevated indoor radon levels are detected later on [138]. This approach balances cost efficiency with adaptability and allows for straightforward upgrades if mitigation becomes necessary in the future.

Radon-resistant construction practices are being adopted in many countries as awareness of radon-related health risks increases throughout government agencies and international organizations. While the specific measures vary according to local radon conditions and regulations, the primary objective is consistent: to protect building occupants from radon exposure and to minimize the need for costly post-construction mitigation.

Existing Structures

Among the various mitigation options available for existing homes, SSDs are widely recognized as the most effective approach [53]. This technique involves installing a system of pipes beneath the building's foundation that vents radon gas directly outdoors, thereby establishing a pressure difference. By maintaining a lower pressure beneath the slab than inside the house, SSD systems effectively block radon gas from entering indoor spaces. Systematic reviews of radon mitigation interventions have identified SSD as the most successful method, with effectiveness reported as high as 97.5% in Canada and 96.5% in the United States [10], [139].

SSD systems can be distinguished as either active or passive. Active SSD systems employ an electric fan to sustain continuous negative pressure, ensuring steady removal of radon gas. Passive SSD systems depend on natural pressure gradients and the stack effect to achieve similar results. Both approaches utilize the same fundamental principle, though their performance can be affected by external variables. A study in Québec, Canada, examined the performance of passive SSD systems in both new and retrofitted homes, finding that these systems often reduced radon concentrations to below the Canadian guideline. However, certain features, such as heat recovery ventilators with reduced supply air settings, poorly insulated vent stacks, or openings in ground floor bathrooms, diminished effectiveness,

especially during cold weather when frost accumulated in attic spaces, restricting the airflow in uninsulated stack vents [140].

If installing an SSD is not feasible, balanced mechanical ventilation provides an alternative mitigation solution. This strategy increases air exchange rates, thereby diluting indoor radon concentrations. For example, Dehnert et al. (2021) demonstrated that a wireless, automatically controlled ventilation system, triggered by radon sensors, was able to lower radon in a German apartment building from 8,000 to 800 Bq/m^3 [86]. This finding highlights the potential for enhancing existing ventilation systems as a cost-effective means of radon risk reduction while also conserving energy.

Comparisons of radon levels in Finnish homes revealed that houses with balanced ventilation, which involves both supply and exhaust with heat recovery, showed reductions in radon concentration by as much as 20 – 47% compared to homes using only mechanical exhaust ventilation [141]. This outcome is supported by research in Norway, where balanced ventilation systems in detached homes significantly reduced radon levels compared to those with solely mechanical exhaust ventilation [142].

Despite these benefits, a systematic review by Khan et al. (2019) indicated that active ventilation methods display moderate effectiveness, typically ranging from 25 – 75% in studies conducted in Norway, the United States, and the United Kingdom [53]. Combining mechanical ventilation with active SSD can further enhance indoor air quality and energy efficiency. For instance, in Romania, the use of both systems together reduced radon from 425 to 75 Bq/m^3 and achieved up to an 86% reduction in energy consumption [143]. This demonstrates that it is possible to achieve effective radon mitigation while maintaining energy-efficient building practices.

Other mitigation strategies include sealing cracks and openings in the structure and using air filtration systems with high-efficiency particulate air filters. However, research has shown that sealing entry points alone is the least effective technique, largely due to the challenge of thoroughly identifying and sealing all potential pathways. Even with substantial effort, if any openings are missed, the radon reduction can vary greatly and rarely eliminates the risk, with

effectiveness ranging from 0 – 40% [144], [145]. Sealing is best used in combination with SSD or other methods. The effectiveness of air filtration depends on the interaction between radon progeny and particulate matter in the indoor environment [146], [147]. Some studies suggest air cleaners can help by reducing particulate matter concentrations, but they may inadvertently increase the proportion of unattached radon progeny, which is considered more harmful to human health than attached progeny [148], [149], [150].

While SSD remains the most reliable mitigation method for existing buildings, its performance can be influenced by building design and use patterns. For new construction, there are opportunities not only to incorporate these mitigation techniques into building designs but also to implement preventive measures before occupancy.

2.8 Global Regulations, Standards, and Guidelines

As mentioned previously, the WHO identifies radon as a confirmed human carcinogen and recommends indoor radon thresholds of 100–300 Bq/m^3 [5]. This recommended range serves as a reference for countries around the world as they develop national guidelines and regulatory frameworks. The WHO handbook on indoor radon presents policy options aimed at reducing health risks from residential radon exposure and emphasizes the need for a national annual average residential radon concentration reference level of 100 Bq/m^3. If achieving this level is not feasible, the handbook states that the reference value should not exceed 300 Bq/m^3. In addition, the International Commission on Radiation Protection (ICRP) advises that radon exposure should always be reduced as much as reasonably possible, within the same range outlined by the WHO [151]. These international recommendations have significantly shaped the development of national radon regulations. However, the adoption and enforcement of radon policies vary widely across countries, reflecting differences in radon prevalence, regulatory systems, and public health strategies.

2.8.1 European Countries

Nordic countries, including Finland, Sweden, and Norway, which experience some of the highest indoor radon concentrations globally, have addressed radon risk in their building codes, though the extent of recency of updates varies by country. [56]. Each country has

established its national reference level and developed comprehensive strategies that combine systematic radon testing, amendments to building regulations, and public awareness campaigns. Norway, in particular, has adopted one of the most proactive frameworks in the region by mandating the implementation of prevention measures in all new construction and requiring radon testing after building completion [55]. Standard preventive measures typically include the installation of a radon-impermeable barrier together with a passive SSD system, which may be augmented with an active fan if measured radon concentrations exceed the action level. Regulatory changes to Norway's building code implemented in 2010, which set an action level at 100 Bq/m^3 and a maximum limit at 200 Bq/m^3, led to a statistically significant reduction in average radon concentrations in detached houses by nearly 50% [142]. In contrast, building codes in Finland and Sweden require that the design and construction process address radon prevention, but do not specify detailed measures [55], [152].

At the broader European level, the European Union (EU) adopted Directive 2013/59/Euratom, which sets out basic safety standards for protection against ionizing radiation and obliges EU member states to establish legal requirements for radiation protection [153]. This directive has spurred further research and initiatives across Europe, leading to the creation of the European Indoor Radon Map and the development of national radon action plans [154], [155]. Several other European countries have long-established radon policies and have continued to update them in light of new research findings. For example, building regulations in the United Kingdom have required radon prevention measures for new homes located in designated radon-affected areas, where 3 – 10% of homes are expected to exceed the national action level of 200 Bq/m^3, since 1992 [156]. More recently, the UK introduced a target level of 100 Bq/m^3 to guide prevention in new construction and remediation efforts in existing buildings [157].

2.8.2 North America and Other Countries

Unlike many European countries with unified regulatory frameworks, nations such as Canada and the United States exhibit substantial variation in radon regulations due to their complex administrative structures. In the United States, the Environmental Protection Agency (EPA) recommends an indoor radon limit of 4 pCi/L, which is approximately 148 Bq/m^3.

However, the formulation and enforcement of radon policies are managed at the state level, resulting in differing standards for testing and mitigation across the country [158]. For instance, a recent study leveraged the mandatory disclosure of radon information during real estate transactions to develop a detailed radon map, but only 35 of the lower 48 states require such disclosures. This highlights the inconsistent nature of radon policies at the state level. As an illustration, New Jersey mandates radon testing for all ground-contact multi-family housing units, whereas states like Wyoming do not maintain any statewide radon regulations [159], [160].

In Canada, regulatory responsibilities for radon prevention and mitigation measures largely fall on provincial and territorial governments. The National Building Code of Canada recommends the installation of a capped rough-in pipe in new residences, except for multi-family homes, to facilitate potential future SSD installations. Nevertheless, provincial and territorial authorities decide whether to adopt these recommendations, resulting in regional variability in radon mitigation practice [161]. For example, British Columbia has established one of the most comprehensive frameworks in the country, requiring a full radon mitigation system in new construction within designated high-radon zones and rough-in provisions elsewhere [162]. Testing for radon remains the responsibility of homeowners, who must arrange for measurement and any mitigation if elevated concentrations are detected. Limited public awareness of radon among Canadians contributes to the likelihood that many homes remain unmitigated, thereby increasing public health risks [13]. Notably, the forthcoming 2025 National Building Code of Canada will introduce stricter measures, including requirements for passive vertical SSD systems in all dwellings and residential buildings with ground-contact spaces or basements, such as ground-contact units in multi-family buildings [163]. If provinces and territories choose to adopt these updated provisions, stricter radon regulations may be implemented in certain regions.

Elsewhere, other countries have adopted a range of approaches. In China, the national standards set a mandatory limit of 200 Bq/m^3 for newly constructed dwellings, with recommended levels of 100 Bq/m^3 for new homes and 300 Bq/m^3 for existing residences [164]. While South Korea currently lacks formal radon regulations for buildings, national studies have

been undertaken to evaluate radon concentrations, to inform future mapping efforts and protective measures for the public [117].

2.9 Summary of Literature Review

This review demonstrates the complex and multifaceted nature of radon exposure in residential environments, with substantial evidence linking elevated indoor radon concentrations to a variety of geological, environmental, and building-related factors, with building design and ventilation practice playing notable roles. While progress has been made in mapping radon risk, predictive models that can integrate diverse risk factors remain moderate to weak in predictive power. Therefore, the performance and reliability of measurement tools remain an important consideration, particularly as consumer-grade ERMs are increasingly used alongside traditional passive detectors.

Comprehensive mitigation strategies, including sub-slab depressurization and enhanced ventilation, are well supported by research. National and international guidelines and policies emphasize the importance of accurate measurement and effective mitigation strategies, yet significant variability exists in approaches across different jurisdictions. Despite increased awareness of national governing bodies in regions with high radon potential, gaps persist in public understanding, regulatory implementation, and tailored risk assessment for diverse building types. Thus, this review emphasizes the ongoing need for robust, context-specific research that develops predictive models tailored to national and regional contexts, validates the effectiveness of new monitoring technologies in real-world conditions, and expands the evidence on radon exposure in multi-family environments.

Chapter 3 – Methodology

Chapter 3 outlines the methodology and analytical framework employed to address the three objectives identified in Chapter 1: developing and validating predictive models for residential radon concentrations; evaluating the accuracy and reliability of low-cost electronic radon monitors (ERMs); and characterizing indoor radon patterns in high-rise and multi-family dwellings in Canada. To address the first objective (O1), the chapter details the sourcing, preprocessing, and encoding of two Canadian datasets and describes the development and validation of random forest (RF) regression models to identify key predictors of indoor radon concentrations. Statistical analyses, including both parametric and non-parametric techniques, are applied to explain relationships between building characteristics and radon levels.

Additionally, this chapter presents the design and execution of short- and long-term collocation experiments comparing multiple low-cost ERMs to professional-grade reference instruments in real homes to address the second objective (O2) and the measurements of radon concentration in high-rise multi-family buildings to address the third objective (O3). Detailed protocols for device placement, calibration, data logging, and performance evaluation are provided, utilizing metrics such as linear regression, RMSE, Spearman correlations, Bland-Altman analysis, and confusion matrices. The influence of indoor environmental factors, meteorological conditions, and air exchange rates on radon variability and sensor performance is assessed using the methods described here. The findings are reported in Chapter 4, with the discussions presented in Chapter 5.

3.1 Predictive Modelling

Predictive modelling was conducted to address the objective of the development and evaluation of predictive models for radon exposure risk estimation in Canadian residences. Two comprehensive Canadian datasets, each containing detailed information on building features and measured radon concentrations, were used as the basis for this analysis, as described in Sections 3.1.1 and 3.1.2. A combination of statistical methods and machine

learning techniques was employed to explore and quantify the relationships between key variables and radon levels. Linear regression and correlation analyses were first used to explore direct associations and identify significant predictors. Subsequently, RF regression models were used for a deeper investigation into the relative importance of each variable and the overall predictive capability of the model. To further assess the generalizability and robustness of these models, cross-dataset training and validation were performed, evaluating the extent to which predictive insights could be transferred between distinct regional and national datasets. All analysis was conducted in Python version 3.12.7.

3.1.1 Health Canada (HC) Dataset Description

The Health Canada (HC) dataset comprises data from the Cross-Canada Survey with approximately 13,800 residential dwellings distributed across 121 health regions nationwide, provided by Health Canada through a data sharing agreement. Health regions, as delineated by provincial health authorities, were selected as the geographic unit of analysis to ensure balanced representation of both urban and rural populations and to mitigate potential oversampling in major metropolitan centers. Conducted over two years (2009–2011) by Health Canada's National Radon Program, the survey aimed to estimate the proportion of Canadians residing in homes with radon concentrations exceeding the national guideline of 200 Bq/m^3 [8]. Long-term radon measurements (minimum three months) were collected during the autumn and winter heating seasons. The sampling frame excluded dwellings constructed on stilts and units in high-rise multi-family buildings situated above the second floor. For this study, the dataset was interpreted as representative of single-family homes, which we acknowledged as a study limitation. Reported radon concentrations below 15 Bq/m^3 were standardized to 15 Bq/m^3. In addition to radon measurements, the dataset contains 20 variables detailing building characteristics and contextual information. Further details regarding variable handling are provided in Section 3.1.3. This dataset has previously been analyzed by Chen (2021) to investigate the influence of housing characteristics on radon levels in Canada [165]. Given the existing literature on this aspect, the present study focused exclusively on the development of predictive models using this dataset, rather than re-examining the relationships between building characteristics and radon concentrations.

3.1.2 British Columbia Radon Data Repository (BCRDR) Dataset Description

The British Columbia Radon Data Repository (BCRDR) dataset comprises 44,410 radon measurements collected from a diverse range of building types throughout British Columbia. The BCRDR was established by the BCCDC to address the fragmented nature of radon data collection across the province. Individual datasets held by industry professionals, government agencies, and research organizations were insufficient on their own to provide comprehensive risk assessments at a localized scale [106]. To create a combined resource, the BCCDC aggregated voluntary contributions from multiple organizations, resulting in a repository that supports the development of the interactive British Columbia Radon Map. A data sharing agreement between our research team and the BCCDC was established to analyze the data and explore relationships between different factors influencing radon concentrations. Each measurement in the BCRDR includes information on the average radon concentration for the building reported, along with ten additional building-specific parameters. The dataset encompasses both residential and non-residential structures, with approximately 88% of measurements derived from long-term tests conducted over a three-month period. The coverage of data extends from 1992 to the present, a comprehensive representation of radon measurements across multiple decades. Preprocessing of the dataset and handling of the variables are discussed in further detail in Section 3.1.3. It is important to acknowledge that the BCRDR includes data from Health Canada surveys, which introduces the possibility of overlapping data points between datasets. In the present study, the BCRDR dataset was employed both for the development and validation of predictive models of indoor radon concentration and for the examination of variable relationships using statistical analysis techniques.

3.1.3 Dataset Preprocessing

The preprocessing of datasets was conducted to ensure data integrity and maximize the suitability of the datasets for subsequent statistical and machine learning analyses. The primary target variable, indoor radon concentration, typically exhibits a right-skewed distribution, which can compromise the assumptions of many statistical analyses and hinder the interpretability of results. As a result, radon concentrations were log-transformed prior to

both linear regression and RF analysis, a step widely implemented in radon-related studies and literature to normalize the distribution of data [166], [167], [168]. Given the study's focus on residential radon exposure, only data pertaining to residential buildings were included in the analysis. Non-residential data were excluded by filtering datasets based on building type to avoid confounding by building type and ensuring the relevance of findings to Canadian residences.

For the HC dataset, the initial dataset consisted of 13,815 data points. After removing entries with unknown values in any category, 13,642 data points remained, corresponding to a data loss of 1.25%. The BCRDR dataset underwent a more extensive filtering process. The original dataset comprised 44,410 entries. Approximately 5% of the data points were removed due to unknown values across all categories, resulting in 42,189 valid measurements. Of these, 18,994 were identified as non-residential buildings, including commercial, healthcare, educational, and unspecified non-residential types. These were excluded from both statistical and machine learning analyses, as nearly half of these non-residential entries lacked sufficient building-specific information to minimize introducing further uncertainty. After these steps, the final BCRDR dataset comprised 23,040 residential data points, representing 54% of the filtered dataset. Notably, 14% of the dataset labelled as residential buildings had unknown building types; however, these records were retained under the assumption that they were likely residential.

Variables in the Datasets

To prepare the datasets for input into the RF regression model, several additional preprocessing steps were performed. The target variable, indoor radon concentration (Bq/m^3), was log-normalized prior to input into all regression models. The selection and processing of variables in both the HC and BCRDR datasets were guided by the purpose of maximizing the predictive power for indoor radon concentrations while ensuring interpretability and minimizing redundancy. Variables were retained or excluded based on their relevance to building characteristics, environmental factors, and geographic context, as well as the quality and completeness of the data. Parameters deemed redundant, insufficiently detailed, or unrelated

to these three factors were omitted to streamline the modelling process and reduce noise. Recent research has also demonstrated that RF regression models face performance limitations when processing datasets that contain high cardinality categorical variables; therefore, we reduced the number of categorical variables to help improve the performance of the RF model [169], [170]. For the HC dataset, out of an initial set of 20 variables, 12 were retained for analysis after evaluation. Within the BCRDR dataset, 10 variables were initially available, of which 7 were ultimately included in the RF model. A comprehensive summary of all variables, including detailed descriptions and processing methods, is provided in Table A1 of Appendix A.

For both datasets, responses such as “Other”, “Unknown”, “No Response”, or “Not Sure” were treated as missing values. These were subsequently handled using iterative multiple imputation, a technique used for addressing missing values, ensuring that the predictive models were not biased by incomplete information. Iterative multiple imputation handles the missing data by estimating and replacing missing values by training predictive models using the known values and using the model to estimate and replace the missing entries [171].

To maximize the predictive accuracy of the RF regression model, all variables were systematically encoded according to their respective data types and levels of cardinality. Forward Sortation Areas (FSAs), which serve as key spatial identifiers, were initially subject to target encoding, facilitating the transformation of these high-cardinality categorical variables into meaningful numerical representations. Concurrently, FSAs were linked with census divisions through the use of official Canadian boundary files, which enabled both the assignment of spatial coordinates and the incorporation of mean radon concentrations at the census division level as continuous predictor variables. This dual strategy enabled a direct comparison of categorical encoding and the use of spatially derived continuous features. The comparison showed the benefits of the latter in leveraging the strengths of RF algorithms, particularly in reducing the uncertainty inherent in categorical spatial data, which was thus used in the subsequent analyses. All other categorical variables, such as building type, heating system, year of construction, and basement configuration, were encoded using one-hot encoding. This approach converts each categorical attribute into a set of binary variables,

preserving its non-ordinal nature and preventing the introduction of misleading ordinal associations. Through this comprehensive encoding process, both spatial and building-related variables were made fully compatible with the RF regression framework, ensuring that the model could successfully use the entire dataset to identify the key predictors of indoor radon levels.

3.1.4 Statistical Analysis

Statistical analyses were conducted exclusively on the BCRDR dataset to evaluate the influence of building characteristics and environmental factors on indoor radon concentrations within British Columbia. This approach was selected since the HC dataset has previously undergone this type of analysis in the literature, and the present study intended to further explore relationships between these factors and radon concentrations, providing a geographically specific yet similar evaluation utilizing the BCRDR dataset. Descriptive statistics were calculated to summarize the radon concentrations across different building characteristics. Given the log-normal distribution of indoor radon concentrations, the geometric mean (GM) and geometric standard deviation (GSD) were selected as the most appropriate measures for these analyses, in accordance with established literature [50], [165], [172]. To discover patterns and differences in radon levels amongst different variables, comparisons were made across important categorical characteristics such as building type, year of construction, heating system, and season. Table 2 summarizes the data points included for statistical analysis of the categorical characteristics in the BCRDR dataset.

Table 2: Summary of Data Points for Statistical Analysis of BCRDR Data

Type of Analysis	Inclusion Criteria of Data	N (Total included in analysis)	Percentage of Total Data (N_T = 42,189)
Building Type	Data points with residential building values.	11,313	27%
Multi-family vs. Single-family Buildings	Paired matching multi-family and single-family buildings by FSA.	220 paired FSAs; 11,183 data points	27%
Year of construction	Data points with year built values.	8,959	42%
Heating Type	Data points with heating type values.	7,189	17%
Season	Data points with season values.	42,044	100%

To further investigate the relationships between radon concentration and predictive variables, linear regression analyses were conducted, with the coefficient of determination (R^2) used to quantify the proportion of variance in radon levels explained by specific building features. In particular, regression models were used to explore the relationship between radon concentrations in single-family and multi-family residences, with comparisons matched by Forward Sortation Area (FSA) to control for geographic variation. When multiple measurements were available within each building category in a given FSA, GMs were first calculated separately for multi-family and single-family homes within each FSA. The values reported for each category represent the GM of these FSA-specific GMs, as the data again followed a log-normal distribution. As the distribution of radon concentrations for certain variables did not meet the assumptions of normality, non-parametric tests were employed. The Mann-Whitney U-test was used to assess the statistical significance of differences in radon concentrations between two groups. Spearman rank correlation tests were also employed to assess the strength and direction of monotonic relationships between radon concentrations in different building categories.

3.1.5 Random Forest (RF) Regression Model Development

To assess the predictive capabilities of different features for indoor radon concentrations, an RF regression model was developed and applied separately to both the HC and BCRDR datasets. This is pertinent to our objective to determine whether the RF model could synthesize

a varied range of input factors and effectively forecast radon concentrations, thus identifying the most influential predictors and helping to prioritize risk initiatives.

For each dataset, the RF model was trained and evaluated using an 80/20 split, with 80% of the data allocated to the training set and 20% reserved for testing. This approach ensured that model performance could be assessed on unseen data, providing an unbiased estimate of generalizability. In addition to the standard train-test split, model validation incorporated several key metrics: mean squared error (MSE), root mean squared error (RMSE), mean absolute error (MAE), and the coefficient of determination (R^2). The out-of-bag (OOB) score, a built-in validation method for RF models using bootstrap aggregation, was also calculated to provide an additional measure of model accuracy without the need for a separate validation set.

To further safeguard against overfitting and maintain model resilience, two additional validation procedures were implemented. First, the MSE was compared between the training and test sets to ensure that the model generalized effectively and was not simply memorizing the training data. Second, 5-fold cross-validation was performed, in which the dataset was partitioned into five subsets, with the model trained on four folds and tested on the remaining fold in each iteration. The performance metrics from each fold are averaged, providing a more stable estimate of generalizability and reducing the variability associated with a single train and test split. The cross-validation MSE, averaged across all folds, provided an estimate of the model's expected performance on new data and helped to mitigate the effects of data partitioning variability.

Hyperparameter tuning was conducted using a randomized search approach, leveraging the 'RandomizedSearchCV' function from scikit-learn. This method explored defined parameters within an RF model to identify the optimal configuration for each dataset, including the number of trees, maximum tree depth, minimum samples required to split a node, minimum samples per leaf node, and the number of features considered at each split. The hyperparameter search was guided by cross-validated MSE, ensuring that the selected parameters maximized predictive accuracy while minimizing overfitting. The final RF model parameters for each dataset, determined through this hyperparameter tuning process, are summarized in Table 3.

These settings reflect the unique characteristics of each dataset, and the trade-offs required to achieve optimal performance.

Table 3: Summary of Random Forest (RF) Model Parameters from Hyperparameter Tuning

Random Forest (RF) Model Parameters	HC Model	BCRDR Model
Number of trees	363	300
Maximum tree depth	25	12
Minimum samples required to split a node	16	10
Minimum samples per leaf node	4	8

Feature Selection and Importance

A critical aspect of interpreting the RF regression models lies in understanding which features most strongly influence the prediction of indoor radon concentrations. However, a notable limitation of our analysis is that the majority of input variables for both datasets are categorical rather than ordinal or continuous. As a result, standard feature importance metrics provided by the RF model tend to rank each category (e.g., each building type) separately, rather than evaluating the overall contribution of the broader feature group (building type as a category). This makes direct interpretation and comparison of feature importances more challenging, particularly when categories are numerous or imbalanced.

To address this, a leave-one-out (LOO) feature importance strategy was employed using OOB score as the primary metric for assessing model performance. The OOB error score, which is calculated using bootstrap samples not included in each tree's training set, serves as an unbiased estimate of model accuracy and generalizability. This approach involves establishing a baseline OOB error with all features included. Subsequently, the LOO strategy was applied to quantify the importance of each feature. In each iteration, a single group of related categories, for example, all building type categories, was removed, and the RF model was retrained with the remaining features and the resulting OOB error score. By comparing the OOB error of the baseline model (with all features included) to the OOB error after dropping each feature group, the relative importance of each group can be quantified. Specifically, a larger increase in OOB error upon removal of a feature group indicates a greater contribution of that group to the predictive power of the model. This LOO approach allows for a robust, group-level assessment

of feature importance, mitigating the interpretive challenges posed by high-cardinality categorical variables to identify which building, environmental, or spatial factors most strongly influence indoor radon levels.

Cross-Dataset Model Training

To further evaluate the generalizability and robustness of the developed RF regression models, a cross-dataset model training approach was implemented. Specifically, the model trained on the BCRDR dataset was applied to predict radon concentrations in the HC dataset. This approach allowed for an assessment of how well patterns and relationships learned from one regional dataset could be transferred to a broader, national context.

In order to facilitate meaningful cross-dataset predictions, it was necessary to harmonize the feature sets between the two datasets. Several preprocessing steps were undertaken to ensure that the input variables were directly comparable. First, categories unique to the HC dataset, such as “Trailer” and “Pre-Fabrication” within the building type variable, were removed so that the building type categories matched those present in the BCRDR data. This ensured that the model would not encounter previously unseen categories when applied to the HC dataset. Additionally, variables present in the HC dataset but absent from the BCRDR dataset, specifically, heating fuel type, foundation type, and air conditioning system, were excluded from the HC data before model application. This step was critical to ensure that the feature spaces were aligned and to prevent the introduction of bias or error due to missing predictors in the cross-dataset prediction process.

Further, all overlapping categorical variables were carefully reviewed and recoded to ensure consistent naming conventions and category definitions. For example, categories within building type, heating system, and floor level were matched and standardized across both datasets. This harmonization method entailed mapping categories with comparable meanings to a single label and ensuring that categorical variables were encoded consistently, reducing the likelihood of misclassification or information loss during model transfer.

3.2 Evaluation of Low-Cost ERMs

The evaluation of low-cost ERMs was conducted through two collocation tests: one short-term (approximately 7 days) and one long-term (98 days), each comparing the performance of multiple low-cost ERMs against a professional-grade reference instrument. Both studies took place in Canadian residences to capture the exposure in real, occupied homes. The short-term test was designed to assess multiple homes to capture a wide range of building types, ages, and indoor radon concentrations, allowing for an assessment of ERM performance under diverse real-world conditions. The findings from the short-term test also guided the selection of sensors for the subsequent long-term field measurement of multi-family buildings (O3), ensuring a reliable tool was used for monitoring. A subsequent long-term test was conducted to assess the performance of the sensors aligned with the three-month deployment of passive detectors recommended by Health Canada.

Sensor performance was assessed using several statistical analysis techniques. These included linear regressions to evaluate agreement between ERMs and reference instruments, as well as calculation of percent ratios, relative percent errors, coefficient of variation, and root mean squared error. Bland-Altman plots were generated to visualize any systematic differences between device types, and confusion matrices were used to determine the ability of ERMs to correctly classify radon concentrations relative to established safety thresholds. In addition to device performance comparison, the influence of building environmental parameters, such as indoor temperature, relative humidity, and ventilation, on sensor performance was examined. The effects of meteorological factors on temporal changes in radon concentrations, as recorded by the reference instrument during the long-term test, were also explored. All analysis was conducted in Python version 3.12.7.

3.2.1 Experimental Set-up

The short-term test was designed to evaluate the performance of four low-cost ERMs relative to a calibrated research-grade reference instrument (RAD7; Durridge) under real-world residential conditions. Testing was carried out in seven distinct homes in Waterloo, Canada, from May 30th, 2024, to July 29th, 2024. The selected homes represented a mix of single-family

detached houses and units within high-rise multi-family buildings, ensuring that the study captured a wide range of building types, construction years, and radon exposures. Each home was monitored for a continuous period of seven days to encompass typical fluctuations in environmental conditions and indoor radon concentrations, which ranged from 0 – 2,000 Bq/m^3 during the study period.

In single-family homes, sensors were positioned at the lowest lived-in level, the basement, where radon concentrations are often the highest. In multi-family buildings, devices were placed in living rooms, reflecting common living spaces. During each test, all ERMs and the reference instrument were collocated at least 10 cm of each other to maintain adequate airflow around each device. This protocol ensured consistency in data collection. Special attention was given to the operation of the RAD7 reference instrument, which relies on a desiccant to dry the incoming air stream and maintain measurement accuracy. The desiccant's effectiveness was monitored through visual inspection, with a colour change from blue to pink indicating saturation. While the desiccant was typically replaced at the end of each test (every seven days), there were instances where it was completely pink by the end of the test, raising concerns about potential humidity interference. To address this, RAD7's proprietary software was used to apply humidity correction to the radon measurements whenever necessary.

A summary of the site characteristics, including building type, year of construction, and specific testing locations within each home, is provided in Table 4. The typical experimental set-up of the devices during each test is illustrated in Figure 7.

Table 4: Summary of Site Information

Site	Building Type	Year of Construction	Testing Location
A	Detached House	1895	Unfinished basement
B	Detached house	1969	Finished basement
C	Detached House	1999	Unfinished basement
D	Multi-Family Building	2023	10th Floor living room
E	Multi-Family Building	1974	11th Floor living room
F	Detached House	1890	Unfinished basement
G	Multi-Family Building	2019	5th Floor living room



Figure 7: Typical experimental set-up of collocated devices.

The long-term collocation test was designed to evaluate the accuracy and stability of low-cost ERMs over an extended duration. A total of 15 types of ERMs, comprising three units per type, were assessed concurrently with a calibrated, research-grade reference instrument (AlphaGuard PQ2000; SARAD), as well as two solid-state alpha-track detectors. Monitoring was conducted over a test period of 98 days (approximately three months), from December 3rd, 2024, to March 12th, 2025, in alignment with Health Canada recommendations on radon testing during the heating season and on the lowest occupied level of the home [173]. The study took place in the basement of a detached, single-family home in Waterloo, Ontario, originally constructed in 1895 and without any major modifications (Site A from the short-term test). The basement was equipped with a walk-out entrance, separated from the upper floors.

All ERMs and the reference instrument were situated on a table at a height of 60 cm from the floor, in accordance with the ANSI/AARST guidelines for residential radon measurement [174]. To minimize the influence of wall proximity, drafts, or localized airflows and to ensure representative sampling, all devices were placed a minimum of 30 cm away from exterior walls and at least 1 m away from any windows, doors, or other openings. Due to space constraints, sensors of the same device type were positioned less than 10 cm apart; however, particular care was taken to avoid obstructing air inlets, preserving adequate airflow, and minimizing

potential device interference. Throughout the testing period, all ERMs were checked regularly for proper operation, and data were downloaded at the end of the monitoring period for subsequent analysis. The experimental set-up is depicted in Figure 8.



Figure 8: Experimental set-up of devices for long-term collocation test.

The basement environment was representative of typical living conditions, being in routine use by household occupants for daily activities such as laundry, exercise, workshop, and storage. Although direct access to the upper floors was not available, some air exchange occurred through floor gaps, resulting in a generally well-mixed airspace. All basement windows remained closed for the duration of the study by the occupants to maintain stable indoor conditions and comply with standard measurement protocols.

For both the short-term and long-term tests, preprocessing of data from sensors with internal datalogging capabilities involved synchronizing all device timestamps and resampling the data to the nearest hour to allow for direct comparison between the devices.

3.2.2 Devices Evaluated

A diverse selection of low-cost ERMs was evaluated to assess their performance across both short-term and long-term tests. The choice of devices was guided by their accessibility to Canadian consumers available for purchase on online marketplaces or physical stores, their technical features, and their representation in both laboratory studies and the consumer market. As mentioned previously, for the short-term test, a total of four ERMs were tested alongside a single professional-grade reference instrument. In contrast, the long-term collocation test involved a wider range of sensors, with 15 distinct ERM models, with three units of each model deployed, resulting in a total of 45 ERMs.

Reference Instruments

For both collocation studies, reference-grade instruments were used as benchmarks for evaluating ERM performance. In the short-term test, the reference instrument was the RAD7 (Durridge). For long-term collocation, the AlphaGuard PQ2000 (SARAD) served as the primary reference instrument, complemented by two Radtrak3 (Radonova) solid-state alpha-track detectors. These reference devices provided high-accuracy, validated measurements against which the consumer-grade ERMs could be assessed. Table 5 summarizes the devices with their technical specifications and other additional parameters measured by the reference instrument.

Table 5: Summary of reference instruments

Test	Manufacturer	Model	Detection Method	Accuracy	Sampling Frequency*	Additional Parameters
Short-term	*Durridge*	RAD7	Electrostatic collection and silicone detector	±5%	Hourly	Temperature; Relative humidity
Long-term	*SARAD*	AlphaGuard PQ2000	Pulsed ionization chamber	±3%	Hourly	Temperature; Relative humidity; Atmospheric pressure
	Radonova	Radtrak3	Alpha track detector	±6% after 3 months at 200 Bq/m^3	N/A	N/A

**Sampling frequency options range from every 2 minutes to 24 hours. The table shows the sampling frequency selected during the tests.*

Consumer-Grade Sensors

There was some overlap in the ERMs used for both the short-term and long-term tests. Notably, the RadonEye RD200 by Ecosense and the INK-RD2 by Inkbird were included in both tests, while the Airthings Wave was used in the short-term test, and the newer Airthings Wave Plus was evaluated in the long-term test. The selection of ERMs for the short-term test was primarily based on their internal datalogging features, which were essential for recording and retrieving hourly measurements via Wi-Fi or Bluetooth. This ensured that data could be reliably accessed and analyzed after deployment. Devices were also selected based on findings from Warkentin et al. (2020), which assessed ERM performance in laboratory settings against Canadian regulatory standards [175]. Additionally, a review of the most popular devices on Amazon, focusing on those priced at or below 300 CAD, helped ensure the study reflected devices commonly purchased by Canadian consumers. To broaden the range of devices tested, one commercial-grade sensor (Spirit) was included in the short-term study. Priced at approximately 1,000 CAD, this device is marketed for use in commercial buildings and institutions and recommended by the C-NRPP. Its inclusion provided a valuable benchmark for the performance of mid-grade sensors in comparison with both consumer-grade and research-grade instruments. For the long-term collocation test, the selection of ERMs was coordinated by Health Canada, with all devices chosen based on their availability to Canadian consumers

and a price point below 400 CAD (pre-tax). Each ERM was assigned a unique physical label and identification number to ensure traceability throughout the testing process. The full list of devices from both tests, along with their manufacturers, detection methods, technical specifications, sampling frequency, and data-logging capabilities, is summarized in Table 6.

Table 6: Summary of ERMs evaluated for both short-term and long-term collocation tests

Manufacturer	Model	Label (Long-Term Tests Only)	Detection Method	Accuracy reported by Manufacturer	Sampling Frequency	Data-logging Capabilities
Devices included in both tests						
Ecosense	RadonEye RD200	RE-4 RE-5 RE-6	Pulsed ionization chamber	±10% after 10 hours at 370 Bq/m^3	Hourly	App
INKBIRD	INK-RD2	RD2-2 RD2-4 RD2-5	Pulsed ionization chamber	±10%	Daily	App
Short-Term Test Devices						
Airthings	Wave	N/A	Diffusion chamber with silicone detector	±10% after 7 days at 200 Bq/m^3; ±5% after 2 months	Hourly	App
Radonova	Spirit	N/A	Silicone detector with alpha spectrometry	< 20% after 2 hours at 200 Bq/m^3	Hourly	App
Long-Term Test Devices						
Airthings	Wave Plus	WP-5 WP-6 WP-7	Diffusion chamber with silicone detector	±10% after 7 days at 200 Bq/m^3 ±5% after > 1 month	Hourly	App
Airthings	View Plus	VP-4 VP-5 VP-6	Diffusion chamber with silicone detector	±10% after 7 days at 200 Bq/m^3 ±5% after > 1 month	Hourly	App
Airthings	Corentium Home	CH-5 CH-6 CH-7	Diffusion chamber with silicone detector	±10% after 7 days at 200 Bq/m^3 ±5% after > 1 month	Daily	Camera*

CRADTEC	PRM-02H	CRAD-4 CRAD-5 CRAD-6	Diffusion chamber with silicone detector	±10% after 2 days at 200 Bq/m^3 ±5% after 2 months at 200 Bq/m^3	Daily	Camera*
Ecosense	EcoBlu	EB-4 EB-5 EB-6	Pulsed ionization chamber	±14% after 10 hours at 370 Bq/m^3	Daily	Camera*
Ecosense	EcoQube	EQ-4 EQ-5 EQ-6	Pulsed ionization chamber	±10% after 10 hours at 370 Bq/m^3	Hourly	App
Funny Kitchen	HRDM-02	FK-4 FK-5 FK-6	Diffusion chamber with silicone detector	±10% after 7 days ±5% after 2 months	Daily	Camera*
Hanchen	Home Digital Radon Detector	HAN-4 HAN-5 HAN-6	Diffusion chamber with silicone detector	±10% after 2 days at 200 Bq/m^3 ±5% after 2 months at 200 Bq/m^3	Daily	Camera*
INKBIRD	INK-RD1	IBD-4 IBD-5 IBD-6	Diffusion chamber with silicone detector	±10%	Daily	Camera*
LifeBasis	RN-55	LB-4 LB-5 LB-6	Diffusion chamber with silicone detector	±10% after 7 days ±5% after 2 months	Daily	Camera*
LifeBasis	Smart Radon Detector	LCA-4 LCA-5 LCA-6	Diffusion chamber with silicone detector	±10% after 10 hours at 370 Bq/m^3	Daily	App
Safety Siren	Pro Series 4	PS4-4 PS4-5 PS4-6	Diffusion chamber with silicone detector	±12% after 7 days at 925 Bq/m^3 ±5% after 1 month of monitoring at 925 Bq/m^3	Daily	Camera*
SunRadon	Lüft Home Radon	LU-5 LU-6	Diffusion chamber with silicone detector	±10% after 7 days at 148 Bq/m^3	Two-day average	App

**A time-lapse camera was used to record measurements for ERMs without internal datalogging capabilities. Photos were taken every hour, and measurements were manually extracted after testing.*

Upon completion of the long-term test, hourly or daily radon measurements were retrieved from devices with datalogging functionality via their respective mobile applications or online portals. For devices lacking datalogging support, a time-lapse camera was positioned to capture hourly photographs of the device display screens. These images were manually transcribed at the end of the study to extract radon concentration readings. In most cases, 12-hour readings were obtained, while 24-hour readings were used for sensors that experienced display issues, such as blinking screens at the time of image capture. Figure 9compares the original photo captured by the time-lapse camera and the colour grading applied for easier extraction of the radon concentration readings. As shown in the picture, some measurements were not displayed due to the blinking screens of certain ERMs.



Figure 9: Original photo captured from time-lapse camera (left), processed photo for manual data extraction (right).

During the long-term test, some data loss occurred due to equipment malfunctions. Specifically, the IBD-4 sensor lost power around December 24, 2024, at 5:45 pm, and was not restored until the battery was replaced on December 30, 2024. The sensor subsequently failed again on January 13, 2025. Additionally, the camera used for data logging stopped recording on December 30, 2024, at 11:37 am and was not reset until January 12, 2025, at 12:12 pm. As a result, all sensors without datalogging capability experienced a loss of measurements during this interval, accounting for approximately 13% of the total testing period. Furthermore, a persistent connectivity issue prevented any data collection from the LU-4 sensor throughout

the entire duration of the test. The sampling intervals, total number of radon measurements, and the percentage of available data for each device are detailed in Table 7.

Table 7: Summary of sampling frequency, total number of radon measurements, and percentage of available data for ERMs in long-term collocation test

Label	ERM	Sampling Frequency	Total number of radon measurements	Percentage of available data
Reference	AlphaGuard	Hourly	2374	100%
CH	Corentium Home	Every 12-hours	172	86.4%
CRAD	CRADTEC	Every 12-hours	173	86.7%
EB	EcoBlu	Every 12-hours	181	90.9%
EQ	EcoQube	Hourly	2370	99.8%
FK	Funny Kitchen	Every 12-hours	171	85.9%
HAN	Hanchen	Every 12-hours	173	86.7%
IBD	Inkbird RD1	Every 12-hours	180	90.5%
LB	LifeBasis RN-55	Every 12-hours	180	90.5%
LCA	LifeBasis Smart Radon Detector	Daily	99	99%
LU	Lüft	Two-day average	49	98%
PS4	Safety Siren Pro Series	Every 12-hours	172	86.4%
RD2	Inkbird RD2	Daily	99	99%
RE	RadonEye	Hourly	2371	99.9%
VP	View Plus	Hourly	2374	100%
WP	Wave Plus	Hourly	2373	99.9%

3.2.3 Performance Evaluation Metrics

The performance of low-cost ERMs was assessed using statistical and analytical methods to ensure a thorough evaluation of accuracy, reliability, and agreement with the reference instruments. The selection of metrics was tailored to the objectives and data characteristics of both the short-term and long-term collocation tests. Table 8 summarizes the evaluation

metrics applied in each phase. The details of each metric are described following the table, with environmental and meteorological analysis methods presented in Section 3.2.4.

Table 8: Performance Evaluation Metrics used in short-term test vs. long-term test

Method	Short-Term Test	Long-Term Test
Time-series plots	X	X
Linear Regression	X	X
Root Mean Squared Error (RMSE)	X	X
Spearman Rank Correlation	X	X
Mann-Whitney U-test	X	X
Bland-Altman Plots	X	X
Confusion Matrix	X	X
Percent Ratio		X
Relative Percent Error (RPE)		X
Coefficient of Variation (CV)		X
Environmental Analysis		X
Meteorological Analysis		X

Time-series concentration plots were visually inspected to qualitatively assess the temporal changes in ERM readings relative to the reference instrument over the duration of monitoring, examining how closely the ERM readings followed the reference instrument. Linear regression analysis was employed to determine the degree to which ERM measurements could be predicted from those of the reference instrument, with the coefficient of determination (R^2) indicating the proportion of variance in ERM readings explained by the reference data. The RMSE was calculated to quantify the mean difference between ERM and reference measurements, as shown in Equation Equation (1):

$$RMSE = \sqrt{\sum_{i=1}^{n} \frac{\left(C_{ERM} - C_{ref}\right)^2}{n}} \qquad \text{Equation (1)}$$

where n denotes the number of paired measurements between each ERM unit and the reference instrument, and C_{ERM} and C_{ref} represent the radon concentrations reported by the

ERM and the reference device, respectively, at each measurement interval (e.g., hourly, 12- or 24-hour concentrations).

Given that the measurement data did not conform to a normal distribution, non-parametric methods were utilized. Spearman rank correlation was used to assess monotonic relationships between device readings, and Mann-Whitney U-tests were applied to compare the distributions of ERM and reference measurements.

To investigate systematic bias and the degree of agreement across the full range of observed radon concentrations, Bland-Altman analysis was conducted. The mean difference (bias) and the upper and lower limits of agreement (LoA) were determined using Equations (2 - 4):

$$Bias = \frac{\sum(C_{ERM} - C_{ref})}{n} \quad \text{Equation (2)}$$

$$Upper\ LoA = Bias + 1.96 \times \sigma \quad \text{Equation (3)}$$

$$Lower\ LoA = Bias - 1.96 \times \sigma \quad \text{Equation (4)}$$

where σ represents the standard deviation of the differences between ERM and reference measurements.

Confusion matrices, following the methodology of Rey et al. (2024), were constructed to evaluate the classification performance of ERMs in identifying radon concentrations above or below established guideline thresholds [20]. Specifically, a threshold of 200 Bq/m^3 (the Canadian guideline) was used for the short-term test, while a lower threshold of 100 Bq/m^3 (the World Health Organization (WHO) guideline) was applied in the long-term test, selected based on the range of concentrations observed. A sensitivity analysis was also performed to explore the effects of changing the threshold parameter. From these matrices, key performance indicators such as accuracy, precision, recall, and F1 score were calculated as follows (Equations 5 – 8):

$$Accuracy = \frac{TP + TN}{TP + FP + FN + TN} \quad \text{Equation (5)}$$

$$Precision = \frac{TP}{TP + FP} \quad \text{Equation (6)}$$

$$Recall = \frac{TP}{TP + FN} \quad \text{Equation (7)}$$

$$F1\ Score = \frac{2 \times Precision \times Recall}{Precision + Recall} \quad \text{Equation (8)}$$

where TP, TN, FP, and FN denote true positives, true negatives, false positives, and false negatives, respectively. True positives represent the number of measurements that were correctly identified as above the threshold, with true negatives representing when the measurements were below the threshold. False positives and negatives represent the number of measurements that were incorrectly categorized either above or below the threshold.

For the long-term collocation test, additional metrics were introduced to provide a more detailed characterization of device performance and intra-device variability. The percent ratio, defined as follows (Equation 9), compared the radon concentrations measured by the ERM to those of the reference instrument at matching sampling frequencies:

$$Ratio\ (\%) = \frac{C_{ERM}}{C_{ref}} \times 100\% \quad \text{Equation (9)}$$

In addition, the relative percent error (RPE), commonly reported in radon monitor validation studies and outlined by Public Health England [124], [176], was calculated by Equation (10):

$$Relative\ percent\ error\ (\%) = \frac{\overline{C_{ERM}} - \overline{C_{ref}}}{\overline{C_{ref}}} \times 100\% \quad \text{Equation (10)}$$

where $\overline{C_{ERM}}$ and $\overline{C_{ref}}$ refer to the mean radon concentrations recorded by the ERM and the reference instrument, respectively.

To evaluate intra-sensor variability across individual ERM units of the same device type, the coefficient of variation (CV) was computed using Equation (11).

$$CV = \frac{\sigma_{type}}{\mu_{type}} \times 100\% \quad \text{Equation (11)}$$

where σ_{type} denotes the standard deviation and μ_{type} denotes the mean of the measurements from the three units of each ERM type. According to US EPA guidelines, the acceptable CV for ERMs are up to 10% and has been used in previous studies [122], [177], [178].

3.2.4 Environmental and Meteorological Analysis

A variety of indoor environmental and meteorological variables were monitored to investigate their potential influence on ERM performance and the temporal variability of radon concentrations recorded by the reference instrument during the long-term test. Hourly measurements of atmospheric pressure, temperature, and relative humidity were logged using the reference instrument. Concurrently, hourly outdoor temperature, humidity, and precipitation data were obtained from the historical records of Environment and Natural Resources Canada, utilizing data from the Waterloo International Airport, located approximately 20 km from the test site [179]. Particulate matter ≤2.5 μm in diameter ($PM_{2.5}$) and carbon dioxide (CO_2) concentrations were monitored by two air quality monitors (Air Master AM7, Weesky Instruments), installed in both the basement and the first-floor living room. Although several ERMs included in the study are capable of monitoring additional environmental parameters such as CO_2, $PM_{2.5}$, PM_{10}, VOCs, temperature, and relative humidity, the performance of these supplementary measurements was not evaluated in this work.

To investigate the relationship between ventilation and indoor radon concentrations, periods of continuous decline in CO_2 concentrations longer than four hours in duration were identified throughout the monitoring period. These intervals, presumed to occur when the house was unoccupied, were used to estimate the building's air change rate following the methodology described by Du et al. (2024) [180]. The effects of these estimated air change rates, along with other measured indoor and outdoor environmental parameters, on radon concentrations recorded by the reference monitor were subsequently analyzed using Spearman rank correlation tests.

3.3 Multi-Family Buildings

As described in Chapters 1 and 2, the indoor radon exposure in multi-family high-rise residential buildings remains understudied, despite their growing prevalence in urban environments. To address this gap, the prevalence and distribution of radon concentrations, as well as the building and environmental characteristics, were measured. The research was conducted in two phases: preliminary screening and a subsequent field deployment for long-term data collection in the selected building. The preliminary screening involved visiting multiple high-rise residential buildings across Waterloo and Kitchener, ON and measuring radon concentrations in the lobbies and identifying the ones with concentrations above the ambient background levels.

Following the screening, a 12-storey student dormitory residence at the University of Waterloo was selected for in-depth study. Sensors were deployed on both occupied and unoccupied floors, with student participants recruited from residential floors and additional instrumentation placed in communal lounges on unoccupied levels. Each monitoring location was equipped with three types of sensors: a low-cost ERM, an air quality sensor, and a passive alpha-track detector. This multi-instrument approach enabled both continuous and integrated measurements of radon, as well as the assessment of other indoor air quality parameters. The field deployment spanned three months during the Canadian heating season as recommended by Health Canada [173]. Statistical analyses were conducted to examine differences in radon concentrations across floors, while indoor environmental parameters, such as air exchange rates, were measured and analyzed. The relationship between meteorological data, such as outdoor temperature and relative humidity, and indoor radon concentrations was also explored to better understand the factors driving radon variability in high-rise multi-family environments. All analysis was conducted in Python version 3.12.7.

3.3.1 Preliminary Screening

A total of 61 high-rise residential buildings within the Waterloo and Kitchener areas were tested during the preliminary screening phase. Buildings were selected based on their residential status and location within the Forward Sortation Areas (FSAs) of Waterloo and

Kitchener. High-rise buildings were defined according to the Ontario Building Code (OBC) as those having seven or more storeys or where the floor level of the highest storey of the major occupancy exceeds 18 meters above grade [181]

Testing was conducted between October 16th, 2024, and November 1st, 2024. Measurements were taken in the lobby area on the first floor of each building, with each test lasting between 30 minutes to one hour, depending on initial readings. The AlphaGuard PQ2000 was used for all measurements, recording radon concentrations every 10 minutes. The duration of each test was sufficient to obtain an initial estimate of radon levels in the building. Following the completion of testing across all buildings, one building was selected for further study based on accessibility and having radon concentrations above typical background levels.

3.3.2 Sensor Selection and Calibration

For the second phase of the study, which involved detailed field measurements in a selected high-rise building, the RadonEye (Ecosense) ERM was chosen as the primary radon sensor. This selection was based on the results of the short-term collocation test described in Section 3.2 and results from the literature, where RadonEye demonstrated strong accuracy and precision compared to other consumer-grade ERMs evaluated [19], [124], [175].

To further ensure the consistency and reliability of the field measurements, a calibration test was conducted with all 12 RadonEye sensors intended for deployment, corresponding to the number of floors in the selected building. During calibration, all units were placed on a flat surface at least 60 cm above ground level in an unfinished basement mechanical room. A fan was used to promote air mixing and ensure uniform radon distribution throughout the calibration area. The set-up is illustrated in Figure 10. The average radon concentration across all sensors during calibration was 25 Bq/m^3.



Figure 10: Experimental set-up for collocation test for calibration factors of RadonEyes.

To account for intra-sensor variability, a calibration factor (CF) was calculated for each RadonEye unit using Equation (12):

$$CF_i = \frac{\overline{C_i}}{\overline{C_{all}}} \qquad \text{Equation (12)}$$

where CF_i represents the calibration factor for sensor i, $\overline{C_i}$ and $\overline{C_{all}}$ represent the average radon concentration measured by the sensor i and by all sensors during calibration, respectively. This calibration factor was then used to adjust subsequent field measurements from each sensor to minimize measurement differences caused by sensor discrepancies.

3.3.3 Long-term Field Measurement

The study site for multi-family building field measurements was Claudette Millar Hall (CMH), a student dormitory residence located on the University of Waterloo campus. Constructed in 2017, CMH is a 12-storey building featuring a mix of single- and double-occupant rooms, with all washrooms located in shared spaces separate from the dormitory rooms. The first floor

houses various amenities, including a cafeteria, meeting rooms, and study spaces, while floors 2 through 12 each contain a communal lounge. The basement is reserved exclusively for mechanical equipment and storage and is not accessible to residents.

Sensor Deployment

With the support of the University of Waterloo Campus Housing, a recruitment campaign was launched in January 2025 to engage student participants for in-unit sensor placement. Recruitment efforts included targeted email communications and posters distributed throughout CMH with a 20 CAD incentive upon completion of the test to encourage participation. The goal was to install all sensors by mid-February to capture data during the Canadian heating season, when indoor radon concentrations are typically highest.

Sensor installation was completed by February 19th, 2025, and all devices were retrieved on May 21st, 2025, resulting in a minimum data collection period of 91 days for each deployment. Due to occupancy patterns during the winter semester, only floors 2, 3, 10, 11, and 12 were available for in-unit sensor placement with student participants. On the unoccupied floors, sensors were installed in the lounges (floors 4 – 9) and a meeting room on the first floor.

At each deployment location, three types of sensors were used: a RadonEye (Ecosense) electronic radon monitor, an Air Master AMP7 (Weesky Instruments) air quality sensor for CO_2 measurements, and a Radtrak3 (Radonova) alpha-track detector. Sensors were positioned according to best practices, always at least one meter away from exterior walls, windows, doors, vents, and other openings to minimize the influence of drafts and ensure representative sampling. The typical sensor arrangement and deployment locations are illustrated in Figure 11 below.



(a) (b)

(c) (d)

Figure 11: (a) Sensors deployed in each unit, (b) typical dorm room, (c) typical dorm room with sensor placement, (d) typical lounge with sensor placement.

During the retrieval phase, some data loss and equipment issues were encountered. One alpha-track detector was misplaced and could not be included in the final analysis. On floor 4, the Air Master sensor failed to record CO_2 measurements, while on floor 5, the same sensor was found unplugged on April 18th, resulting in limited CO_2 data for that floor. Additionally, on floor 12, all sensors were unplugged on April 18th, terminating data collection for the remainder of the study period on that floor.

3.3.4 Differences in Concentrations

To characterize spatial and temporal variation in radon concentrations across the monitored floors, a combination of statistical analyses was conducted. For each floor, calibration factors calculated in Section 3.3.2 were applied to raw radon data to ensure comparability across devices before further analyses. An analysis of variance (ANOVA) test was conducted to compare the means of the radon concentrations on each floor and evaluate if there were statistically significant differences between the floors. Time series plots were generated to visualize real-time fluctuations in radon levels and identify any unusual events over the monitoring period. When considerable spikes (i.e., elevated concentrations from the background level) were observed in the time series, focused analyses of environmental and operational factors were conducted immediately before, during, and after these peaks to identify the potential causes.

3.3.5 Environmental and Meteorological Analysis

Meteorological variables relevant to indoor radon dynamics and air exchange rates were analyzed, as described in Section 3.2.4. Hourly outdoor temperature, relative humidity, precipitation, and atmospheric pressure data were obtained from the Waterloo International Airport weather station. To evaluate the potential influence of meteorological conditions on indoor radon concentrations, Spearman rank correlation analyses were performed between each environmental variable and the radon measurements recorded by the respective RadonEye sensor on each floor. The relationship between estimated air exchange rates and indoor radon concentrations was assessed via both Spearman rank correlation and linear regression analyses.

Chapter 4 – Results

This chapter presents the results of three distinct research projects, each directly addressing one of the thesis objectives introduced in Chapter 1. Discussion and interpretation of these findings, limitations, and comparison with existing literature will be provided in Chapter 5.

4.1 Predictive Modelling Results

This section presents results to address the first objective of this thesis: evaluating the predictive accuracy of statistical and machine learning models for estimating residential radon concentrations in Canadian homes. Results from the statistical exploration of the British Columbia Radon Data Repository (BCRDR), including descriptive summaries and distributions of radon concentrations across building types, years of construction, heating types, and seasons, are first presented. These analyses highlight observed patterns and differences between multi-family and single-family residences. Next, the results of RF regression models are presented. The results from both the Health Canada (HC) and BCRDR models were evaluated for their national-scale predictive performance and provincial-scale performance, respectively. Finally, the cross-dataset validation results by applying the BCRDR RF model to the HC dataset are presented, examining the generalizability and transferability of RF models between regional and national datasets.

4.1.1 Factors Influencing Radon from the BCRDR Dataset

Statistical analyses conducted on the BCRDR dataset revealed significant variability in residential radon concentrations, with geometric means and distributions differing notably by building-specific characteristics and season. All results presented in this section pertain to the BCRDR dataset, as the HC dataset has already been studied in the literature by Chen (2021) [35]. The sample size, geometric mean (GM), geometric standard deviation (GSD), and arithmetic mean (AM) are reported. Direct comparisons of our work and the study by Chen (2021) are also made to evaluate the similarities and differences between regional and national datasets.

Radon Distribution by Building Type

Table 9 presents the radon distribution by residential building type, revealing differences across building categories across the 11,313 residential measurements.

Table 9: Radon distribution by residential building type

House Type	N	GM (Bq/m^3)	GSD	AM (Bq/m^3)
Apartment Block with 5 or more storeys	11	77	5.1	212
Apartment Block with less than 5 storeys	34	40	2.8	67
Apartment/Condo (unspecified stories)	609	40	4.7	102
Semi-Detached (Duplex)	300	94	3.3	230
Semi-Detached or Attached (unspecified)	19	35	2.2	78
Semi-Detached or Row House	364	32	3.7	50
Single Detached (Bungalow)	2421	58	3.1	115
Single Detached (Multi-Storey)	1720	114	3.5	152
Single Detached (Split Level)	324	43	3.0	95
Single Detached (unspecified)	5381	109	3.6	192
Trailer / Mobile Home	130	50	2.7	115

**N = number of buildings, GM = geometric mean (Bq/m^3), GSD = geometric standard deviation, AM = arithmetic mean (Bq/m^3).*

When examining the overarching building categories, distinct concentration ranges emerge. Apartment buildings demonstrated the most constrained radon concentration range, with geometric means ranging from 40 – 77 Bq/m^3 (n = 654). Notably, apartment blocks with ≥ 5 storeys exhibited the highest geometric mean within this category at 77 Bq/m^3 (n = 11). This elevated concentration in high-rise buildings contrasts with the lower concentrations observed in apartment blocks with ≤ 5 storeys (40 Bq/m^3) and unspecified apartments (40 Bq/m^3). Semi-detached housing showed geometric means of 32–94 Bq/m^3 (n = 683), with duplexes exhibiting the highest values (94 Bq/m^3) and row houses the lowest (32 Bq/m^3). Single-detached homes displayed the widest range, with geometric means spanning 43–114 Bq/m^3 (n = 9,846), where multi-storey configurations recorded the highest concentrations (114 Bq/m^3). However, it is important to note that the sample size for apartment buildings with ≥ 5 storeys was limited to only 11 cases, potentially limiting the representativeness of this building type in the broader British Columbia context.

A comparison with the HC dataset, as reported by Chen (2021), further contextualizes these findings [165]. In the HC dataset, the GM for single-family homes across Canada ranged from

20 to 62 Bq/m^3, with the highest GM found in bungalows and the lowest in trailer or mobile homes. Interestingly, this pattern differs slightly from the results of the present study, in which multi-storey single-detached homes recorded the highest GM among single-family dwellings. Furthermore, while the overall GM reported for British Columbia in the HC dataset was 33 Bq/m^3, the GM across all building types reported in this study is prominently higher, at 55 Bq/m^3. It should be noted that the mean reported by Health Canada represented a population-weighted radon concentration, which may partially account for these differences. Another distinction is that the HC dataset did not include multi-family building types, rendering direct comparison of radon concentrations in these categories within a Canadian context unfeasible.

Comparing these results to international data, such as that from South Korea, reveals that the distribution of radon concentrations from single-family and multi-family homes is aligned with the findings from the BCRDR dataset. A national assessment there reported a GM of 36 Bq/m^3 for multi-family dwellings, closely matching the concentrations found in apartment blocks with fewer than five storeys and unspecified apartments in this study [117]. In both the present study and the South Korean study, single-family homes exhibited higher GMs (80 Bq/m^3 in South Korea) than their multi-family counterparts. These comparisons highlight the consistent observation that single-family residences typically have higher indoor radon concentrations than multi-family buildings, both in Canada and internationally.

To further explore the relationship between residential building types and the log-transformed radon concentrations, linear regression and Spearman rank correlations were conducted to evaluate the correlation between radon concentrations in multi-family versus single-family dwellings. The analysis focused on floor-specific comparisons, as summarized in Table 10, with measurements categorized by floors tested. Single-family homes included single-detached and semi-detached dwellings, while trailers and mobile homes were excluded due to their distinct construction characteristics, being typically raised off the ground, making floor-tested comparisons inappropriate. To eliminate geographical confounding variables, multi-family and single-family homes were matched by Forward Sortation Areas (FSAs).

Table 10: Summary of statistics for multi-family buildings vs. single-family buildings

Floor Tested		Multi-Family	Single-Family	Linear Regression			Spearman Correlations
	N*	GM (Bq/m^3)	GM (Bq/m^3)	Slope	Intercept	R^2	ρ^+
Main floor or higher	80	20	28	0.70	0.62	0.54	0.70
At or below grade	37	65	66	1.01	-0.69	0.72	0.83
All apartments	103	23	33	0.87	0.04	0.61	0.73

**N = number of paired matches of multi-family homes and single-family homes with the same FSAs. Total number of data points included = 11,183, with 220 paired FSAs.*
+The p-values are smaller than 0.05 for all tests.

Single-family homes consistently exhibited higher radon concentrations across all floor categories tested. However, the magnitude of the difference varied substantially by floor level. For measurements at or below grade, the difference was minimal (65 vs. 66 Bq/m^3), differing by only 1 Bq/m^3. In contrast, main floor or higher measurements showed a more pronounced difference (20 vs. 28 Bq/m^3), representing a 40% increase in single-family homes compared to multi-family buildings. The linear regression analysis revealed moderate to strong correlations between multi-family and single-family radon concentrations, with Spearman correlation coefficients (ρ) from 0.70 – 0.83 ($p < 0.05$). For all apartments, 61% of the variance in multi-family radon concentrations can be explained by corresponding single-family concentrations within matched FSAs. The strongest relationship was observed for at or below grade measurements ($R^2 = 0.72$, $\rho = 0.83$), suggesting that basement-level radon concentrations in both building types respond similarly to underlying geological and soil conditions.

These findings align closely with those reported from Finland's national radon survey, which conducted similar analyses on single-family and multi-family buildings. The study found a slope of 1.04 for ground-contact apartments and 0.60 for apartments without direct ground contact when compared to single-family homes, suggesting highly comparable radon exposure for ground-contact floors and lower exposures for upper-level apartments [182]. Notably, the BCRDR dataset produced comparable slopes of 1.01 for or below grade (ground-contact) floors and 0.70 for main floor or higher, consistent with this observation. The slope for ground-contact floors in both datasets suggests that, in the absence of other mitigating factors, radon concentrations on these floors in apartments and single-family homes are nearly equivalent.

The strength of these relationships provides confidence that linear regression models can be used to estimate mean multi-family building concentrations at a national scale. Although it is important to note that this relationship should not be used to predict concentrations in individual buildings due to the various factors discussed earlier, as linear regression models are limited by their lack of capability to account for multicollinearity.

Accordingly, these three established linear regression models were then applied to predict multi-family radon concentrations at a national scale using existing single-family data (n = 13,785) from the HC dataset. Figure 12 presents a comparative box plot analysis of radon concentrations across Canadian provinces and territories, contrasting actual single-family measurements with predicted multi-family concentrations based on floor-tested categories.

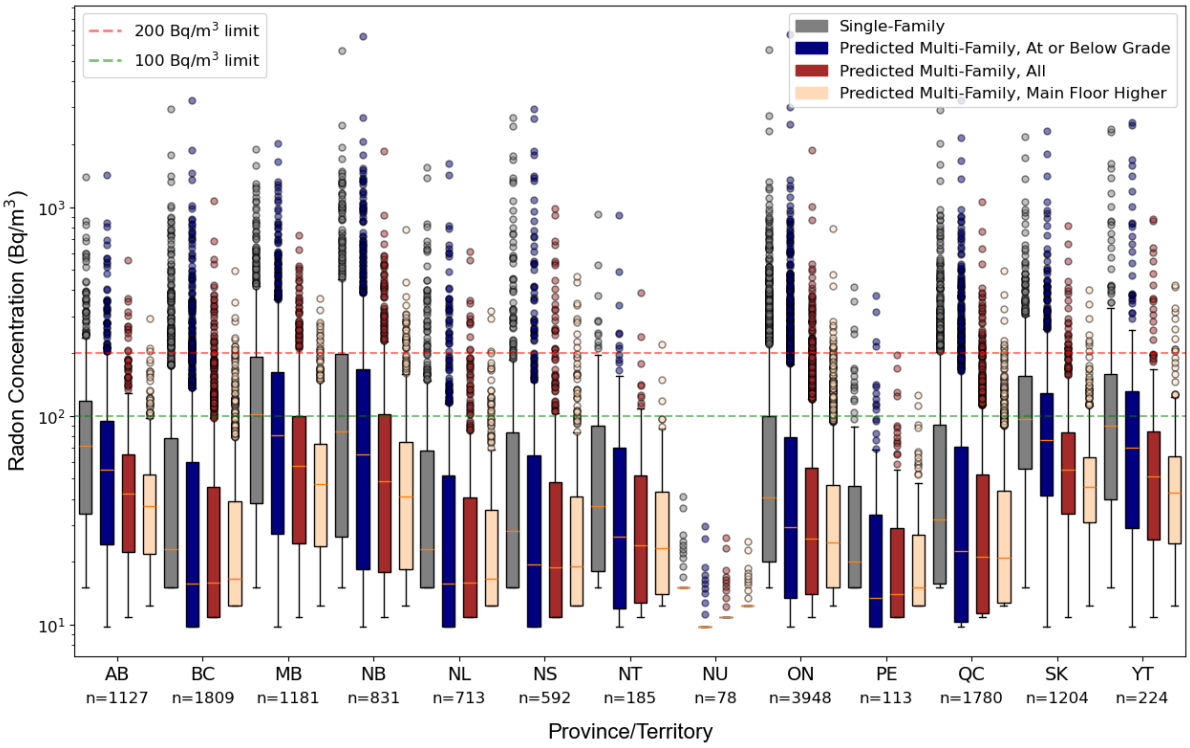


Figure 12: Radon concentrations in Canada for single-family vs. predicted concentrations for multi-family buildings by province or territory. In each box plot, the orange line represents the median concentration, while the bottom and top halves of the box indicate the second and third quartiles, representing the interquartile range. The whiskers extend to the most extreme data points within 1.5 times the interquartile range. Outliers are shown as individual points.

Although the median radon concentrations for all building types remain below the Canadian guideline, in certain regions, homes at the 75th percentile exceed the 100 Bq/m^3 threshold. The presence of extended interquartile ranges and long upper whiskers in the boxplots indicates a positively skewed distribution in several provinces, suggesting that a subset of homes with elevated radon levels is driving these patterns. Manitoba, New Brunswick, Saskatchewan, and the Yukon consistently display the highest radon concentrations across both single-family dwellings and all predicted multi-family categories. This pattern suggests that, in these provinces and territories, a meaningful proportion of both single-family and ground-contact multi-family homes may be at risk of exceeding recommended radon thresholds. While multi-family units situated on upper floors generally exhibit a lower risk exposure, the predicted concentrations for ground-contact units closely mirror those observed in single-family homes.

Radon Distribution by Age, Heating Type, and Season

The relationship between building age and radon concentration reveals an increase in radon concentration with respect to construction year, as summarized in Table 11 and illustrated in Figure 13. The analysis of 8,959 residential homes across different construction periods demonstrates significant variability in radon concentrations based on year of construction. To further analyze the increasing trend of radon concentrations with year of construction, 1981 was selected for construction era classifications following the introduction of energy-efficient design measures [9].

Table 11: Radon distribution by year of construction

Year Built	N	GM (Bq/m^3)	GSD	AM (Bq/m^3)
1920 or before	176	41	3.6	85
1921 to 1945	372	56	3.7	120
1946 to 1960	827	53	3.5	116
1961 to 1970	955	54	3.6	122
1971 to 1980	1893	57	3.5	122
1981 to 1990	1192	48	3.8	116
1991 to 2000	1336	67	3.5	150
2001 to 2010	1321	81	3.6	175
2011 or after	887	71	3.9	166
1981 or Newer (New Homes)	4736	86	3.2	167
1980 or Older (Old Homes)	4223	66	3.7	151

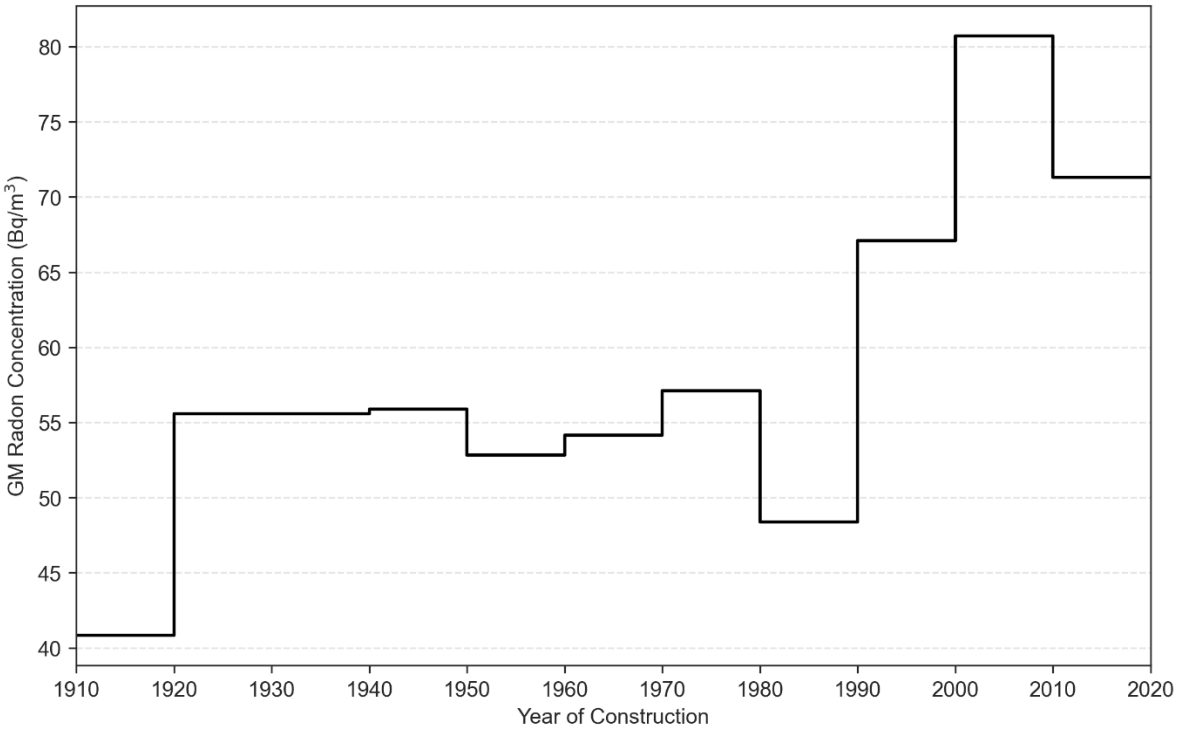


Figure 13: Year of Construction vs. GM Radon Concentration

Homes built in 1920 or before exhibited the lowest geometric mean radon concentration at 41 Bq/m^3. The 1921 – 1980 period shows relatively consistent radon concentrations, with geometric means ranging from 53 – 57 Bq/m^3. This stability suggests that construction practices during this era maintained similar radon entry characteristics, with the peak occurring in the 1971 – 1980 period (57 Bq/m^3). A notable inflection point occurs in the 1981-1990 period, where concentrations decrease to 48 Bq/m^3; however, this trend reverses dramatically in subsequent decades. Homes built between 1991 – 2000 show a significant increase to 67 Bq/m^3, while the 2001 – 2010 period exhibits the highest geometric mean across all construction periods at 81 Bq/m^3. This peak represents a 33 Bq/m^3 increase compared to the 1981 – 1990 period, suggesting that modern construction practices may inadvertently contribute to radon accumulation. Recent construction trends (2011 or after) show a slight decline to 71 Bq/m^3, though concentrations remain elevated compared to earlier construction periods. New homes (1981 or newer, n = 4736) demonstrate statistically significant (Mann-Whitney U-test, $p << 0.001$) higher radon concentrations compared to older homes (1980 or

older), with geometric means of 66 vs. 55 Bq/m^3, respectively, representing a 20% increase in newer construction.

These findings are consistent with national-level patterns reported by Chen (2021), who observed a steady increase in radon concentrations from 25 Bq/m^3 in homes built before 1920 to 57 Bq/m^3 in homes constructed after 2010 [165]. While both datasets reveal a small dip in concentrations around 1980, the most pronounced increase in the present study occurs in the 2000s, rather than immediately following 1981. This pattern aligns with emerging international evidence, as discussed in the literature review, where countries such as Russia [80], Greece [183], and China [164] have also documented rising radon concentrations in newer buildings. Across these studies, the adoption of energy-efficient building designs is frequently cited as a contributing factor, as such measures, while reducing energy loss, may increase airtightness inadvertently promoting radon accumulation within indoor environments.

The distribution of radon concentrations by heating system type reveals notable variations, as presented in Table 12. Analysis of 7,189 homes demonstrates that heating system characteristics may influence radon accumulation patterns. Baseboard, forced air, multiple systems, and radiant water heating all exhibited GM radon concentrations between 29 and 40 Bq/m^3, with baseboard heating yielding the lowest levels. The highest concentrations were observed in homes with "Other" heating systems (GM = 61 Bq/m^3; n = 751), nearly double those found in baseboard-heated homes. The "Other" category includes heating types not identified elsewhere, possibly encompassing wood or pellet stoves, fireplaces, or kerosene heaters, most likely associated with rural residences. However, specific details on these systems were not available in the dataset.

Table 12: Radon distribution by heating type

Heating Type	N	GM (Bq/m^3)	GSD	AM (Bq/m^3)
Baseboard	161	29	3.2	67
Forced air	4756	34	3.5	77
Multiple systems	1228	35	3.2	79
Radiant water	293	40	3.0	79
Other	751	61	3.1	125

Furthermore, these findings are generally consistent with those from the Health Canada dataset analyzed by Chen (2021), which reported geometric means ranging from 34 Bq/m^3 for radiant water heaters to 52 Bq/m^3 for forced air systems, with baseboard heating yielding intermediate values at 42 Bq/m^3 [165]. While the specific ranking of heating systems by radon concentration differs between datasets, the overall range remains comparable. This consistency indicates a modest association between heating system type and indoor radon concentrations.

The seasonal analysis of 42,044 radon measurements from the BCRDR dataset reveals distinct temporal patterns in residential radon concentrations as summarized in Table 13. Heating season measurements (n = 38,542) demonstrated a GM of 49 Bq/m^3, while cooling season measurements (n = 5868) showed elevated concentrations at 61 Bq/m^3.

Table 13: Radon distribution by season

Season	N	GM (Bq/m^3)	GSD	AM (Bq/m^3)
Heating	36431	48	4	108
Cooling	5613	61	3	123

This outcome contrasts with the guidance from Health Canada, which recommends radon testing during the heating season based on elevated indoor radon levels over the cooling season. While the literature generally supports the adjustment of radon measurements to account for temporal variations, there has been a recent study that has challenged the applicability of seasonal correction factors, particularly in regions with pronounced seasonal climates. Stanley et al. (2019) found largely comparable radon concentrations in both heating and cooling seasons for homes situated in the North American prairie region [11]. Their pairwise assessment of radon measurements from the heating and cooling seasons revealed that approximately half of the buildings displayed negligible seasonal differences, while the remaining homes were evenly split between higher winter and higher summer concentrations. The authors suggest potential causes of this diminished difference may stem from the effects of using air conditioning over natural ventilation in summer months, due to increasingly warmer temperatures. This finding resonates with the patterns observed in the present dataset. Collectively, these observations suggest that the long-standing practice of applying seasonal

correction factors may warrant re-evaluation, particularly in regions where emerging empirical data indicate inconsistent seasonal effects.

4.1.2 Random Forest (RF) Regression

RF regression was employed to evaluate the ability of multiple building, environmental, and geographic variables to predict residential radon concentrations. The HC dataset and BCRDR dataset served as the basis for this analysis at the national and provincial levels, respectively. The RF model for the HC dataset (n = 13,642) demonstrated moderate predictive performance, while the BCRDR dataset (n = 23,040) demonstrated a stronger performance in comparison, across a few key evaluation criteria as summarized in Table 14.

Table 14: Random Forest (RF) Model Evaluation Metrics

Model Evaluation Metric	Values	
	HC Model	**BCRDR Model**
Mean Squared Error (MSE)	0.77	0.77
Root Mean Squared Error (RMSE)	0.87	0.88
Mean Absolute Error (MAE)	0.72	0.68
Coefficient of Determination (R^2)	0.27	0.45
Out-of-Bag (OOB) Score	0.28	0.45
Training MSE	0.62	0.68
Testing MSE	0.77	0.77
Cross-Validation MSE	0.77	0.86

Both RF models yielded the same mean squared errors (MSE) of 0.77 and similar root mean squared error (RMSE) of 0.87 (HC model) and 0.88 (BCRDR model), however the BCRDR model showed a better mean absolute error (MAE) of 0.68 on the test set, indicating better precision in individual predictions. Lower values for MSE, RMSE, and MAE generally indicate a better-performing model. MSE quantifies the average of the squared differences between predicted and observed values, providing a measure that penalizes larger errors more heavily. RMSE, the square root of MSE, indicates better predictive accuracy when the values are closer to 0. MAE indicates the average of the absolute differences between predicted and actual values. Both RMSE and MAE are reported in the same units of Bq/m^3 as the predicted variable. The R^2 for the HC model was 0.27 with a similar out-of-bag (OOB) score of 0.28, indicating that just over a

quarter of the variance in log-transformed radon concentrations could be accounted for by the included predictors. The testing MSE (0.77) was the same as the cross-validation MSE, suggesting that the model has stable performance across different data splits. However, the difference between the training (0.62) and testing MSE (0.77) values suggests that the model may be overfitting. In contrast, the RF model applied to the BCRDR dataset demonstrated improved predictive performance compared to the national HC dataset. Most notably, the R^2 increased to 0.45, representing a substantial improvement over the national model and indicating that nearly half of the variance in log-transformed radon concentrations could be explained by the included predictors. An OOB score of 0.45 closely matched the R^2 value, confirming model stability, which the HC dataset also exhibited for its respective model. Similarly to the HC dataset, the training MSE of 0.68 and testing MSE of 0.77 showed some signs of overfitting, though with a smaller performance gap. Analysis of feature group importance provided insight into which variables were most influential in predicting radon concentrations, as displayed in Figure 14. For both the HC and BCRDR datasets, the geographic-related variable, FSA, emerged as the dominant predictor, accounting for 28.7% and 29.5% of the total model importance, respectively, confirming the critical role of spatial location in determining residential radon concentrations. For the HC dataset, among building-related predictors, floor tested, year of construction, basement type, and building type also demonstrated considerable contributions to model accuracy with the increase of OOB error score at 6.9 – 10.1%. Other structural and mechanical variables, such as heating systems, air conditioning, and foundation type, in addition to season effects, further enhanced the predictive performance, contributing a modest increase in OOB error score.

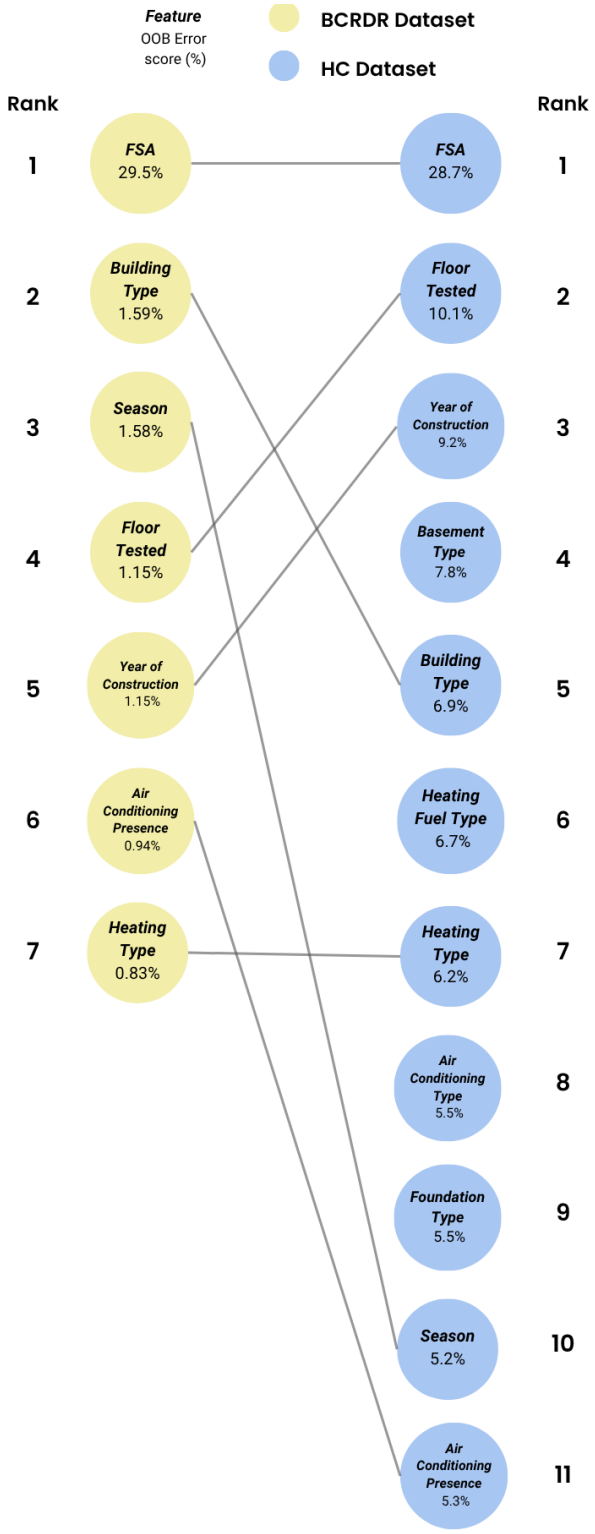


Figure 14: Ranked feature importances by increase in OOB error score for HC and BCRDR models.

Feature importance analysis for the BCRDR dataset revealed some notable differences in the relative contribution of building characteristics, as shown in Figure 14. Building type emerged as the second most important feature group at 1.59% as opposed to floor tested for the HC dataset, followed closely by seasonal factors at 1.58%. Other building characteristics, including floor level, year built, air conditioning, and heating system, each contributed between 0.84% and 1.15% to the model's predictive power. Comparing these models' performance metrics to those in published literature further emphasizes their strength. For instance, one research group's RF models reported an R^2 of only 0.14 and RMSE of 0.83 while using similar multivariate approaches to study factors influencing radon concentrations [184]. Both the HC and BCRDR models in this analysis achieved higher R^2 values (0.27 and 0.45, respectively) with similar or only marginally higher RMSE values, indicating comparatively better explanatory power. Another recent RF study in Switzerland achieved an R^2 of 0.31 and RMSE of 0.74, outperforming the HC model but still behind the BCRDR model in explained variance, though with a somewhat lower RMSE [185]. Importantly, the geographic or spatial variable emerged as the most important factor in both this and other international studies, such as elevation from the Switzerland study, demonstrating the importance of spatial determinants in modelling radon concentrations. Seasonal effects were also important in some models, though their rank varied considerably, possibly due to differences in how seasonality was encoded or local climate factors.

Additionally, a recent study by Wu et al. (2023) found that, for their Swedish RF model, year of construction, uranium content in the soil, and balanced mechanical ventilation were the top predictors, further highlighting the importance of both building age and geological variables in radon risk modelling [186]. Collectively, these findings emphasize the influence of spatial variables while revealing that, even with advanced modelling techniques and comprehensive datasets, a substantial fraction of variance in residential radon concentrations remains unexplained, indicating the necessity for continued research into both building and environmental determinants of indoor radon, as well as the importance of in-situ measurements in the meantime.

4.1.3 Cross-Dataset Model Training

To assess the generalizability and transferability of the RF modelling approach across different geographic scales and data sources, a cross-dataset validation was conducted. The BCRDR-trained RF model was applied to predict radon concentrations in the HC dataset, investigating how well regionally specific models perform when extended to national-scale data. As summarized in Table 15, the cross-dataset application revealed substantial limitations in model transferability, with performance deteriorating markedly compared to the dataset-specific models. The MSE increased to 1.46 compared to an MSE of 0.77 for both HC and BCRDR models, with a corresponding RMSE of 1.21 and MAE of 0.93. Most notably, the R^2 was negative (-0.37), indicating that the BCRDR-trained model performed so poorly when applied to the HC dataset that its predictions were less accurate than simply assigning every home the mean radon concentration for all observations.

Table 15: Model Evaluation Metrics for Cross-Dataset Model Training

Model Evaluation Metric	Value
Mean Squared Error (MSE)	1.46
Root Mean Squared Error (RMSE)	1.21
Mean Absolute Error (MAE)	0.93
Coefficient of Determination (R^2)	-0.37

The weak performance of the model is consistent with findings in the literature regarding cross-regional model transferability. Baumann et al. (2025) explored the transferability of RF models trained on German data to predict geogenic radon potential in Belgium [187]. While their models could provide general predictions for the Belgian context, they encountered noteworthy challenges in optimal transferability, mirroring the results of this cross-dataset model. These findings demonstrated that the relative importance and ranking of predictor variables were highly dependent on the region's unique geographic and environmental context. The optimal model configurations varied substantially between Germany and Belgium, and successful prediction required iterative model tuning using validation data from the target region. Baumann et al. (2025) emphasized that without this additional evaluation, applying a German-trained model to Belgian data resulted in suboptimal performance. For instance, they found that the predictors for Germany were completely different from those required for

accurate prediction in Belgium, despite both models using geogenic input parameters such as soil moisture and lithology. These findings reinforce that while the general transferability of RF models is possible, optimal predictive accuracy remains limited without regional considerations. Differences in the importance and performance of predictors, even when similar variables are available, highlight the nuanced interaction between local factors.

4.2 Collocation Test Results

The collocation test results address the second objective of this study, which is to evaluate the accuracy and suitability of low-cost ERMs for residential testing through comparison with research-grade reference instruments. This evaluation employed two field campaigns to assess device performance under distinct operational conditions. The short-term collocation test evaluated low-cost sensors across multiple residential environments, exposing devices to diverse radon concentration ranges and building characteristics, enabling assessment of device performance variability and identification of optimal sensors for subsequent field deployment for Objective 3. The long-term collocation test followed standard measurement protocols recommended by Health Canada, with devices deployed continuously for three months during the heating season in the lowest occupied level of a residence. This extended evaluation incorporated multiple units of each sensor model to evaluate intra-sensor variability and assess long-term measurement stability. The results are organized to first present findings from the short-term multi-site evaluation, followed by the long-term assessment, providing a representation of low-cost ERM performance across different scenarios.

4.2.1 Short-Term Test

Time series plots were used to examine radon concentrations measured by low-cost ERMs and the research-grade reference instrument, RAD7, at each site. Figure 15 & Figure 16 present the hourly radon concentrations at Site D and Site A, respectively. As shown in the figures, while other sensors generally tracked the concentration trends measured by the RAD7, the Wave consistently exhibited a delayed response when approaching daily maximum and minimum values. At Site D, the Wave device required approximately 10 hours to acclimate to the lower concentration range compared to other sensors, following exposure to high radon

concentrations at the previous site (mean concentration = 1,411 Bq/m^3). A similar delayed response was observed across all monitoring locations, as shown in Figure 16 for Site A (mean = 118 Bq/m^3), demonstrating a consistent lag of readings for the Wave at both high and low concentration ranges.

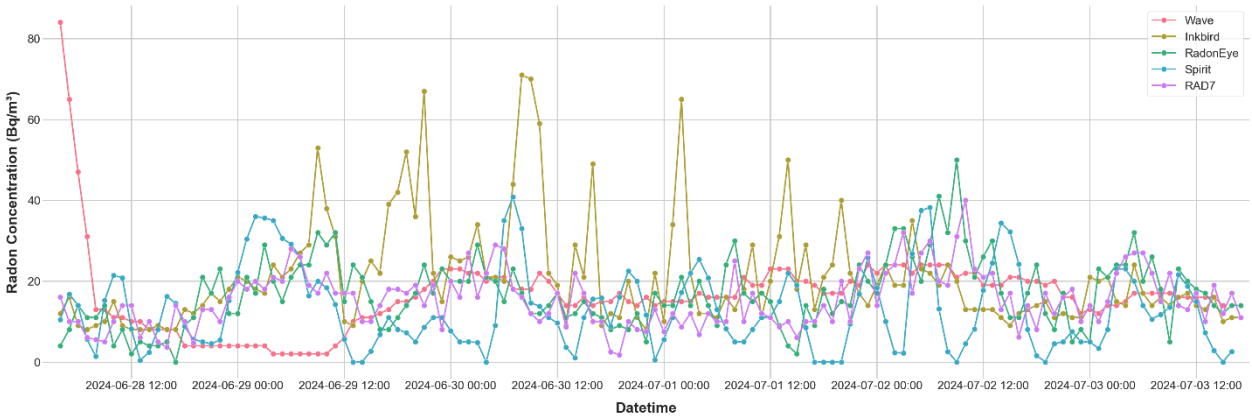


Figure 15: Radon concentration at Site D by all devices from Giang & Li (2025) [188]

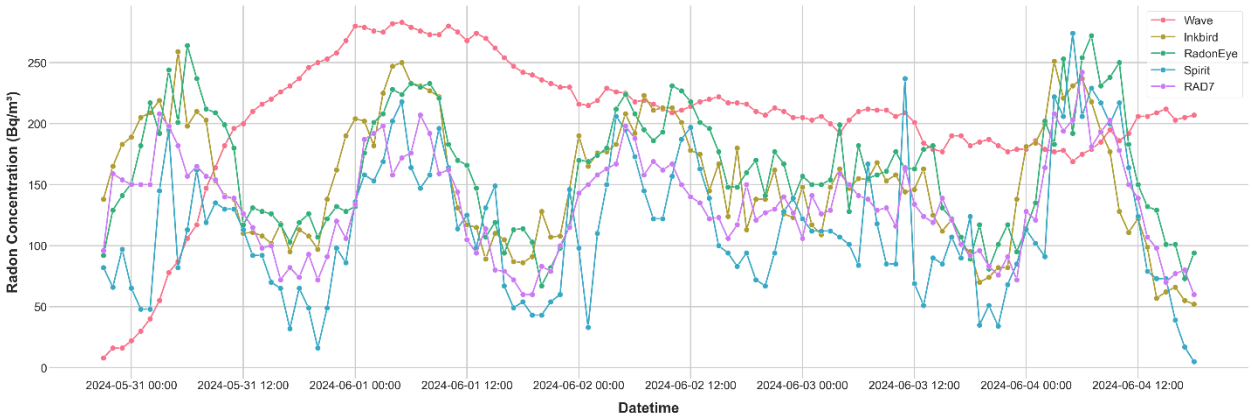
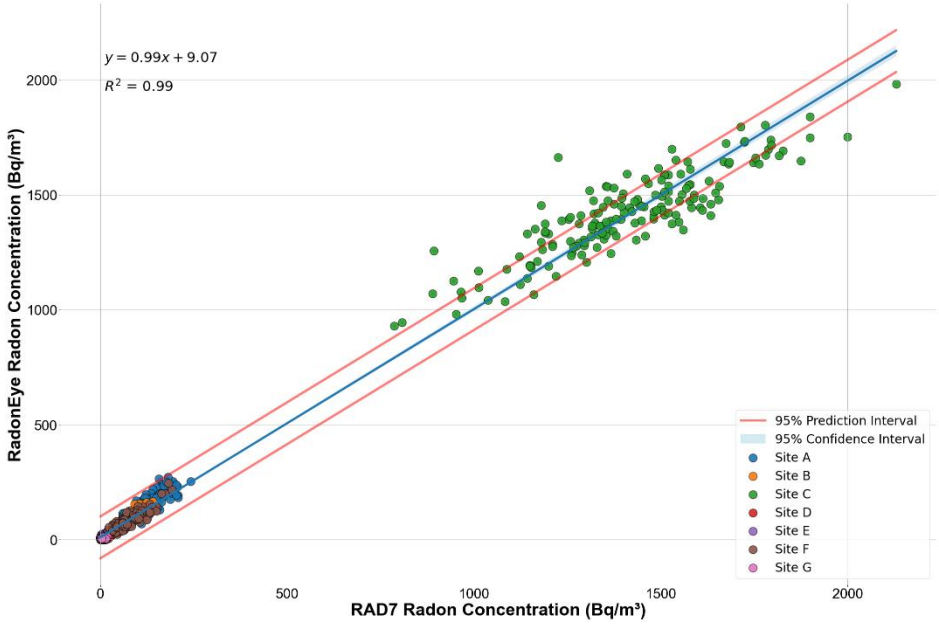


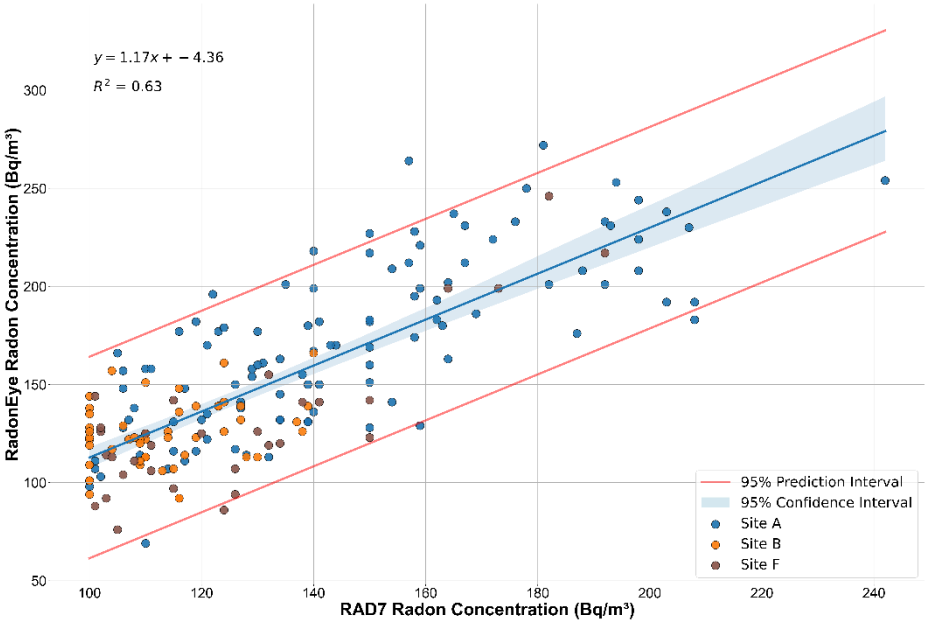
Figure 16: Radon concentration at Site A by all devices

Low-cost ERM performance was assessed using linear regression analysis across all radon concentrations (0–2,000 Bq/m^3) and within three discrete concentration ranges (0–100, 101–300, and >301 Bq/m^3), selected based on exposure levels in our study. Analysis of the complete dataset revealed strong relationships (R^2 = 0.99) and regression coefficients approaching one for all devices, indicating strong agreement with the RAD7 reference instrument. However, concentration-specific analysis demonstrated considerable variability, with R^2 values spanning

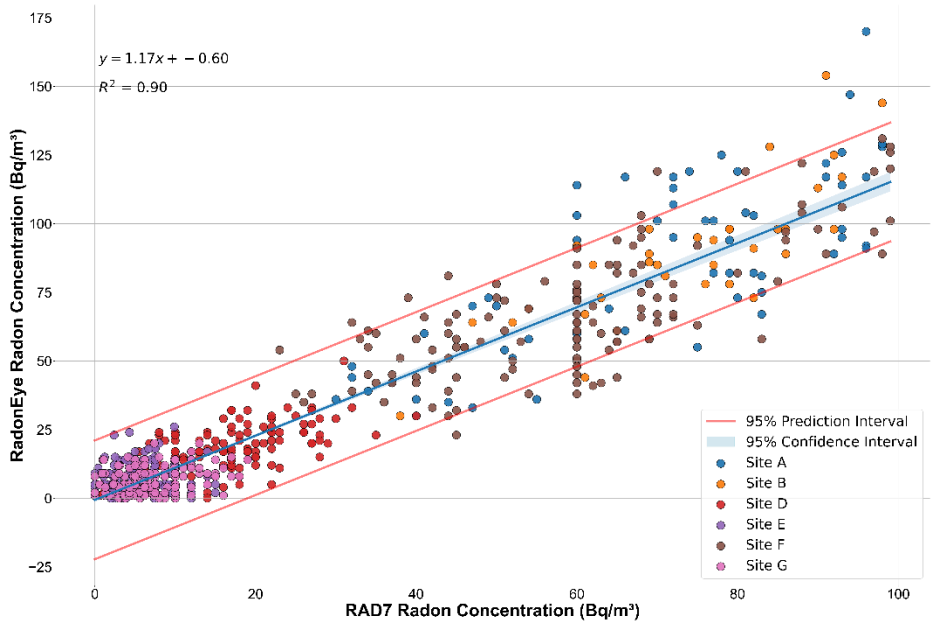
0.01–0.90 and regression coefficients ranging from 0.22–1.66 across the three concentration ranges. Figure 17 illustrates the linear regression relationships between the RadonEye and RAD7 across all measured concentrations and the three concentration ranges.



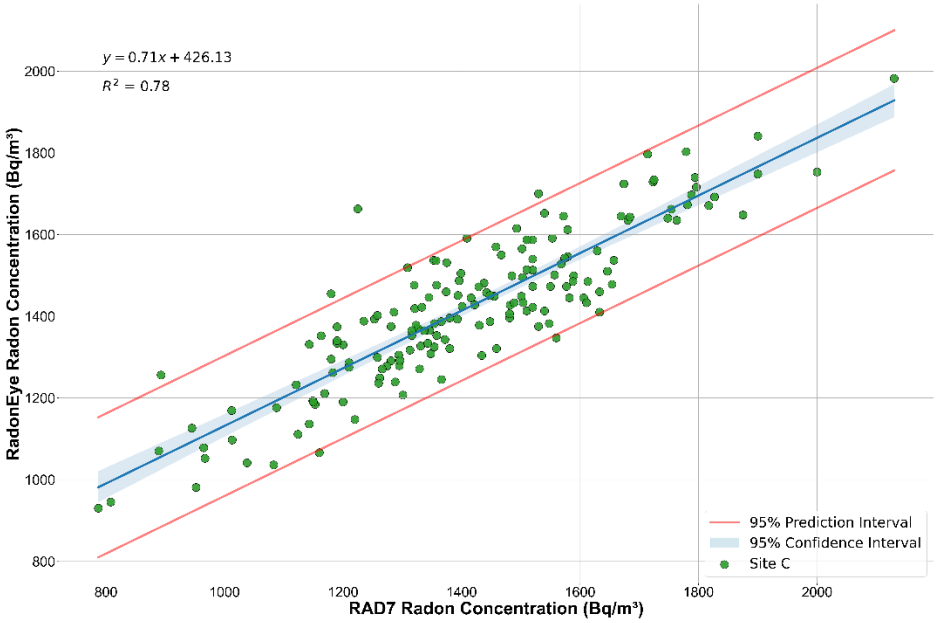
a)



b)



c)



d)

Figure 17: Linear regression of RadonEye vs. RAD7, a) all concentrations (0 – 2,000 Bq/m^3), b) low concentration range (0 – 100 Bq/m^3), c) medium concentration range (101 – 300 Bq/m^3), d) high concentration range (> 301 Bq/m^3) from Giang & Li (2025) [188].

Results from linear regression, Spearman rank correlations, and RMSE values for all the ERMs are summarized in Table 16. Better agreement between the tested devices and the reference instrument was observed at lower concentration levels, with distinct performance variations evident across concentration ranges and device types.

Table 16: Linear Regression, Spearman Rank Correlations (ρ), and RMSE Summary of all low-cost ERMs from Giang & Li (2025)

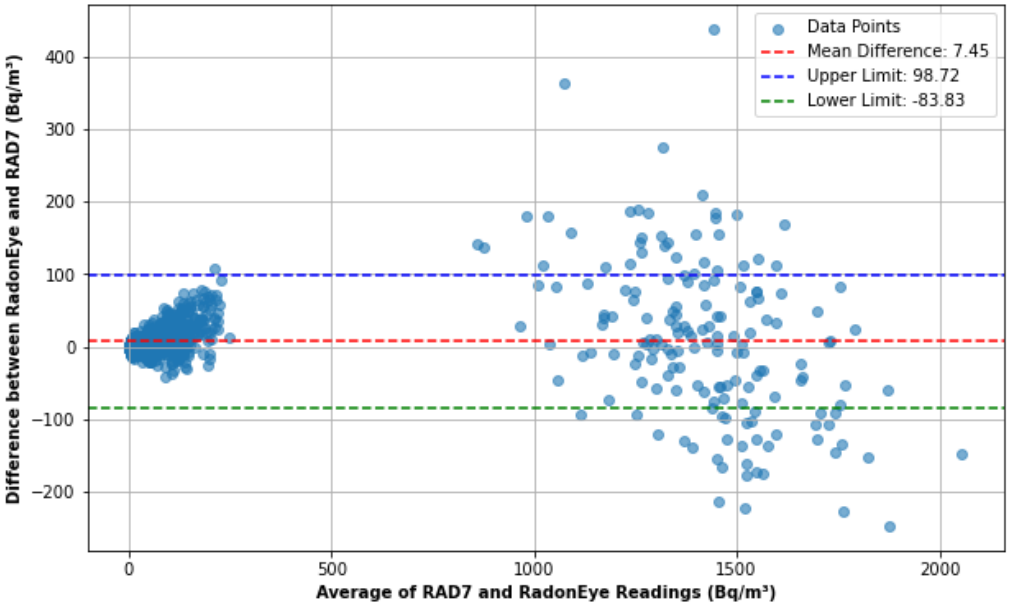
ERMs	**RadonEye**			**Inkbird**			**Spirit**			**Wave**		
Range[+]	*low*	*med*	*high*	*low*	*med*	*high*	*low*	*med*	*high*	*low*	*med*	*high*
Slope	1.17	1.17	0.71	0.88	1.16	0.5	0.91	0.82	0.49	1.66	0.22	0.88
Intercept	-0.6	-4.36	426	3.88	-13.0	723	-0.15	10.8	474	11.8	152	1022
R^2	0.9	0.63	0.78	0.79	0.56	0.41	0.67	0.27	0.23	0.33	0.01	0.05
ρ^*	0.85	0.75	0.85	0.85	0.70	0.59	0.77	0.37	0.47	0.74	0.19	0.28
RMSE	13.0	33.1	111	13.3	32.6	182	19.0	42.2	342	76.6	72.1	341

+low: 0 – 100, medium: 101 – 300, high: > 301 Bq/m^3
**Spearman rank correlations, the p-values are smaller than 0.05 for all tests*

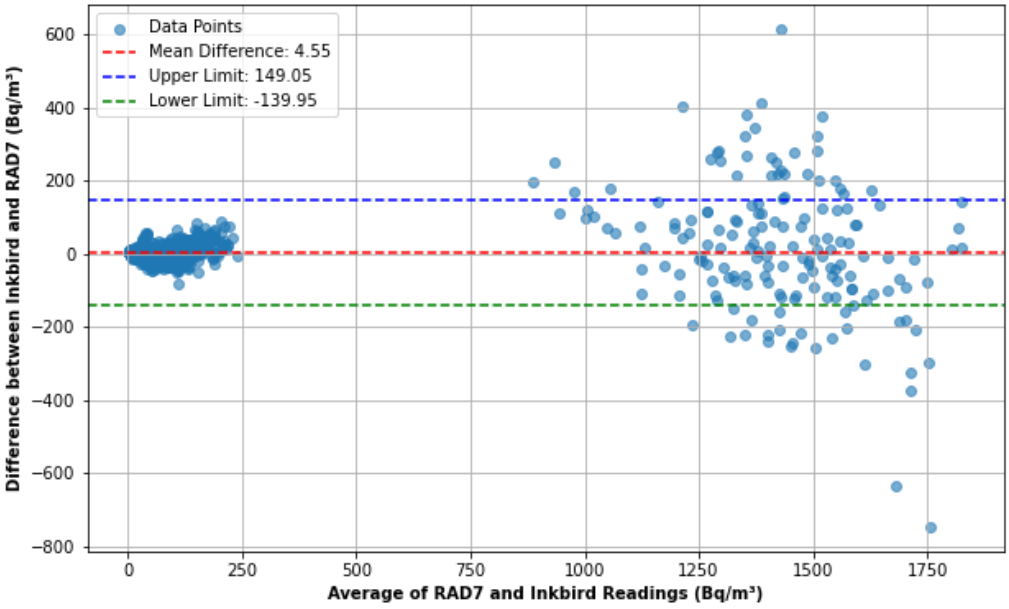
The RadonEye achieved the most consistent performance with RMSE values below 111 Bq/m^3 across all ranges and an aggregate RMSE of 47.2 Bq/m^3. The Inkbird and Spirit devices showed moderate performance characteristics, with the Spirit experiencing a substantial RMSE increase at elevated concentrations. The Wave device displayed considerable measurement variability, recording an overall RMSE of 152 Bq/m^3 and an RMSE of 341 Bq/m^3 in the highest concentration band. Spearman rank correlation analysis supported these findings, with the RadonEye maintaining strong correlations ($\rho = 0.85$, $p < 0.05$) across both low and high concentration ranges. Both Wave and Spirit devices exhibited declining correlation strength from low ($\rho = 0.74–0.77$, $p < 0.05$) to medium and high concentration ranges ($\rho = 0.19–0.47$, $p < 0.05$). Mann-Whitney U-tests show there was no statistically significant difference between the RadonEye and Inkbird with measurements from the reference instrument (RAD7) across most ranges, while revealing significant differences for the Wave in medium concentrations ($p < 0.001$) and the Spirit at high concentrations ($p < 0.001$).

Bland-Altman analysis (Figure 18) quantified measurement agreement between ERMs and the reference instrument. The mean difference represents the average bias of the ERMs. The upper and lower limits of agreement (LoA) indicate the spread of the differences for 95% of

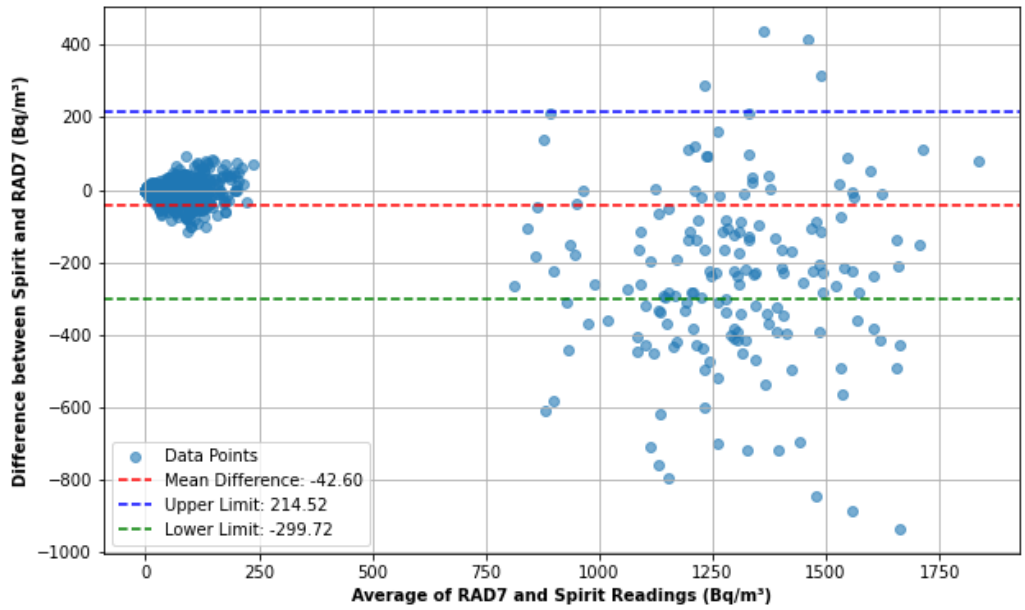
observations. For a reliable and unbiased sensor, the mean difference should be close to zero, and the LoA should be narrow, reflecting minimal and consistent deviation from the reference.



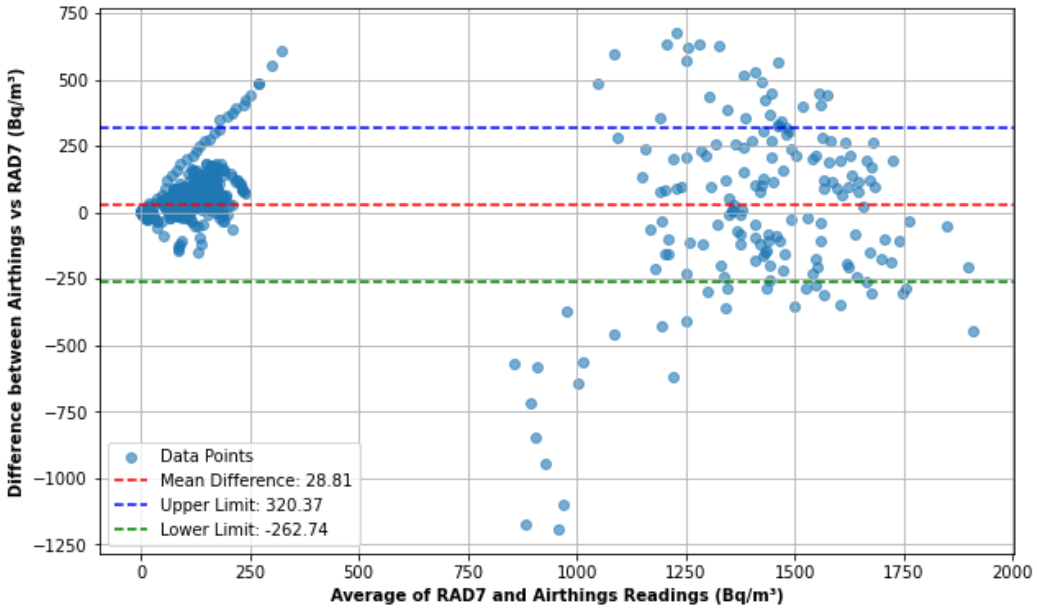
a)



b)



c)



d)

Figure 18: Bland-Altman plots across all concentration ranges per low-cost ERM vs. RAD7, a) RadonEye, b) Inkbird, c) Spirit, and d) Wave from Giang & Li (2025) [188]

The results show that for all sensors, clustering of measurements occurs at lower concentrations, with increasing dispersion at elevated levels, indicating concentration-dependent performance degradation. This suggests that while many ERMs are reasonably

reliable for detecting and quantifying low to moderate radon levels, their measurements can diverge substantially from true values at higher concentrations (> 300 Bq/m^3). Absolute mean differences ranged from 4.55 to 42.6 Bq/m^3, with RadonEye, Wave, and Inkbird devices overestimating concentrations, while the Spirit device underestimated readings. The RadonEye and Inkbird demonstrated narrower agreement limits, with RadonEye showing higher precision. In contrast, the Spirit device showed broader agreement limits and the largest mean difference, indicating lower precision and accuracy. The Wave device showed substantial scattering in measurements, particularly at high concentrations, with the widest agreement limits (-263 to 320 Bq/m^3), and a mean overestimation of 28.8 Bq/m^3.

Classification performance was evaluated using confusion matrix analysis at a threshold of 200 Bq/m^3 in line with the Health Canada guideline, examining accuracy, precision, recall, and F1 scores as summarized in Table 17. The confusion matrix metrics provide insight into the ERM's ability to correctly identify when radon concentrations exceed the threshold. High recall (e.g. 98% for RadonEye) shows the sensor successfully detected nearly all true positive cases above 200 Bq/m^3, whereas high precision indicates that its positive readings were rarely false positives. However, lower recall or precision can indicate underestimation (false negatives) or overestimation (false positives), respectively. For example, the RadonEye's high recall but somewhat lower precision suggests it occasionally gave positive readings when the true value was actually below the threshold. Sensitivity analyses of classification performance with varying thresholds were also conducted and will be discussed in detail in Chapter 5.

Table 17: Confusion Matrix of the Four Tested Sensors against RAD7, Giang & Li (2025) [188]

Sensor	Accuracy	Precision	Recall	F1 Score
RadonEye	97%	86%	98%	92%
Inkbird	98%	89%	99%	94%
Wave	88%	56%	97%	71%
Spirit	99%	94%	98%	96%

All ERMs except for the Wave achieved similar accuracy levels (>97%) and precision values (>86%). The F1 score balances both the ability of a sensor to correctly identify radon concentrations above a threshold (recall) and to limit false positives (precision). In confusion matrix analysis, a high F1 score indicates the sensor effectively captures true positive cases

without excessive false positive cases, whereas a low F1 score reflects poor sensitivity in detecting readings above the threshold. The Spirit device demonstrated optimal overall performance, followed by Inkbird and RadonEye with comparable F1 scores, while the Wave exhibited reduced performance with 56% precision for classifications above 200 Bq/m^3.

4.2.2 Long-Term Test

The long-term collocation test was performed over 98 consecutive days, from December 3rd, 2024, to March 12th, 2025. The radon measurements obtained from the research-grade reference instrument, the AlphaGuard, were used as the benchmark of radon activity in the basement. Over the entire monitoring period, the mean radon concentration recorded by AlphaGuard was 98 Bq/m^3. This value is in close agreement with the mean from two alpha track detectors deployed in parallel, which reported an average concentration of 91 ± 20 Bq/m^3 and 119 ± 20 Bq/m^3. Figure 19 presents the temporal changes of the basement radon concentrations recorded by the AlphaGuard, alongside key indoor and outdoor environmental variables, including temperature, relative humidity, atmospheric pressure, and precipitation. Table 18 summarizes the results of a Spearman rank correlation analysis between outdoor environmental parameters and radon concentrations measured by the AlphaGuard.

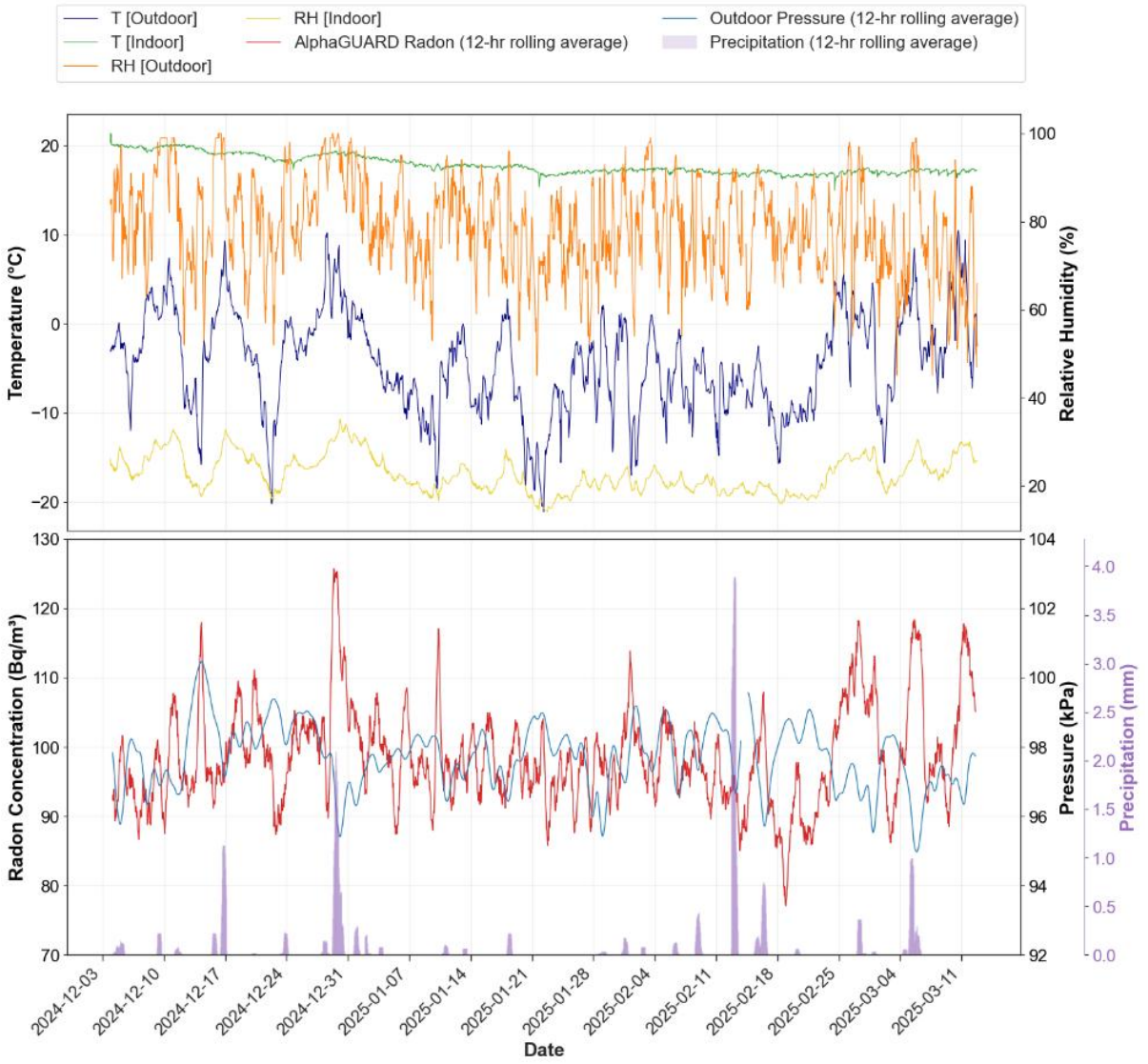


Figure 19: Radon concentration in the basement recorded by the AlphaGuard and the indoor and outdoor environmental conditions.

Table 18: Spearman Rank Correlation of Outdoor Environmental Parameters

Outdoor Environmental Parameter	ρ	Statistically Significant
Temperature (°C)	0.18	$p < 0.001$
Relative Humidity (%)	0.13	
Precipitation Amount (mm)	0.12	
Outdoor Pressure (kPa)	-0.18	

A clear daily pattern is observed, with radon concentration generally varying within the range of 85–120 Bq/m^3. Outdoor temperature, relative humidity, and precipitation each showed a positive, albeit weak, correlation with indoor radon concentrations ($\rho = 0.12 – 0.18$, $p < 0.001$), while outdoor atmospheric pressure was weakly but significantly negatively correlated ($\rho = -0.18$, $p < 0.001$). This relationship is visually evident in Figure 19, where periods of elevated outdoor pressure correspond to reduced radon concentrations. These findings are consistent with Schubert et al. (2018) observed that differences between indoor and outdoor air pressure (i.e., pressure gradients) resulted in strong negative changes in radon concentrations, specifically when outdoor air pressure was higher than indoor air pressure [189]. The study also found that the diurnal variation of indoor radon concentration could be attributed to predominantly changing indoor temperatures, though this is mainly associated with the change in indoor air volume.

The comparative analysis between low-cost ERMs and the research-grade reference instrument revealed a wide range of relative percent errors (RPE) among the tested devices. As mentioned previously in Section 3.2.3, a well-performing sensor is expected to show an RPE within ±10% of the reference instrument. In this long-term collocation test, unfortunately, only six sensors achieved this benchmark, with the majority either significantly underestimating or overestimating radon concentrations, as summarized in Table 19.

Table 19: Relative Percent Errors for Low-Cost ERMs with sensors within ±10% bolded

Sensor ID	Relative Percent Error (RPE) (%)			Average Relative Percent Error (%)
CH-5, CH-6, CH-7	36%	22%	25%	28%
CRAD-4, CRAD-5, CRAD-6	57%	53%	48%	53%
EB-4, EB-5, ***EB-6***	18%	18%	**7%**	14%
EQ-4, EQ-5, EQ-6	30%	28%	29%	29%
FK-4, FK-5, FK-6	-44%	-43%	-44%	-44%
HAN-4, HAN-5, HAN-6	30%	13%	40%	28%
IBD-5, IBD-6	17%	11%		14%
LB-4, LB-5, LB-6	146%	54%	37%	79%
LCA-4, LCA-5, LCA-6	-38%	-24%	-24%	-29%
LU-5*, LU-6*	**10%**	15%		13%
PS4-4*, PS4-5, PS4-6*	**10%**	20%	21%	17%
RD2-2, RD2-4, RD2-5	-36%	-40%	-34%	-37%
RE-4, RE-5, RE-6	**3%**	**4%**	**5%**	4%
VP-4, VP-5, VP-6	16%	17%	24%	19%
WP-5, WP-6, WP-7	30%	18%	13%	20%

Among all devices, the RE-series and notably EB-6 demonstrated the most favourable performance, consistently yielding RPEs between 3–7%. These ERMs are well within the acceptable range for practical use. Other devices, including IBD, LU, PS4, VP, and WP-series, also performed reasonably well, remaining within a ±20% error band. It is important to note that not all the sensors within the same series were ≤20% RPE. Typically, there was one sensor greater than this range, highlighting the variation in RPE even between the same series of sensors. For instance, WP-6 and WP-7 have an RPE of 13 and 18% respectively, while WP-5 shows an RPE of 30%. Conversely, several sensors exhibited a strong bias in their measurements. The FK-series, LCA-series, and RD2-series persistently underestimated radon concentrations, with RPEs ranging from -24% to -44%. In contrast, certain devices, such as LB-4, showed extreme overestimation, recording RPEs as high as 146%, indicating a substantial positive bias. The CRAD-series also tended to overestimate, with RPEs between 48 – 57%.

Examination of other statistical performance metrics, such as the coefficient of determination (R^2) from linear regression, root mean square error (RMSE), and Spearman's rank correlation coefficient (ρ), provides further insight into sensor reliability as summarized in Table 20. The coefficient of determination, RMSE, and Spearman rank correlation coefficient

columns have colour gradients applied to the values of each ERM concerning each other, with darker colours indicating better performance. For instance, the coefficient of determination column shows values with poor R^2 (close to 0) as very light blue or white, whereas greater R^2 values are shown as a darker blue (greatest R^2 = 0.2234).

Table 20: Summary of linear regression, RMSE, and Spearman Rank Correlations for Long-term Test with Statistically Significant ERMs bolded

Sensor	R^2	Slope	Intercept	RMSE (Bq/m^3)	ρ
CH-5	0	0.01	132.6	47.34	0.01
CH-6	0.0031	0.14	105.96	37.13	0.09
CH-7	0.0035	-0.15	137.62	39.7	0.01
CRAD-4	0.0001	0.04	150.04	70.23	0.1
CRAD-5	0.0078	0.25	126.05	62.05	0.09
CRAD-6	0.0108	-0.35	180.74	62.6	0.03
EB-4	0.0514	0.49	67.92	30.05	**0.16**
EB-5	0.0619	0.48	68.98	28.08	**0.21**
EB-6	0.0389	0.34	72.44	21.09	**0.17**
EQ-4	0.092	0.49	79.47	34.9	**0.28**
EQ-5	0.0787	0.44	82.21	33.36	**0.24**
EQ-6	0.0934	0.49	78.98	34.07	**0.28**
FK-4	0.0155	-0.25	79.61	50.59	0.03
FK-5	0.013	-0.24	79.08	50.38	-0.07
FK-6	0.0108	-0.2	74	50.21	0.03
HAN-4	0.0239	0.39	90.02	41.35	0.13
HAN-5	0.0316	0.4	72.05	28.33	0.1
HAN-6	0.0373	0.65	73.92	53.82	**0.18**
IBD-5	0.0291	0.47	69.1	35.24	**0.19**
IBD-6	0.0566	0.64	47.13	31.29	0.12
LB-4	0.035	1.34	110.56	163.83	**0.16**
LB-5	0.0222	0.58	94.4	68.49	0.11
LB-6	0.0057	0.32	103.52	60.6	0.04
LCA-4	0.1767	0.22	40.25	36.76	**0.33**
LCA-5	0.1615	0.24	51.11	24.39	**0.29**
LCA-6	0.1563	0.24	51.44	24.18	**0.34**
LU-5	0.0272	0.2	88.92	21.56	0.15

LU-6	0.044	0.21	92.93	22.05	0.21
PS4-4	0.0119	0.23	85.3	26.72	0.11
PS4-5	0.0076	0.18	100.77	31.25	0.1
PS4-6	0	0	119.17	31.16	0.04
RD2-2	0.2234	0.21	43.39	34.55	**0.42**
RD2-4	0.1986	0.2	40.52	38.31	**0.36**
RD2-5	0.1382	0.19	47.03	32.71	**0.31**
RE-4	0.0998	0.42	60.02	16.58	**0.28**
RE-5	0.0866	0.39	64.1	16.94	**0.26**
RE-6	0.0863	0.4	64.66	17.54	**0.26**
VP-4	0.0143	0.19	95.75	25.79	**0.13**
VP-5	0.0189	0.25	91.29	28.49	**0.12**
VP-6	0.0073	0.15	107.9	32.83	**0.06**
WP-5	0.0002	-0.02	130.07	37.89	-0.01
WP-6	0.0001	0.02	114.96	28.72	0.01
WP-7	0.0059	0.12	99.06	24.43	**0.09**

Overall, the R^2 values across all sensors were notably low, with most devices registering values well below 0.1, and seven sensors equal to zero. These low R^2 values indicate that, for the majority of sensors, very little of the variance in the ERM readings could be explained by AlphaGuard reference measurements. Only a handful of sensors, such as the LCA and RD2, achieved R^2 values in the range of 0.15 – 0.22, suggesting a moderately improved, though still weak, ability to match the reference instrument readings. With respect to RMSE, which shows the absolute error magnitude, the results were similarly varied. Sensors such as the LB-4 and CRAD displayed much higher RMSE values (up to 164 Bq/m^3 and 70 Bq/m^3, respectively), reflecting larger deviations from reference concentrations. Regarding Spearman rank correlations, only a minority of ERMs demonstrated significant, positive, monotonic relationships with the AlphaGuard ($\rho < 0.3$). For instance, the LCA and RD2 were among the strongest, with $\rho = 0.31 – 0.42$ ($p < 0.05$). With RMSE values ranging from 16 to 18 Bq/m^3, the top-performing sensors, most notably the RE, showed a reasonably close match to the AlphaGuard on an absolute value basis. However, their R^2 values (~0.10) are not the highest among all sensors, as shown in Figure 20.

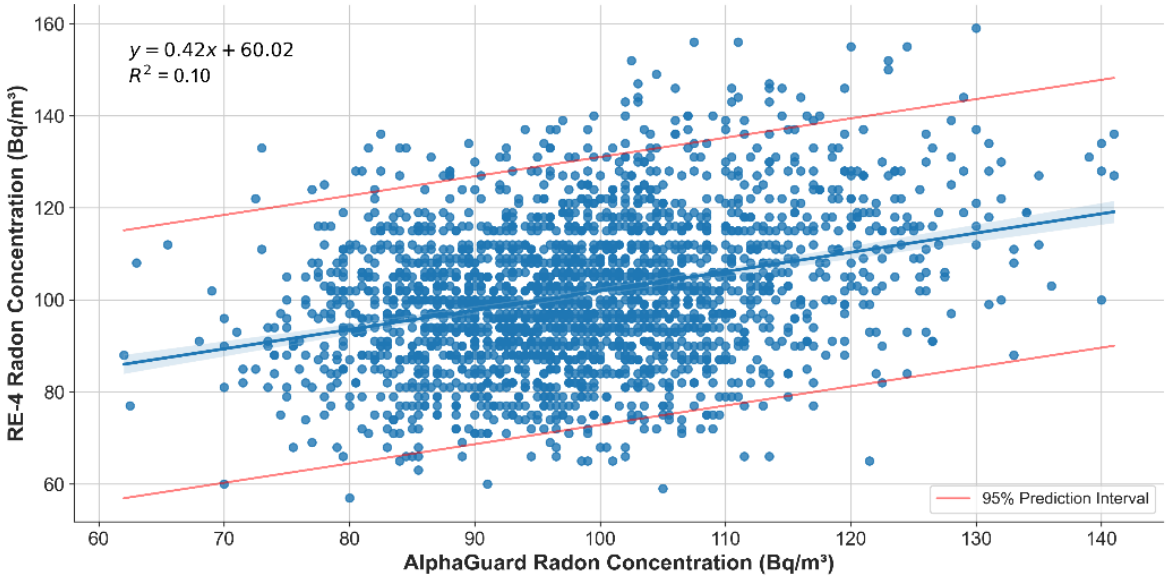


Figure 20: Linear regression of RE-4 vs. AlphaGuard

Despite the low R^2, they are among the better performers in the other evaluation metrics. Their low RPE (3 – 5%) and low RMSE (16 – 18 Bq/m^3) emphasize their agreement with the reference instrument. Moreover, the RE also achieves one of the highest Spearman correlations (ρ = 0.26 – 0.28) observed in the dataset, demonstrating both accuracy and consistency. In contrast, Figure 21 illustrates the linear regression performance of CRAD-4 to show a representative sample of ERMs' lower bounds of performance.

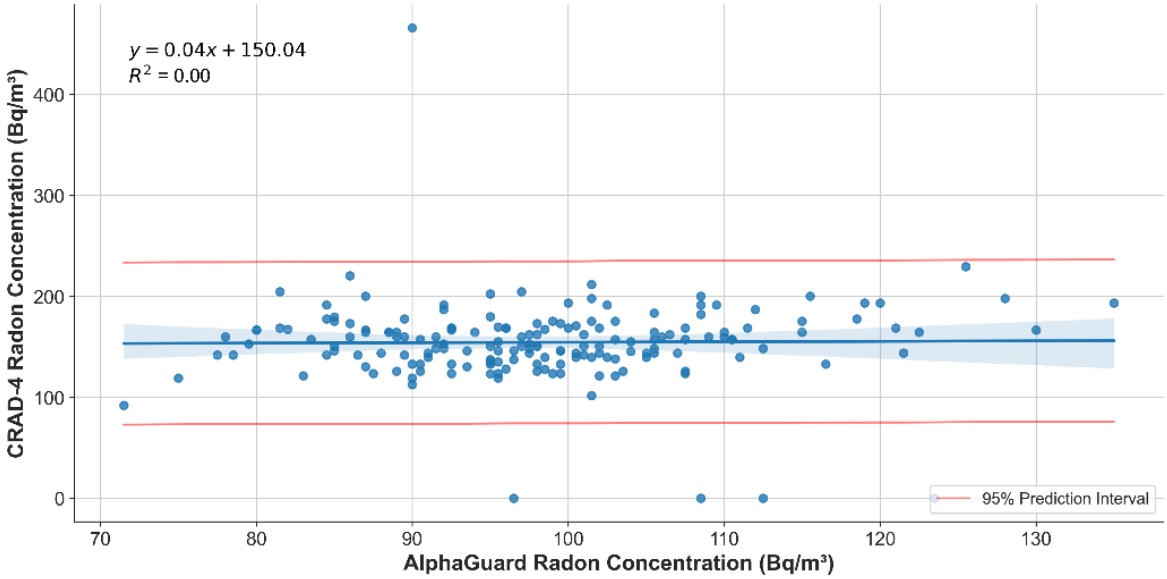


Figure 21: Linear regression of CRAD-4 vs. AlphaGuard

The CRAD failed to track the reference instrument with an RPE up to 57%, $R^2 \sim 0$, and high RMSE. Similarly, the LB-4 exhibited considerable positive bias (RPE = 146%) and the highest absolute error (RMSE = 164 Bq/m^3), paired with a weak R^2 (0.04). The FK and LCA consistently underestimated radon concentrations, as seen by their large negative RPEs. However, the LCA showed moderate R^2 and the highest rank correlations (up to 0.34), indicating they may still be adequate for relative trend detection, instead of absolute value measurements. Finally, moderate performing sensors, such as from the EB and EQ, demonstrated moderate RPEs (7–30%), relatively low RMSEs, and mid-range correlation coefficients.

Figure 22 presents the percent ratio distributions for all ERMs relative to the reference instrument. The percent ratio reflects the ERM's measured radon concentration as a percentage of the AlphaGUARD's measurements at matching sampling intervals, with 100% indicating perfect agreement.

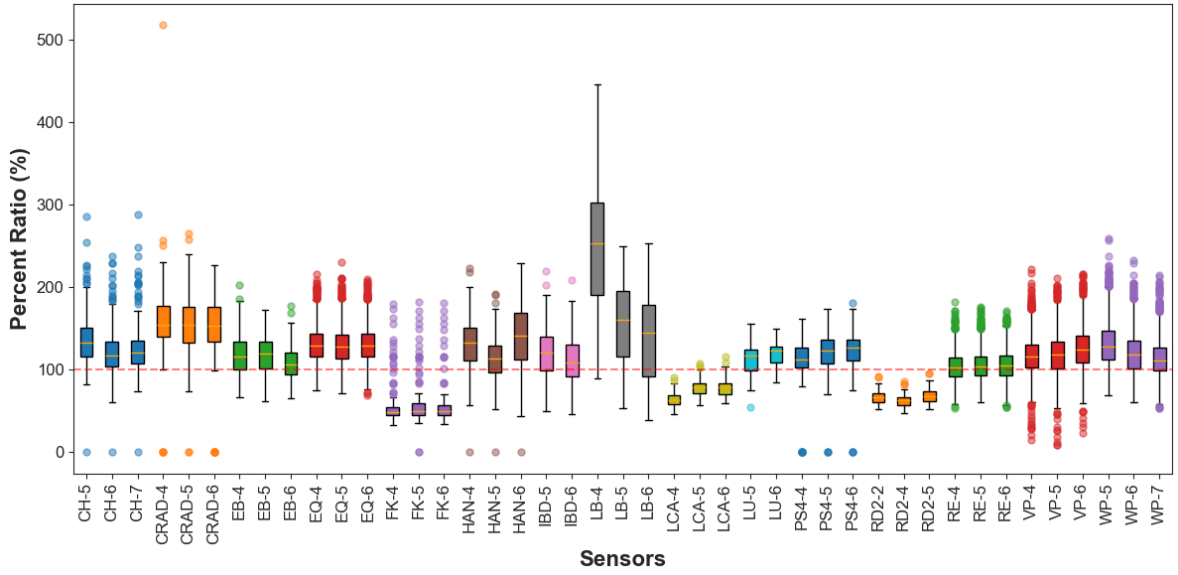


Figure 22: Percent Ratios of ERMs against AlphaGuard at matching sampling intervals. In each box plot, the orange line represents the median concentration, while the bottom and top halves of the box indicate the second and third quartiles, representing the interquartile range. The whiskers extend to the most extreme data points within 1.5 times the interquartile range. Outliers are shown as individual points.

Across the various sensors, the percent ratios were also highly variable, with the median values for most sensors deviating substantially from the 100% line. Sensor groups (e.g., CH, CRAD, EQ, HAN, LB, PS4, VP, WP) clustered above 100% indicate systematic overestimation of radon levels. In contrast, sensors such as the FK, LCA, and RD2 consistently reported below 100%, reflecting significant underestimation. There is also a noticeable variation within the same sensor groups. For instance, LB-4 presents with a considerably higher percent ratio than LB-5 or LB-6. The RE exhibited medians closest to 100% showing the best agreement with the reference instrument among all tested ERMs.

Figure 23 displays the coefficients of variation (CV), representing the relative variability in repeated measurements (as % of the mean) within a type of sensor. A lower CV indicates that the individual device of the same model captures highly similar readings at each timestamp, indicating the intra-sensor performance is more consistent, while a higher CV signals greater measurement instability between the units.

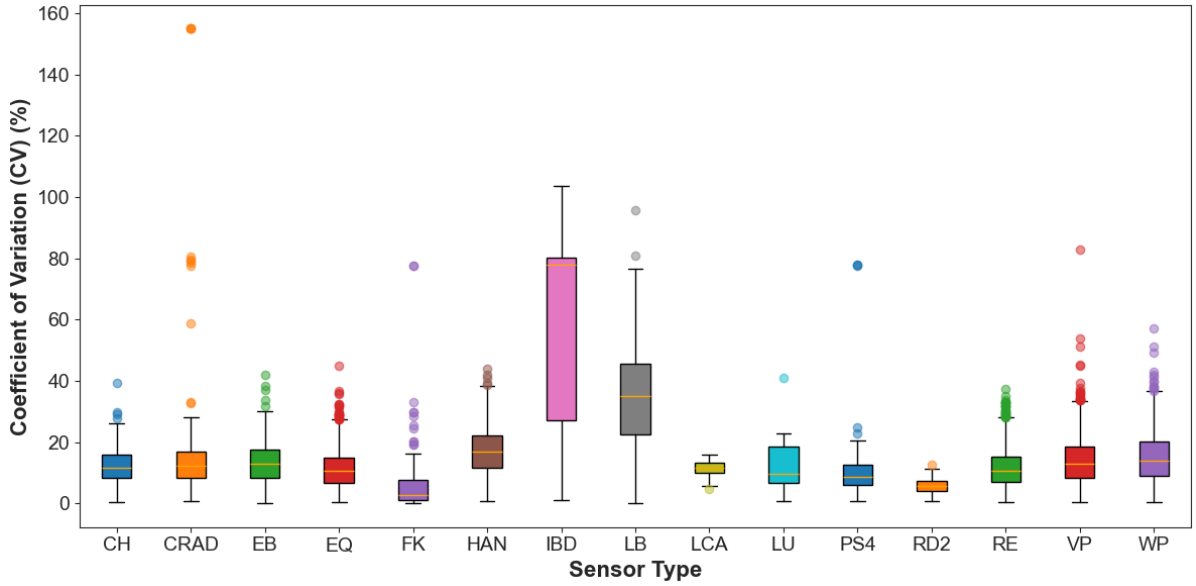


Figure 23: Coefficient of variation of ERM. In each box plot, the orange line represents the median concentration, while the bottom and top halves of the box indicate the second and third quartiles, representing the interquartile range. The whiskers extend to the most extreme data points within 1.5 times the interquartile range. Outliers are shown as individual points.

Overall, the majority of ERMs maintained relatively low median CVs (< 20%), suggesting reasonable within-model repeatability. However, a few sensors, most prominently IBD and LB, matching their performance in percent ratios, had notably high median CVs and exhibited extreme outliers (> 80%). These elevated CVs indicate substantial variability between measurements by different units from the same model. FK and LCA sensors, while generally underestimating, maintained relatively low CVs, indicating that while they were biased, they produced consistent readings. According to US EPA guidelines, the acceptable mean CV for ERMs is up to 10% [178]. In this analysis, only four out of the fifteen unique ERM types (FK, RD2, PS4, and LU) met this threshold. The remaining ERMs generally exhibited CVs between 10% and 20%..

The Bland-Altman analysis provides a further quantification of the agreement between each low-cost ERM and reference instrument. The mean difference represents the average bias of the ERMs. The upper and lower limits of agreement indicate the spread of the differences for approximately 95% of observations. For a reliable and unbiased sensor, the mean difference should be close to zero, and the limits of agreement should be narrow, reflecting minimal and consistent deviation from the reference. The Bland-Altman analysis showed substantial differences in bias and limits of agreement across all ERMs (see Table A3). Only a few sensors demonstrated low bias and narrow limits of agreement, while most showed substantial positive or negative bias and wide limits, indicating poor agreement and inconsistency with the reference instrument. Figure 24 - Figure 26 show examples of certain ERMs that show best overall agreement, consistent underestimation, and overestimation, respectively.

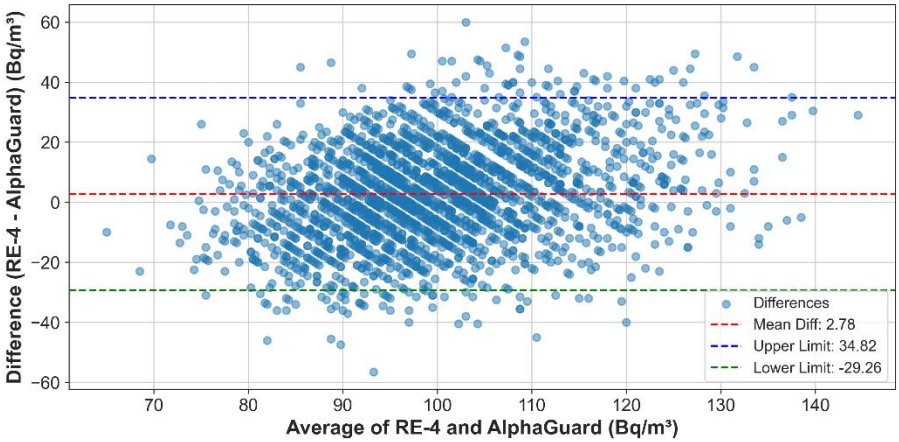


Figure 24: Bland-Altman plot for RE-4 vs. AlphaGuard

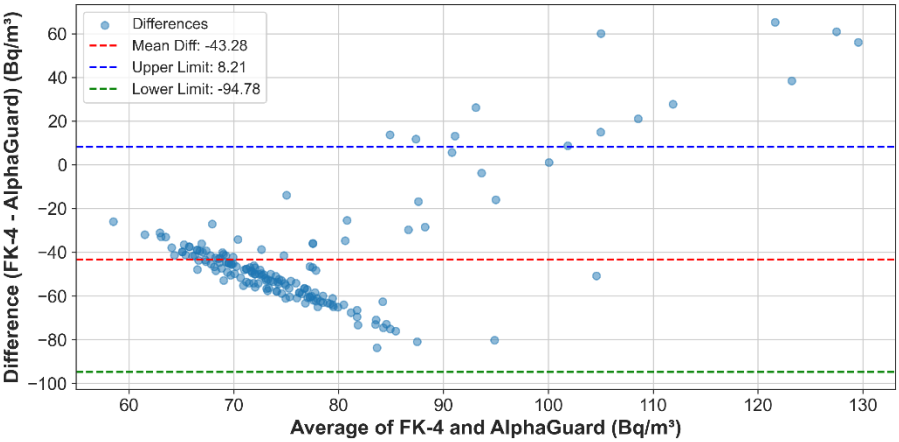


Figure 25: Bland-Altman plot for FK-4 vs. AlphaGuard

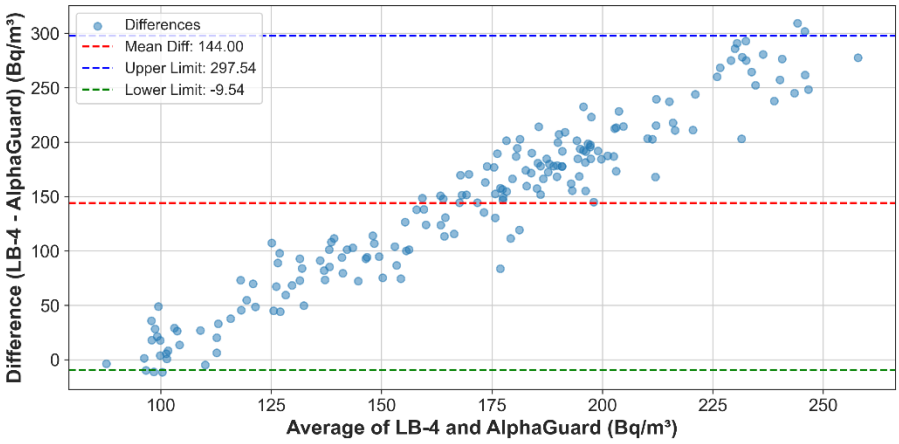


Figure 26: Bland-Altman plot for LB-4 vs. AlphaGuard

Among the ERMs evaluated, RE-4, FK-4, and LB-4 represent distinct patterns in agreement with the reference instrument as revealed by the Bland-Altman analysis. The RE-4 sensor showed a mean difference of 2.78 Bq/m^3 with upper and lower LoA ranges of 64.08 Bq/m^3. The values for RE-4 indicate a low average bias and comparatively narrow spread. The FK-4 sensor had a mean difference of –43.28 Bq/m^3, with a LoA range of 102.99 Bq/m^3. This large negative mean difference and widespread points indicate that FK-4 consistently recorded lower radon concentrations than the reference, with considerable variability in measurements. Particularly, the plot shows a negative trend, suggesting the underestimation gets worse at higher radon concentrations. In contrast, the LB-4 sensor exhibited a mean difference of 144.00 Bq/m^3 and a very wide range of LoA of 307.08 Bq/m^3.. The high positive bias and extensive spread for LB-4 indicate that this sensor consistently overestimated radon concentrations, and this overestimation becomes more pronounced at high radon concentrations.

Table 21 presents the summary statistics derived from the confusion matrix analysis for each sensor, including accuracy, precision, recall, and F1 score. A threshold of 100 Bq/m^3 was used to evaluate the ERMs based on the range of measured radon concentrations and the recommended World Health Organization (WHO) limit. The colours on the table reflect the performance of each confusion matrix statistic, with values closer to 0 representing poor performance, as indicated by white, and values with strong performance closer to 1 as indicated by a dark green, relative to the values in each respective parameter.

Table 21: Summary of Confusion Matrix for Long-Term Collocation Test

Sensor	Accuracy	Precision	Recall	F1 Score
CH-5	0.43	0.41	0.99	0.58
CH-6	0.49	0.43	0.87	0.57
CH-7	0.41	0.39	0.9	0.54
CRAD-4	0.39	0.39	0.96	0.55
CRAD-5	0.4	0.39	0.96	0.56
CRAD-6	0.37	0.38	0.91	0.53
EB-4	0.46	0.4	0.75	0.52
EB-5	0.49	0.42	0.79	0.55
EB-6	0.52	0.42	0.63	0.51
EQ-4	0.45	0.43	0.96	0.59

EQ-5	0.45	0.43	0.96	0.59
EQ-6	0.45	0.43	0.96	0.59
FK-4	0.56	0.18	0.03	0.05
FK-5	0.57	0.2	0.03	0.05
FK-6	0.57	0.22	0.03	0.05
HAN-4	0.45	0.41	0.85	0.55
HAN-5	0.5	0.43	0.78	0.55
HAN-6	0.45	0.4	0.87	0.55
IBD-5	0.52	0.44	0.83	0.57
IBD-6	0.53	0.43	0.63	0.51
LB-4	0.39	0.39	0.96	0.55
LB-5	0.46	0.41	0.87	0.56
LB-6	0.46	0.4	0.7	0.51
LCA-4	0.61	0	0	0
LCA-5	0.61	0	0	0
LCA-6	0.61	0	0	0
LU-5	0.43	0.34	0.71	0.46
LU-6	0.47	0.43	0.9	0.58
PS4-4	0.45	0.4	0.82	0.54
PS4-5	0.45	0.41	0.91	0.57
PS4-6	0.41	0.39	0.9	0.55
RD2-2	0.61	0	0	0
RD2-4	0.61	0	0	0
RD2-5	0.61	0	0	0
RE-4	0.61	0.53	0.61	0.57
RE-5	0.58	0.5	0.65	0.56
RE-6	0.57	0.49	0.65	0.56
VP-4	0.48	0.44	0.8	0.56
VP-5	0.48	0.43	0.78	0.56
VP-6	0.45	0.42	0.89	0.57
WP-5	0.44	0.42	0.93	0.58
WP-6	0.47	0.43	0.79	0.55
WP-7	0.51	0.45	0.75	0.56

Notably, the LCA and RD2 exhibit values of 0.61 for accuracy but zero for precision, recall, and F1 score. This combination indicates that while they were able to correctly identify all true negatives (measurements ≤ 100 Bq/m^3), they failed to correctly identify any true positive cases (> 100 Bq/m^3), likely due to systematic underestimation of the sensors. This suggests that these models may miss all instances of hazardous radon exposure above guideline thresholds, highlighting a notable limitation for their use in screening tests. Sensors such as the RE report higher values for all four metrics. RE-4 has an accuracy of 0.61, a precision of 0.53, a recall of 0.61, and an F1 score of 0.57. RE-5 and RE-6 have slightly lower but comparable values in the same metrics, but a higher recall score, indicating their more successful detection of true positives above the threshold, even though there were also more false positives identified. These sensors have the highest overall accuracy and balanced combinations of precision and recall among the devices tested. The FK display relatively high accuracy (0.56 – 0.57) but low values for precision (0.18 – 0.22), recall (0.03), and F1 score (0.05), highlighting difficulty in identifying true positives. For many other ERMs, the accuracy, precision, recall, and F1 score are generally in the range of 0.40–0.53.

Overall, the confusion matrix results indicate a wide disparity in the ability of the different ERMs to correctly classify observations at a threshold of 100 Bq/m^3, with only a few sensors achieving a combination of high precision and recall; therefore F1 score. The variability across these metrics highlights differences in both correct identification rates among the tested sensors.

4.2.3 Comparison of Short-Term & Long-Term Tests

Across both short-term and long-term collocation tests, the RadonEye (RE) sensors consistently demonstrated strong performance relative to both research-grade reference instruments, the RAD7 and AlphaGuard, respectively. In the short-term tests conducted across multiple residential environments with large variations in radon concentration, RE sensors achieved high coefficients of determination (R^2 = 0.63 – 0.9) and low RMSE (13 – 111 Bq/m^3) against the RAD7 across all concentration ranges. Similarly, during the long-term deployment in a relatively stable basement environment, the RE sensors closely followed the AlphaGuard

and exhibited a very low RPE of 3 – 5%. They were also among the lowest RMSE values below 18 Bq/m^3. These findings are aligned with previous studies, such as those by Rábago et al. (2024) and Dimitrova et al. (2025), which reported measurement errors of ≤15% after one week of exposure in a laboratory at mean exposure of 200 Bq/m^3 and 8% after a year-long test comparing RE sensors to alpha-track detectors, respectively [19], [190].

Although the RE sensors performed well among the other ERMs in each testing scenario, differences between short-term and long-term results were apparent. For example, Bland-Altman analysis indicated that while RE sensors performed well in both tests, the short-term test results had slightly wider LoA and a higher mean difference (by 4.67 Bq/m^3). Similarly, confusion matrix analysis revealed a notable drop in F1 score for the long-term test (56%) compared to the short-term test (92%). This pattern was not unique to RE sensors; other ERMs demonstrated comparable shifts in performance between testing durations, with F1 scores and mean differences generally reflecting greater accuracy during the short-term test.

Examining other ERMs, the RD2 was evaluated in both tests and consistently ranked near the middle of its cohort in short-term deployments. The long-term test, however, showed a marked trend toward underestimation compared to the AlphaGuard, with RPEs from -34% to -40%. Despite this, the RD2 exhibited good within-device repeatability (CV = 6%), though the underestimation persisted in Bland-Altman analysis, where mean differences ranged from -36.85 to -30.81 Bq/m^3 with wide LoA from -9.14 to -52.47 Bq/m^3. In confusion matrix analysis, RD2 failed to detect any true positives in the long-term test, resulting in zero values for precision, recall, and overall F1 score, whereas it had achieved an F1 score of 94% in the short-term context. This outcome is coherent with the underestimation indicated by RPE analysis, as the sensor only reported true negatives and false negatives. It is important to note that the RD2 sensors have been recalled by Health Canada due to inaccurate radon measurements, emphasizing the unreliability of certain ERMs on the market and the need for regulatory testing [191].

The CH sensors, which are the Corentium Home (formerly called Canary) models, exhibited RPE values between 22% and 36%. Prior research by Daraktchieva et al. (2024) reported a notably higher RPE of 60.9% after three months under low-radon conditions, whereas the

findings in this study more closely align with those of Warkentin et al. (2020) and Gunning et al. (2016), which documented measurement errors at or below 20% [124], [128], [175]. These differences may be attributable to variations in experimental design, including concentration ranges and test durations. For instance, the narrower concentration range and limited fluctuations seen during the long-term test, as opposed to the short-term test with wide ranges and exposure to weekly fluctuations, saw discrepancies in F1 scores. The short-term test encompassed a broader spectrum of radon exposures, increasing the likelihood of detecting true positives or false positives above the 200 Bq/m^3 threshold, thereby inflating the performance of the confusion matrix metrics.

Furthermore, the Wave sensor used in the short-term test is the predecessor to the WP sensors evaluated in the long-term deployment. While the Wave sensor demonstrated higher R^2 values in short-term tests, its long-term RMSE values (24–38 Bq/m^3) were comparable to those observed at low- and medium-concentration ranges in the short-term test (19–42.2 Bq/m^3). Differences in F1 scores and Bland-Altman outcomes persisted, with better F1 scores in the short-term but smaller mean differences and narrower LoA in the long-term context.

Across both testing durations, a common observation is that high measurement variability and response delays to radon fluctuations were prevalent among many ERMs. This observation is corroborated by previous research [19], [127]. For instance, Daraktchieva et al. (2024) found that the Wave sensor had a response time of up to 15 hours, achieving stable readings only after 27 hours, and reported high overestimation (up to 90%) under some conditions. The corresponding RPE for the Wave was 47.7% after three months of testing in a low-radon chamber (145 Bq/m^3). In the present study, however, the RPE for the WP sensor after a 90-day deployment ranged from 13% to 30%, suggesting that the Wave may indeed perform better during long-term monitoring, as recommended by the manufacturer, which advises a minimum 30-day test period to ensure reliable results. The Wave's reliance on rolling 24-hour averages may also influence its ability to capture daily extremes, potentially explaining differences in performance between short- and long-term tests.

4.3 High-Rise Multi-Family Building Results

This section addresses the third objective of this research project: investigating the prevalence and variability of radon concentrations in high-rise multi-family residential buildings. The results presented here focus on both a preliminary screening, which offers a snapshot of radon levels across a selection of multi-family buildings in the Kitchener/Waterloo region, and a detailed case study of Claudette Millar Hall (CMH), where radon sensors were deployed on every floor of the 12-storey building over a three-month period. The findings encompass a statistical analysis and comparison of radon concentration distributions between floors, as well as air exchange rate analysis during a period of interest to assess how ventilation may affect indoor radon levels. In addition, meteorological factors that may influence observed patterns within the building were explored.

4.3.1 Preliminary Screening

The preliminary screening of multi-family buildings in the Kitchener/Waterloo region encompassed 61 buildings across various postal code areas, providing a snapshot of radon concentrations in this residential sector as summarized in Table 22.

Table 22: Summary of Preliminary Screening of Multi-Family Buildings

Building ID	Measured Radon Concentration (Bq/m^3)	Error (±)	Test Location	Postal Code Region
Building 1	37.75	12.94	1st Floor	N2L
Building 2	28.13	10.19	1st Floor	N2L
Building 3	15.31	6.88	1st Floor	N2L
Building 4	20.13	8.19	1st Floor	N2L
Building 5	17.88	7.53	1st Floor	N2L
Building 6	15	6.84	1st Floor	N2L
Building 7	13	6.19	Basement	N2L
Building 8	13	6.19	1st Floor	N2L
Building 9	12.81	6.19	1st Floor	N2L
Building 10	12.75	6.16	1st Floor	N2L
Building 11	12.63	6.19	Basement	N2L
Building 12	12.19	6.84	1st Floor	N2L
Building 13	1.88	3	1st Floor	N2L
Building 14	15.25	6.78	1st Floor	N2J

Building 15	13.06	6.19	1st Floor	N2J
Building 16	13	6.16	1st Floor	N2L
Building 17	10.81	5.5	1st Floor	N2J
Building 18	10.81	5.5	1st Floor	N2J
Building 19	8.31	4.81	1st Floor	N2J
Building 20	4.13	3.38	1st Floor	N2L
Building 21	4.06	3.38	Basement	N2J
Building 22	20.38	8.19	1st Floor	N2G
Building 23	20.13	8.16	1st Floor	N2L
Building 24	17.88	7.53	1st Floor	N2L
Building 25	17.75	7.53	1st Floor	N2G
Building 26	15.25	6.84	1st Floor	N2L
Building 27	13.06	6.19	19th Floor	N2G
Building 28	10.63	5.47	1st Floor	N2J
Building 29	8.56	4.81	1st Floor	N2J
Building 30	8.5	4.81	1st Floor	N2J
Building 31	8.38	4.81	1st Floor	N2J
Building 32	1.88	3	19th Floor	N2G
Building 33	17.5	7.53	1st Floor	N2J
Building 34	15.38	6.84	1st Floor	N2J
Building 35	10.81	5.5	1st Floor	N2J
Building 36	8.56	4.81	1st Floor	N2J
Building 37	40.5	13.63	1st Floor	N2J
Building 38	33	11.56	1st Floor	N2J
Building 39	29.13	10.19	1st Floor	N2J
Building 40	24.88	9.5	1st Floor	N2H
Building 41	21.75	8.88	1st Floor	N2J
Building 42	17.38	7.53	1st Floor	N2H
Building 43	12.88	6.19	1st Floor	N2G
Building 44	42	13.44	1st Floor	N2A
Building 45	26.25	10.19	1st Floor	N2A
Building 46	20.13	8.19	1st Floor	N2B
Building 47	19.88	8.19	1st Floor	N2B
Building 48	19.88	8.19	1st Floor	N2J
Building 49	19.38	8.19	1st Floor	N2A
Building 50	18	7.53	1st Floor	N2B
Building 51	38	12.94	1st Floor	N2L
Building 52	22.5	8.88	1st Floor	N2K
Building 53	17.75	7.53	1st Floor	N2L

Building 54	13.13	6.19	1st Floor	N2C
Building 55	10.75	5.5	1st Floor	N2H
Building 56	10.56	5.5	1st Floor	N2L
Building 57	5.75	4.13	1st Floor	N2H
Building 58	5.16	4.13	1st Floor	N2C
Building 59	4.13	3.38	1st Floor	N2H
Building 60	4.13	3.38	1st Floor	N2H
Building 61	1.95	3	1st Floor	N2H

Overall, the measured radon concentrations were low, ranging from a minimum of 1.95 Bq/m^3 to a maximum of 42 Bq/m^3, with corresponding measurement uncertainties spanning from ±3 to ±13.63 Bq/m^3. This is consistent with prior surveys indicating that multi-family buildings tend to exhibit lower radon concentrations [64]. However, the presence of a few buildings with concentrations above 30 Bq/m^3 suggests that building-specific factors, such as foundation design, local geology, or ventilation practices, may still contribute to elevated exposures in some cases. In addition, as some studies have found ground-contact units in multi-family buildings with comparable radon levels to single-family homes within the same areas, it would be expected that some of the multi-family buildings have elevated levels [50], [192]. The majority of measurements were conducted on the first floor, while three buildings were tested in basement locations, and two buildings had additional measurements on the 19th floor. Geographically, the buildings were distributed across multiple postal code regions, with the N2J and N2L regions representing the largest clusters of tested buildings. Notable observations include Building 44 recording the highest concentration at 42 Bq/m^3, followed by Building 37 at 40.5 Bq/m^3 and Building 51 at 38 Bq/m^3, while several buildings in the N2H region recorded the lowest concentrations, all below 6 Bq/m^3. Notably, Building 1 in Table 22 corresponds to Claudette Millar Hall (CMH), a residence building at the University of Waterloo. CMH was selected for long-term monitoring due to its relatively higher first-floor radon concentration (37.75 Bq/m^3) compared to other screened buildings, in addition to the accessibility and partnership with the building management team to facilitate extended testing.

4.3.2 Claudette Millar Hall (CMH)

Following a month-long recruitment campaign in January 2025, sensor installation occurred from February 3rd to February 19th, 2025, with the deployment lasting 91 days from the last sensor installation date. Floor 12 was the only exception to the full deployment duration, as the sensor was disconnected on April 18th by the occupant/custodial staff without contacting the research team, resulting in only 66 days of testing data. Before analyzing radon concentrations from each floor, calibration factors were applied to the 12 RadonEye sensors based on the results of the calibration test described in Section 3.3.2. The calibration factors applied to each floor ranged from 0.96 to 1.05.

Table 23: Calibrated Factors Applied to Radon Concentration by Floor

Floor	*1*	*2*	*3*	*4*	*5*	*6*	*7*	*8*	*9*	*10*	*11*	*12*
Calibration Factor	0.97	0.96	1.03	1.02	1.02	0.96	1.02	0.99	0.98	0.97	1.05	1.04

The time series analysis of calibrated radon concentrations across all floors is shown in Figure 27. Overall, the concentrations were low during the measurement period, ranging from February 3rd to April 21st.. The most significant observation was a substantial spike in radon concentrations recorded on all floors, approximately between April 22nd and April 30th, 2025. Additionally, Floor 10 exhibited a smaller spike at the beginning of the testing period from February 10th to February 12th before returning to consistent baseline levels. The potential cause of this spike is explored further later in this section. The data also displayed clear diurnal patterns with daily maxima and minima across all measurement periods.

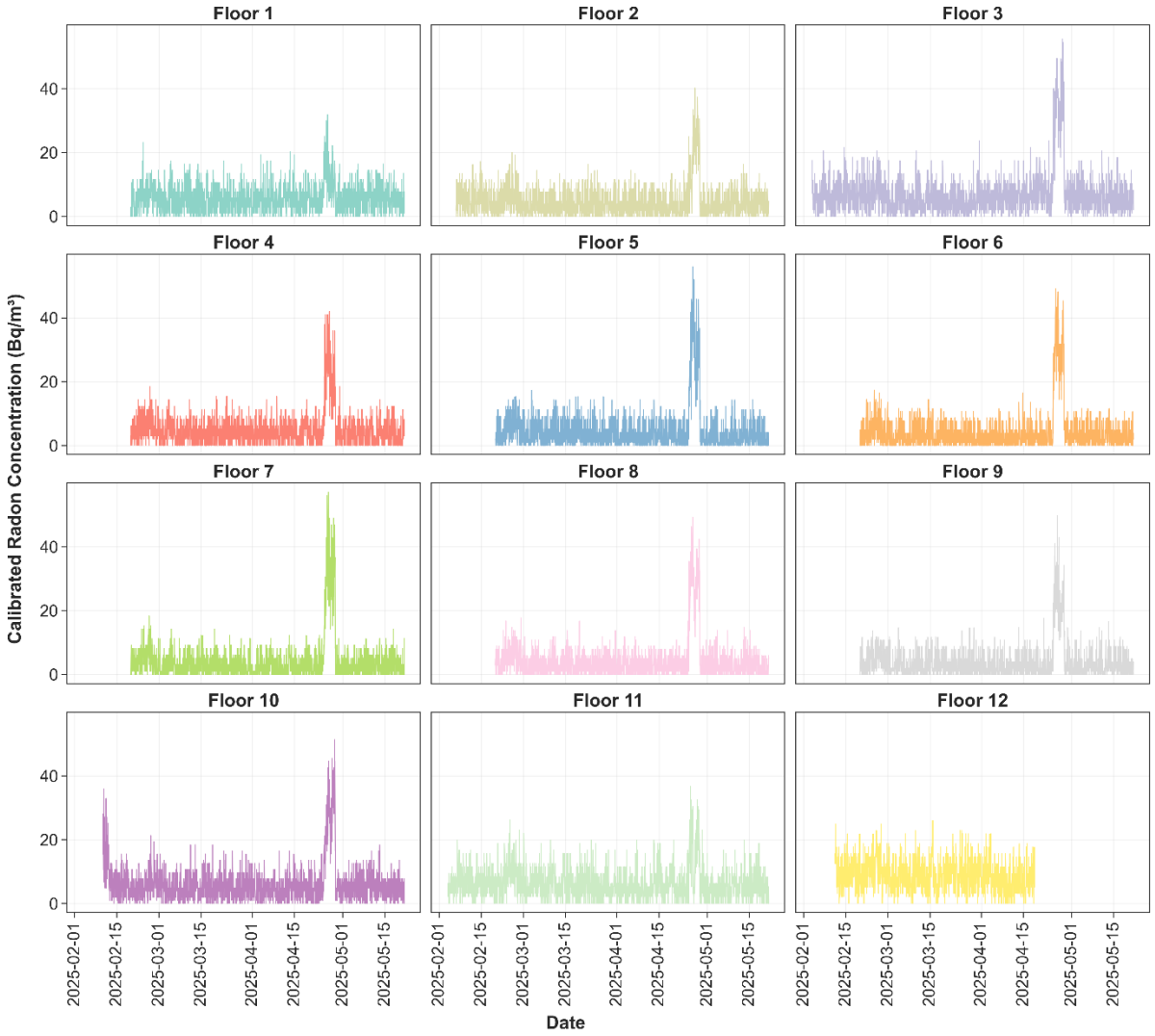


Figure 27: Time series of calibrated radon concentrations across all floors.

Figure 27 shows the mean radon concentration in comparison to the alpha track sensors, and Figure 28 shows the mean calibrated radon concentrations with 95% error bars for comparison across floors. It was confirmed through ANOVA analysis that there are statistically significant differences between the calibrated radon concentrations on each floor of CMH ($F = 132.86$, $p < 0.001$).

Table 24: Comparison of Mean Reported by Sensor vs. Alpha-Track Detector

Floor	*1*	*2*	*3*	*4*	*5*	*6*	*7*	*8*	*9*	*10*	*11*	*12*
AM (Bq/m³)	5.8	4.6	6.9	5.0	4.6	4.1	4.2	4.3	3.7	6.1	6.2	8.9
Alpha-track detectors (Bq/m³)*	< 31	< 15	< 15	35 ± 16	< 15	34 ± 24	< 15	< 15	< 15	< 15	N/A	< 20

**Values with '<' are reported with an upper limit of 90% confidence. All other values are reported with uncertainty with a 95% confidence interval.*

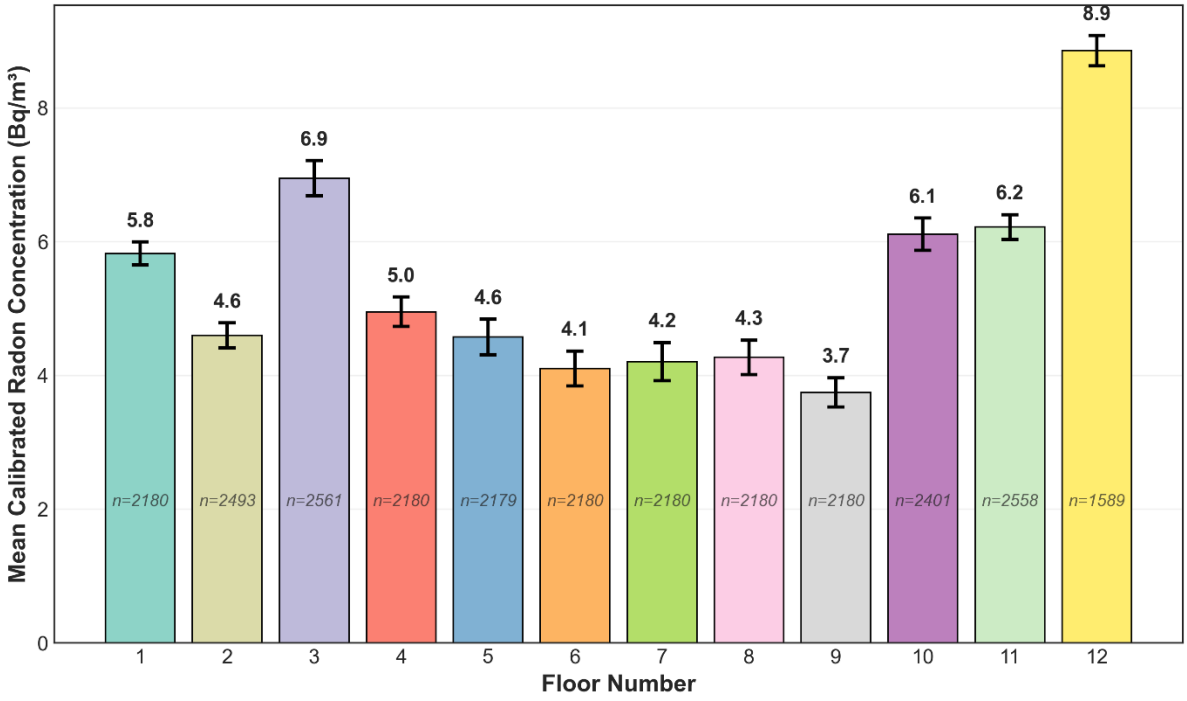


Figure 28: Arithmetic means of calibrated radon concentrations reported on top of 95% error bars, with 'n' representing the number of data points collected on each floor.

The RadonEye sensors generally demonstrated good agreement with the alpha-track detectors, particularly given the low concentration ranges observed. However, some discrepancies were noted, especially on Floors 1, 4, and 6. These differences may be attributed to the error margins inherent to alpha-track detectors, which are reported at a 95% confidence interval, as well as their distinct detection mechanisms. For example, on Floor 4 and Floor 6, the alpha-track detectors reported values of 35 ± 16 Bq/m^3 and 34 ± 24 Bq/m^3, respectively, whereas the RadonEye sensors measured lower mean values. On most other floors, alpha-track detectors reported concentrations below their detection limit (< 15 Bq/m^3 or < 31 Bq/m^3), which is consistent with the low means observed by the RadonEye sensors. Examining the calibrated

radon concentrations, Floor 12 recorded the highest mean radon concentration at 8.9 Bq/m^3, while Floor 9 reported the lowest at 3.7 Bq/m^3. Notably, floors without occupants where sensors were placed in lounges (Floors 4 through 9) generally exhibited among the lowest concentrations. The box plot distribution analysis shown in Figure 29 further illustrates these patterns, with the concentration spike visible as outliers in the data. Floor 12 showed minimal outliers due to measurement termination before the start of the spike.

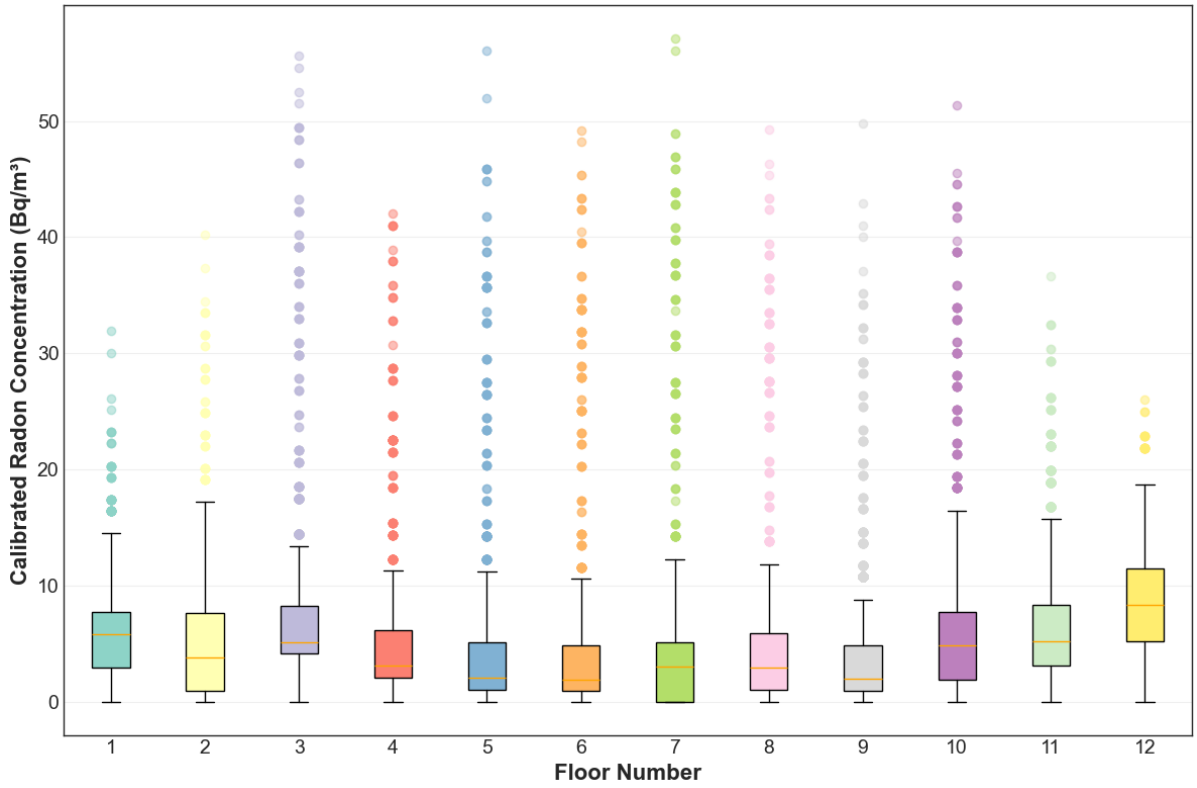


Figure 29: Box plot of radon concentration distributions by floor. In each box plot, the orange line represents the median concentration, while the bottom and top halves of the box indicate the second and third quartiles, representing the interquartile range. The whiskers extend to the most extreme data points within 1.5 times the interquartile range. Outliers are shown as individual points.

While no clear monotonic trend emerged from the CMH results, there is a general decrease in radon concentration with an increase in floor level up to Floor 9. This pattern is consistent with previous findings from Man and Yeung (1999) in an 18-storey Hong Kong building, as well as Valmari et al. (2012) in Finnish multi-family residences [52], [182]. However, the detection of

the highest mean radon concentration on the 12th floor of CMH deviates from these earlier studies, suggesting that additional factors, such as radon exhalation from building materials or unique ventilation patterns, may influence upper-floor concentrations. Valmari et al. (2012) noted that upper-floor apartments in Finnish multi-family buildings sometimes exhibited radon levels comparable to those in surrounding low-rise buildings, supporting the notion that construction materials, such as concrete, may contribute to elevated concentrations in high-rise settings [182].

Further evidence is provided by Jeong and Chon (2013), who found that the 11th floor of a 15-storey building had mean radon concentrations similar to those measured on lower floors of other buildings after three months of passive testing (63 Bq/m^3 on the 11th floor, 67 Bq/m^3 on the first and second floors of a two-storey building, and 48 Bq/m^3 on the third floor of a four-storey building) [84]. These observations suggest that upper floors can exhibit radon concentrations comparable to or even exceeding those on lower floors.

Air exchange rate analysis was conducted to investigate whether changes in ventilation rates contributed to the observed concentration spike. Table 25 presents air exchange rates estimated based on CO2 measurements for the period from April 15th to May 7th, 2025, categorized into before, during, and after the spike periods.

Table 25: Air Exchange Rate Analysis during April 15th, 2025 – May 7th, 2025

Floor	Air Exchange Rate (h^{-1})		
	Before Spike	**During Spike**	**After Spike**
1	0.44	0.33	0.41
2	0.63	0.30	0.09
3	0.23	0.10	0.17
6	0.06	0.12	0.15
7	0.11	0.08	0.55
8	0.09	0.10	0.41
9	0.10	0.17	N/A
10	0.15	0.15	0.13
11	0.83	0.40	0.15

The majority of floors showed decreased ventilation rates during the spike period, followed by recovery afterward. This trend is expected as lower air exchange rates reduce the removal of

indoor radon, resulting in increased concentrations. This finding is aligned with the established relationship between reduced air exchange and increased indoor radon levels documented in the literature. For example, Floor 1 decreased from 0.44 h^{-1} before the spike to 0.33 h^{-1} during the spike, then increased to 0.41 h^{-1} afterward. Several exceptions were observed, including Floors 6 and 9, which recorded higher air exchange rates during the spike and did not correspond with radon reductions, suggesting the influence of additional factors. Floor 10 maintained relatively similar rates throughout all three periods. Floors 7 and 8 showed similar rates before and during the spike but exhibited clear increases afterward. It is also important to acknowledge the limitations of using CO_2 decay measurements to estimate air exchange rates. This method relies on the assumption of occupant patterns to identify decay periods that can introduce some uncertainties. Communications with the Campus Housing facilities team confirmed that there were no specific adjustments made to the HVAC schedules. However, this period would have had minimal occupants due to the transition of students between semesters, which may have corresponded to a reduced load on the mechanical ventilation of the building if demand-controlled ventilation was used for system operation.

Comparable patterns have been documented in international studies. For example, Choi et al. (2022) investigated radon concentrations and ventilation effects within a 12th-floor apartment of a newly constructed building in South Korea [94]. Without active ventilation, radon levels exceeded the national standard of 148 Bq/m^3. However, implementing direct ventilation reduced the radon concentration by 90% or more, highlighting the substantial impact of air exchange rates on upper-floor radon exposures. Meteorological analysis using Spearman rank correlations examined relationships between outdoor environmental parameters and radon concentrations for each floor (see Table A4). The analysis included outdoor temperature, relative humidity, precipitation amount, and outdoor pressure. These correlations were generally weak in magnitude, with only a handful of values with statistical significance, suggesting that while outdoor environmental conditions influence indoor radon levels, there is a weak correlation in the multi-story building context. Temperature and relative humidity showed statistically significant positive correlations for certain floors, though they are small in magnitude, with correlation coefficients up to 0.097. Outdoor pressure exhibited

significant negative correlations on Floors 4, 5, 8, 9, 11, and 12, with the strongest correlation observed on Floor 12 at -0.129. Precipitation amount showed limited correlations, with only Floors 5 and 11 displaying statistically significant relationships at 0.044 and -0.055, respectively.

Chapter 5 – Discussion

Chapter 5 provides an in-depth discussion of the main findings from the research topics presented in this thesis by integrating findings from predictive modelling, electronic radon monitor (ERM) performance evaluation, and policy implications for radon risk management in Canadian residences. The chapter examines the strengths and limitations of random forest (RF) models for radon exposure prediction, evaluates the practical utility and challenges of ERMs, and explores the evolving regulatory and public health landscape. This discussion highlights the interconnectedness between spatial and building-specific factors, the necessity of direct testing alongside predictive tools, and the emerging strategies for increasing radon awareness and mitigation, particularly in multi-family buildings. By synthesizing insights across the three research topics, this chapter aims to inform future research and policy development for improvements in residential radon management.

5.1 Predictive Modelling of Radon Exposure in Canadian Residences

The increasing application of machine learning approaches, particularly RF regression algorithms, has shown promise for radon mapping and predictive exposure modelling in Canadian residences. Recent studies, as well as the present work, have demonstrated that machine learning techniques frequently outperform traditional statistical methods in predicting radon concentrations across varied residential contexts [60], [184], [185], [193], [194]. RF models, in particular, have achieved higher explanatory power and predictive accuracy compared to classical multivariate regression and other statistical approaches, supporting their appeal as analytical tools concerning radon risk exposure.

Despite these advantages, it is important to acknowledge the limitations inherent to RF algorithms, especially when considering their use for radon exposure prediction. One of the most notable constraints is the inability of standard RF models to fully incorporate spatial correlations into predictions. This limitation is particularly consequential, as both the current study and numerous reports in the literature have consistently identified spatial variables among the most important predictors of residential radon concentrations [60], [110], [186],

[193]. For instance, the FSA repeatedly emerged as the dominant predictor in both the Health Canada (HC) and BCRDR datasets. However, this dominance may partly reflect a methodological bias as RF models tend to favour ordinal, target-encoded variables over purely categorical ones, and in this study, FSA was the only spatial variable encoded in this manner [169]. Other building-specific variables, many of which are inherently categorical and were encoded through one-hot methods, may thus have received less importance in the final models, not necessarily because they are less relevant, but due to the limitations of the algorithm in handling categorical data.

Nevertheless, the findings from both the HC and BCRDR RF models reveal that spatial predictors are consistently ranked as the top feature even in the presence of detailed building-specific characteristics, highlighting the necessity of explicitly accounting for spatial patterns in radon prediction models. However, with certain building-specific predictors, such as building type which ranked second in importance in the BCRDR model, cannot be ordinally encoded in a meaningful way due to their categorical nature and potentially high cardinality, therefore, there the selection of predictive modelling approaches needs to ensure it can adequately accommodate both ordinal and high-cardinality categorical features.

In the BCRDR dataset, the RF regression explained up to 47% of the variance in residential log-transformed radon concentrations, while the national HC dataset model accounted for 27%. This suggests that while spatial variables are essential to predictive modelling, they are insufficient to capture the full complexity of radon exposure on their own. Other building-specific factors also play critical roles in predictive power. For instance, from the findings of both datasets, the year of construction has increasingly been a determinant of indoor radon concentrations, as newer Canadian homes tend to have higher levels. This trend is partly attributable to changes in construction practices and evolving building codes. Other key predictors include season, building type, and floor tested. Thus, a well-calibrated predictive model should balance spatial variables with environmental and building-specific factors, which would be reflected in feature importance rankings, to achieve improved predictive performance.

5.2 Performance of Electronic Radon Monitors (ERMs)

The evaluation of ERMs in both short-term and long-term tests revealed a spectrum of performance outcomes, highlighting both the strengths and the limitations of these devices for consumer and public health use. A key observation from the long-term evaluation was the presence of systematic bias among several ERM models. Certain sensors, such as the FK, LCA, and RD2, consistently underestimated radon concentrations, presenting a negative bias. This underestimation is particularly concerning from a public health perspective, as it may result in users being unaware of elevated radon exposures that exceed national guidelines. Conversely, other sensors, including the CRAD and LB, demonstrated systematic overestimation, with relative percent errors (RPE) reaching as high as 146%. Overestimation, while less concerning in terms of health risk, can lead to unnecessary mitigation expenses and undue concern for homeowners. These findings are consistent with previous studies, such as Daraktchieva et al. (2024), which reported substantial overestimation in some consumer ERMs up to 94% [124].

Despite these variations, several sensors demonstrated acceptable agreement with reference instruments, characterized by low relative percent errors (RPE), percent ratios close to 100% (showing minimal bias) and low coefficients of variation (CV), all of which indicate good precision, accuracy and reliability. Notably, sensors that achieved RPE within 10% of the reference instrument offer promise for consumer use. These findings are also supported by other studies that found that ERMs such as the RadonEye (RE) measured within a 10% mean difference of the reference instrument [26], [129]. Warkentin et al. (2020) reported that the ERMs tested generally met an acceptable accuracy threshold of 20% measurement error [175].

It is important to note that the differences between short-term and long-term test results were apparent, particularly in linear regression, correlation coefficients, and RMSE scores. These discrepancies may reflect methodological limitations, such as differences in concentration ranges and test durations. For example, Rey et al. (2024) reported Spearman rank correlation coefficients similar to those observed in this study's short-term tests, but our long-term tests revealed lower and sometimes statistically insignificant correlations, likely due to reduced range in radon concentrations and a larger number of data points [130].

Focusing on long-term results, which align with Health Canada's recommended testing guidelines, the overall recall and precision of most ERMs were often limited, as reflected in lower F1 scores, particularly notable in the long-term test. The F1 score shows the ability of a sensor to capture radon concentrations above a threshold without excessive false positives. A high F1 score shows that the sensor is sensitive to radon measurements above the set threshold and minimally detects false alerts, whereas a low F1 score indicates the sensor is missing true events (false negatives) or incorrectly identifying events as true (false positives), suggesting limited reliability for consumer use. The short-term test results, although sometimes more favourable due to the high F1 scores (71% to 96%), may be misleading due to the greater frequency of certain concentration ranges and the distribution of radon measurements, especially the ones well above the 200 Bq/m^3 threshold, which can artificially inflate performance metrics. To further examine this effect, a sensitivity analysis was conducted by varying the thresholds from the original 200 Bq/m^3 to 300, 150, 100, and 50 Bq/m^3 for the short-term test, as summarized in Table 26. These thresholds were selected in correspondence with the distribution of radon concentrations throughout the entire testing period.

Table 26: Sensitivity Analysis on Confusion Matrix Threshold Parameter for Short-Term Test using F1 Score

Sensor	F1 Score at Threshold (Bq/m^3)			
	300 Bq/m^3	200 Bq/m^3 (Original)	100 Bq/m^3	50 Bq/m^3
RadonEye	100%	92%	84%	89%
Inkbird	100%	94%	86%	86%
Wave	96%	71%	72%	86%
Spirit	100%	96%	79%	84%

Among the ERMs with original F1 scores > 90% at 200 Bq/m^3, performance declined at the 100 Bq/m^3 threshold and showed a modest improvement at 50 Bq/m^3. The Wave exhibited a similar performance at 100 Bq/m^3, with a notable 15% improvement at 50 Bq/m^3. All ERMs demonstrated improved F1 scores at the highest threshold (300 Bq/m^3), with the Wave showing the most substantial improvement by 25%. These findings can be attributed to the distribution of the measurements, as 63% of reference instrument readings were between 0 – 100 Bq/m^3,

14% between 100 – 200 Bq/m^3, less than 2% between 200 – 1100 Bq/m^3, and the remainder at higher concentrations (1,100–1,800 Bq/m^3). The improved performance of the Wave at higher thresholds aligns with its tendency to underestimate radon levels, resulting in better classification when fewer measurements cluster around the new threshold. Conversely, the other ERMs, which showed high F1 scores at 200 Bq/m^3, exhibited decreased performance as the threshold was adjusted closer to the predominant measurement range. This highlights the importance of context, in terms of radon distribution and selecting thresholds used to classify measurements, when interpreting sensor performance. It also raises questions about the reliability of ERMs for consumer use, highlighting that confusion matrices should not be used as the sole method of assessment.

5.3 Policy, Technology, and Future of Radon Testing in Canada

Overall, the findings of this research have direct and important implications for radon policy, public health practice, and the future direction of residential radon risk management in Canada. At the core of this discussion is the persistent challenge of low public awareness regarding radon and its associated health risks, which remains a critical barrier to effective risk reduction. Addressing this gap requires a coordinated approach involving policymakers, public health agencies, researchers, and the general public.

Predictive modelling and radon risk mapping, enabled by advances in machine learning, offer valuable tools for identifying high-risk areas and prioritizing public health interventions. However, the results from this thesis and the literature indicate that these tools cannot fully replace direct measurement. Even the most advanced RF models, which incorporate both geological and building-specific variables, typically explain only a portion of the variance in indoor radon concentrations. For example, recent studies have reported that the highest R^2 values achieved by such models remain weak, with Wu et al. (2023) explaining only 24% of the variance in Swedish residences despite using detailed input data [186]. Petermann et al. (2021) developed an RF-based mapping of geogenic radon potential in Germany, where geological class was identified as the top predictor; however, the model was only able to explain 21% of the variance of radon concentrations [193]. The cross-dataset analysis in this research further

demonstrated the limited transferability and generalizability of predictive models across regions, emphasizing the influence of local factors and the need for context-specific data. Risk mapping and predictive analytics should therefore be understood as complementary to, rather than replacements for direct testing. These tools are most effective when used to inform the strategic allocation of resources, guide targeted awareness campaigns, and support the development of evidence-based policies. They can help identify priority areas for intervention but cannot capture the unique characteristics of individual homes or account for the full range of factors influencing radon exposure. This is particularly important in a country as geographically diverse as Canada, where local geology, building practices, and environmental conditions introduce substantial variability.

Low-cost ERMs have also emerged as promising tools for increasing access to radon testing, particularly through their convenience and immediate results. Their availability in online marketplaces and retail stores has the potential to expand public engagement with radon risk assessment. However, the results of this research, along with recent studies, raise important concerns regarding the accuracy, calibration, and long-term reliability of these devices. Many low-cost consumer ERMs lack calibration or certification of accuracy, and their performance may degrade over time or vary between units. For instance, Daraktchieva et al. (2024) found substantial changes in calibration over time for commonly used ERMs, with differences of up to 63% recorded after several years [124].

Given these findings, ERMs may be most effectively deployed in specific scenarios, such as short-term library lending programs aimed at raising awareness and encouraging initial testing. While short-term tests are less reliable than long-term tests, they can serve as a valuable screening tool, prompting further action if elevated concentrations are detected. ERMs also offer unique advantages for real-time monitoring, particularly before and after home renovations or changes to HVAC systems, which can influence indoor radon levels. Traditional passive long-term detectors are limited in this regard, as they provide only a cumulative exposure estimate over a fixed period.

Nevertheless, the use of ERMs should be approached with caution. User error, device malfunctions, and interface challenges can undermine the effectiveness of ERMs, emphasizing

the need for continued research and refinement. While ERMs hold considerable potential for expanding access to radon testing and raising public awareness, not all ERMs have acceptable performance and have been reviewed by reputable third-party organizations. For instance, the C-NRPP has recommended a list of low-cost ERMS, all of which were reviewed in the long-term tests, to consumers for guidance on which ERM is reliable [195]. Regulatory supervision, third-party testing, and clear consumer guidance are essential to ensure that only ERMs with demonstrated accuracy and reliability are essential to maximize their benefit and protect consumer safety.

While advances in predictive modelling and the availability of low-cost ERMs have broadened the toolkit for risk assessment, these tools cannot replace the foundational role of long-term direct testing using C-NRPP-approved devices, especially as Canadian housing stock diversifies and expands. Recent policy developments in Canada reflect a growing recognition of the need to address radon risk in a wider range of building types. The 2024 update to the National Building Code (NBC) introduced mandatory installation of passive vertical stacks in low-rise residences and ground-contact units of multi-unit buildings, marking a positive step toward prevention [163]. However, the effectiveness of these measures is contingent upon adoption by individual provinces and territories, and their impact is limited to new construction. With projections indicating the addition of a substantial number of new homes over the next decades, it is important to recognize that millions of existing homes remain untested, leaving a significant portion of the population at continued risk of radon exposure.

A further implication of this research is the need to expand radon testing and mitigation efforts beyond single-family homes to include multi-family buildings and other high-risk structures. Evidence from this thesis indicates that upper-floor units in multi-family buildings can, under certain conditions, exhibit radon concentrations equal to or exceeding those of ground-contact units or single-family homes. This challenges the conventional assumption that apartments are inherently lower risk and supports the case for inclusive testing policies. For example, studies investigating the influence of ventilation have shown that inadequate air exchange can lead to elevated radon levels even on upper floors, sometimes surpassing national WHO guidelines [80], [84], [86]. These findings reinforce the complexity of radon

distribution in multi-family dwellings, where factors such as ventilation, spatial location, and building materials interact in unpredictable ways.

Furthermore, the key predictors identified in this research, including spatial variables and building type, reinforce the need for nuanced, data-driven approaches to testing. Although building type ranked as the second and fifth most important feature in the BCRDR and HC models, respectively, it does not consistently emerge as a top predictor in the literature [185], [186], [193]. This variability highlights the importance of considering local context and the limitations of relying solely on predictive models for risk assessment. Instead, targeted testing strategies, informed by both predictive analytics and empirical data, are likely to be the most effective and cost-efficient. Cost-effectiveness analyses have repeatedly shown that focusing interventions in high-risk areas yields the greatest public health benefit, maximizing the number of lives saved per dollar spent [156], [161]. In New Jersey, for instance, regulations require testing of ground-contact units in multi-family buildings. However, Kitto et al. (2022) found that federal protocols mandating testing of only 10% to 25% of ground-contact units failed to identify 32% to 69% of units with radon levels above the EPA action level, depending on building size [160]. Their findings strongly support the implementation of 100% testing for ground-contact units in multi-family residences, as partial testing leaves a substantial number of residents at risk.

The findings from this thesis reinforce the need for ongoing investment in public testing initiatives and awareness campaigns, as these remain the most cost-effective means of identifying and mitigating radon exposure [156], [161], [196]. The evidence strongly supports the case for expanding and refining testing protocols. Testing focus should extend to more than just one residential building type, with particular attention to multi-family homes that are undertested compared to single-family homes. Predictive modelling should not replace testing, but instead, be used as a tool for identifying areas of high risk. A comprehensive approach that combines targeted interventions, robust regulation of testing devices, and persistent public engagement will be most effective in reducing radon-related health risks across Canada. The goal should be to ensure that every Canadian home, regardless of type or location, is assessed

for radon risk and has knowledge of their exposure, ultimately protecting the safety of all Canadians.

Chapter 6 – Conclusions

6.1 Summary & Conclusions

This thesis examined the complex issue of residential radon exposure in Canada through three research objectives: (O1) the development and validation of predictive models for residential radon concentrations using a holistic approach encompassing various geological, seasonal, and building-specific parameters; (O2) the performance assessment of low-cost electronic radon monitors (ERMs); and (O3) a field study characterizing radon concentrations in a high-rise, multi-family building.

The findings from the predictive modelling (O1) demonstrated that residential radon levels in Canada can be partially predicted using machine learning models trained on large-scale datasets. Random forest (RF) regression, applied to both Health Canada (HC) and British Columbia Radon Data Repository (BCRDR) datasets, achieved a maximum R^2 value of 0.47, indicating moderate predictive power and better performance than the conventional linear regression models. Among the input features, FSA consistently emerged as the most influential variable, highlighting the importance of spatial context in radon risk estimation. While these models offer valuable insights for targeted screening, their predictive accuracy remains insufficient for direct substitution of indoor testing. Nonetheless, they provide a promising tool for informing geographically focused interventions.

To address the second objective, low-cost ERMs were collocated against a research-grade reference instrument in both short- and long-term tests to assess their viability for residential radon monitoring. Although certain models demonstrated acceptable levels of accuracy, the majority showed considerable variance when compared to the reference instruments. Notably, response delays, high relative percent errors, and wide limits of agreement were observed in many devices, especially under stable or low-concentration conditions. Some sensors also showed declining performance with increases in radon concentrations. These findings emphasize the need for caution in deploying consumer-grade ERMs for regulatory or exposure assessments and point to the continued value of standardized, long-term testing using validated instruments.

The third objective addressed a significant research gap by monitoring and evaluating radon concentrations in a high-rise student residence over the long term. Results indicated that elevated radon levels are not limited to ground-contact units and can appear on upper floors. The concentrations in the building did not show correlation with building storey height, which contradicts the prevailing assumption that upper-floor units are inherently at low risk. We also observed spikes in radon concentrations, reaching levels up to 57 Bq/m^3 even when the average across all floors was 5.4 Bq/m^3. We suspect that this increase is likely caused by changes in air exchange rates due to changes in HVAC operation patterns at the end of the semester. This further highlights the need for more inclusive testing protocols that extend beyond single-family homes.

Collectively, these studies reinforce the complexity of radon distribution in the built environment and emphasize the limitations of relying solely on predictive models or low-cost devices for risk assessment. A comprehensive approach that integrates empirical testing, spatial analytics, robust sensor validation, and public education is essential to effectively manage residential radon risk in Canada.

6.2 Recommendations for Future Work

Given the moderate performance of current predictive models, future research should prioritize algorithmic refinement, particularly methods that better account for spatial dependence. Techniques such as CatBoost, which is designed to support categorical variables, or spatially explicit RF variants available in R, may yield improved performance and a more accurate ranking of feature importance [197]. Cross-validation across additional provinces and territories will also enhance the transferability and generalizability of radon risk models in the Canadian context.

Further development of ERMs should focus on real-world deployment studies, especially in diverse residential settings and across seasons, to benchmark long-term performance under practical constraints. Evaluation of other environmental conditions and their potential performance impact on the ERMs may also be considered. In addition, future work could also assess the usability, user interface, and data accessibility of these devices as these factors are

important to the adoption and sustained use by consumers. During testing, certain ERMs had technical difficulties with Wi-Fi connections or accessing the internal datalogging for data retrieval, which can all be deterrents for users. Circumventing these issues by selecting sensors that have reliable usability and curating a list of sensors that are easy to use with robust performance can help ensure an accurate estimation of radon exposure. There are also opportunities for ERMs to contribute to public education campaigns and integrate with smart home technologies, such as building automated systems, to help improve awareness and radon protection.

Future fieldwork should explore additional building archetypes, with continued focus on multi-unit dwellings and mixed-use complexes. Given the substantial variability observed across storeys in the same building, larger sample sizes and multi-site studies would enhance our understanding of radon trends and patterns. Moreover, research into the interaction between mechanical ventilation systems, building envelope characteristics, and meteorological influences could uncover new strategies for passive radon mitigation. Finally, policy-oriented research should evaluate the cost-effectiveness of different testing mandates, particularly in under-monitored building types. By coupling refined models with more access to other testing strategies and evidence-backed regulations, public health efforts can more effectively address the long-term risk of radon exposure for all Canadians.

6.3 Summary of Contributions and Publications

I conducted a rapid review comparing radon concentrations in single-family and multi-family residential dwellings that were accepted and presented at the Indoor Air 2024 ISIAQ Conference in Hawaii, US, contributing to international discourse on radon risk assessment across housing types. My work stemming from the short-term collocation tests of low-cost ERMs was selected for a podium presentation at the Healthy Buildings 2025 Conference in Reykjavik, Iceland, accompanied by the submission and acceptance of a peer-reviewed conference paper in the conference proceedings. This work has also been submitted to a special issue of *Indoor Environment* and is currently under review. Additionally, the findings from the short-term collocation test were presented at the invitation-only Radiation and Air

Pollutant Induced Disease (RAPID) Workshop 2024 for Canadian radon researchers and experts to share their findings.

Currently, three manuscripts are in preparation for submission to peer-reviewed journals. The first manuscript is a review paper which examines factors influencing indoor radon concentrations, integrating environmental and building-related predictors. The second details result from long-term collocation testing of low-cost ERMs, providing a comprehensive evaluation of sensor performance over extended monitoring periods. The third manuscript presents findings from the multi-family building field study, with particular focus on floor-by-floor radon variability and the roles of ventilation and building design.

Beyond the radon research, I also contributed to the broader field of indoor air quality. I quantified the particle emissions and the cooking performance of induction stoves, which were presented at the podium for the same Indoor Air 2024 ISIAQ Conference, reflecting broader engagement with topics in indoor air quality and residential environmental health.

References

[1] A. Grzywa-Celińska, A. Krusiński, J. Mazur, K. Szewczyk, and K. Kozak, "Radon—The Element of Risk. The Impact of Radon Exposure on Human Health," *Toxics*, vol. 8, no. 4, p. 120, Dec. 2020, doi: 10.3390/toxics8040120.

[2] Evict Radon National Study, BC Centre for Disease Control, and Health Canada, "Cross-Canada Survey of Radon Exposure in the Residential Buildings of Urban and Rural Communities." Accessed: Nov. 23, 2024. [Online]. Available: https://crosscanadaradon.ca/survey/

[3] R. W. Field, "Radon: An Overview of Health Effects," in *Encyclopedia of Environmental Health*, 2011, pp. 745–753. doi: 10.1016/B978-0-444-52272-6.00095-7.

[4] S. C. Mema and G. Baytalan, "Radon and lung cancer risk," *CMAJ*, vol. 195, no. 24, pp. E850–E850, Jun. 2023, doi: 10.1503/cmaj.230110.

[5] World Health Organization, H. Zeeb, and F. Shannoun, "WHO handbook on indoor radon: a public health perspective," 2009, Accessed: Dec. 02, 2024. [Online]. Available: https://iris.who.int/handle/10665/44149

[6] S. Darby *et al.*, "Radon in homes and risk of lung cancer: collaborative analysis of individual data from 13 European case-control studies," *BMJ*, vol. 330, no. 7485, p. 223, Jan. 2005, doi: 10.1136/bmj.38308.477650.63.

[7] Health Canada, "Radon action guide for provinces and territories: Overview." Accessed: Apr. 21, 2025. [Online]. Available: https://www.canada.ca/en/health-canada/services/health-risks-safety/radiation/radon/action-guides/provinces-territories.html

[8] Health Canada, "Cross-Canada Survey of Radon Concentrations in Homes - Final Report." Accessed: Sep. 14, 2023. [Online]. Available: https://www.canada.ca/en/health-canada/services/environmental-workplace-health/reports-publications/radiation/cross-canada-survey-radon-concentrations-homes-final-report-health-canada-2012.html

[9] S. M. Khan, D. D. Pearson, T. Rönnqvist, M. E. Nielsen, J. M. Taron, and A. A. Goodarzi, "Rising Canadian and falling Swedish radon gas exposure as a consequence of 20th to 21st century residential build practices," *Sci Rep*, vol. 11, no. 1, Art. no. 1, Sep. 2021, doi: 10.1038/s41598-021-96928-x.

[10] F. K. T. Stanley *et al.*, "Comprehensive survey of household radon gas levels and risk factors in southern Alberta," *CMAJ Open*, vol. 5, no. 1, pp. E255–E264, Mar. 2017, doi: 10.9778/cmajo.20160142.

[11] F. K. T. Stanley *et al.*, "Radon exposure is rising steadily within the modern North American residential environment, and is increasingly uniform across seasons," *Sci Rep*, vol. 9, no. 1, Art. no. 1, Dec. 2019, doi: 10.1038/s41598-019-54891-8.

[12] J. A. Simms *et al.*, "Younger North Americans are exposed to more radon gas due to occupancy biases within the residential built environment," *Scientific Reports*, vol. 11, no. 1, 2021, doi: 10.1038/s41598-021-86096-3.

[13] S. M. Khan, D. Krewski, J. Gomes, and R. Deonandan, "Radon, an invisible killer in Canadian homes: perceptions of Ottawa-Gatineau residents," *Canadian Journal of Public Health*, vol. 110, no. 2, pp. 139–148, 2019, doi: 10.17269/s41997-018-0151-5.

[14] S. M. Khan and S. Chreim, "Residents' perceptions of radon health risks: A qualitative study," *BMC Public Health*, vol. 19, no. 1, 2019, doi: 10.1186/s12889-019-7449-y.

[15] O. Alber, C. Laubichler, S. Baumann, V. Gruber, S. Kuchling, and C. Schleicher, “Modeling and predicting mean indoor radon concentrations in Austria by generalized additive mixed models,” *Stoch Environ Res Risk Assess*, vol. 37, no. 9, pp. 3435–3449, Sep. 2023, doi: 10.1007/s00477-023-02457-6.
[16] E. Petermann and P. Bossew, “Mapping indoor radon hazard in Germany: The geogenic component,” *Science of The Total Environment*, vol. 780, p. 146601, Aug. 2021, doi: 10.1016/j.scitotenv.2021.146601.
[17] A. R. Denman *et al.*, “Small area mapping of domestic radon, smoking prevalence and lung cancer incidence - A case study in Northamptonshire, UK,” *Journal of Environmental Radioactivity*, vol. 150, pp. 159–169, 2015, doi: 10.1016/j.jenvrad.2015.08.012.
[18] C-NRPP, “C-NRPP Listed Professional Devices,” C-NRPP. Accessed: Jan. 16, 2025. [Online]. Available: https://c-nrpp.ca/approved-radon-measurement-devices/
[19] D. Rábago *et al.*, “Investigation of the Performance of Various Low-Cost Radon Monitors under Variable Environmental Conditions,” *Sensors*, vol. 24, no. 6, Art. no. 6, Jan. 2024, doi: 10.3390/s24061836.
[20] J. F. Rey, N. Meisser, D. Licina, and J. Goyette Pernot, “Performance evaluation of radon active sensors and passive dosimeters at low and high radon concentrations,” *Building and Environment*, vol. 250, p. 111154, Feb. 2024, doi: 10.1016/j.buildenv.2023.111154.
[21] P. Warkentin, “Canadian National Radon Proficiency Program - 2023 Intercomparison Report,” 2023.
[22] T. R. Beck, E. Foerster, M. Biel, and S. Feige, “Measurement Performance of Electronic Radon Monitors,” *Atmosphere*, vol. 15, no. 10, Art. no. 10, Oct. 2024, doi: 10.3390/atmos15101180.
[23] A. Giang and T. Li, “Rapid Review of Radon Concentrations in Multi-Family Dwellings,” in *18th International Conference on Indoor Air Quality and Climate (INDOOR AIR 2024)*, Honolulu, Hawaii: ISIAQ, 2024, p. 1670.
[24] S. C. Government of Canada, “Focus on Geography Series, 2021 Census - Canada.” Accessed: May 29, 2025. [Online]. Available: https://www12.statcan.gc.ca/census-recensement/2021/as-sa/fogs-spg/page.cfm?lang=E&topic=3&dguid=2021A000011124
[25] V. C. Trassierra, F. Cardellini, G. Buonanno, and P. De Felice, “On the interaction between radon progeny and particles generated by electronic and traditional cigarettes,” *Atmospheric Environment*, vol. 106, pp. 442–450, 2015, doi: 10.1016/j.atmosenv.2014.06.017.
[26] J. McLaughlin, “An overview of thoron and its progeny in the indoor environment,” *Radiation Protection Dosimetry*, vol. 141, no. 4, pp. 316–321, Oct. 2010, doi: 10.1093/rpd/ncq234.
[27] R. W. Field, “Radon: An Overview of Health Effects,” in *Encyclopedia of Environmental Health*, 2011, pp. 745–753. doi: 10.1016/B978-0-444-52272-6.00095-7.
[28] M. Mannan and S. G. Al-Ghamdi, “Indoor Air Quality in Buildings: A Comprehensive Review on the Factors Influencing Air Pollution in Residential and Commercial Structure,” *Int J Environ Res Public Health*, vol. 18, no. 6, p. 3276, Mar. 2021, doi: 10.3390/ijerph18063276.
[29] J.-K. Kang, S. Seo, and Y. W. Jin, “Health Effects of Radon Exposure,” *Yonsei Medical Journal*, vol. 60, no. 7, pp. 597–603, Jul. 2019, doi: 10.3349/ymj.2019.60.7.597.

[30] L. Zhang *et al.*, “Indoor Particulate Matter in Urban Households: Sources, Pathways, Characteristics, Health Effects, and Exposure Mitigation,” *Int J Environ Res Public Health*, vol. 18, no. 21, p. 11055, Oct. 2021, doi: 10.3390/ijerph182111055.
[31] O. US EPA, “Radiation Basics.” Accessed: Jan. 06, 2025. [Online]. Available: https://www.epa.gov/radiation/radiation-basics
[32] National Academy of Sciences, *Health Effects of Exposure to Radon: BEIR VI, Committee on Health Risks of Exposure to Radon (BEIR VI)*. Washington, D.C.: National Academy Press, 1999. doi: 10.17226/5499.
[33] S.-H. Kim, W. J. Hwang, J.-S. Cho, and D. R. Kang, “Attributable risk of lung cancer deaths due to indoor radon exposure,” *Ann Occup Environ Med*, vol. 28, p. 8, Feb. 2016, doi: 10.1186/s40557-016-0093-4.
[34] L. Corrales, R. Rosell, A. F. Cardona, C. Martín, Z. L. Zatarain-Barrón, and O. Arrieta, “Lung cancer in never smokers: The role of different risk factors other than tobacco smoking,” *Critical Reviews in Oncology/Hematology*, vol. 148, p. 102895, Apr. 2020, doi: 10.1016/j.critrevonc.2020.102895.
[35] J. Chen, “A Summary of Residential Radon Surveys and the Influence of Housing Characteristics on Indoor Radon Levels in Canada,” *Health Physics*, vol. 121, no. 6, p. 574, Dec. 2021, doi: 10.1097/HP.0000000000001469.
[36] L. Gulan, J. M. Stajic, D. Spasic, and S. Forkapic, “Radon levels and indoor air quality after application of thermal retrofit measures—a case study,” *Air Qual Atmos Health*, vol. 16, no. 2, pp. 363–373, 2023, doi: 10.1007/s11869-022-01278-w.
[37] S. M. Khan *et al.*, “Rural communities experience higher radon exposure versus urban areas, potentially due to drilled groundwater well annuli acting as unintended radon gas migration conduits,” *Sci Rep*, vol. 14, no. 1, p. 3640, Feb. 2024, doi: 10.1038/s41598-024-53458-6.
[38] M. Trautmannsheimer, W. Schindlmeier, and K. Hübel, “Radon exposure levels of the staff in the drinking water supply facilities in Bavaria, Germany,” *International Congress Series*, vol. 1225, pp. 81–86, Feb. 2002, doi: 10.1016/S0531-5131(01)00517-9.
[39] Y. Manawi, A. Hassan, M. A. Atieh, and J. Lawler, “Overview of radon gas in groundwater around the world: Health effects and treatment technologies,” *Journal of Environmental Management*, vol. 368, p. 122176, Sep. 2024, doi: 10.1016/j.jenvman.2024.122176.
[40] H. Büyükuslu, F. B. Özdemir, T. Ö. Öge, and H. Gökce, “Indoor and tap water radon (222Rn) concentration measurements at Giresun University campus areas,” *Applied Radiation and Isotopes*, vol. 139, pp. 285–291, Sep. 2018, doi: 10.1016/j.apradiso.2018.05.027.
[41] G. P. Bernhardt and C. T. Hess, “Acute exposure from 222Rn and aerosols in drinking water,” *Environment International*, vol. 22, pp. 753–759, Jan. 1996, doi: 10.1016/S0160-4120(96)00179-1.
[42] Health Canada, “Radon - What you need to know factsheet,” Government of Canada, 2024. Accessed: Jan. 07, 2025. [Online]. Available: https://www.canada.ca/content/dam/hc-sc/documents/services/health/publications/radon/radon-what-you-need-to-know-factsheet.pdf

[43] T. Valmari, H. Arvela, and H. Reisbacka, “Radon in Finnish apartment buildings,” *Radiation Protection Dosimetry*, vol. 152, no. 1–3, pp. 146–149, Nov. 2012, doi: 10.1093/rpd/ncs211.
[44] I. Yarmoshenko, G. Malinovsky, A. Vasilyev, and A. Onishchenko, “Model of radon entry and accumulation in multi-flat energy-efficient buildings,” *Journal of Environmental Chemical Engineering*, vol. 9, no. 4, p. 105444, Aug. 2021, doi: 10.1016/j.jece.2021.105444.
[45] A. P. D. Baltrocchi *et al.*, “Mechanisms of Diffusion of Radon in Buildings and Mitigation Techniques,” *Sustainability*, vol. 16, no. 1, Art. no. 1, Jan. 2024, doi: 10.3390/su16010324.
[46] P.-Y. Wu, T. Johansson, M. Mangold, C. Sandels, and K. Mjörnell, “Estimating the probability distributions of radioactive concrete in the building stock using Bayesian networks,” *Expert Systems with Applications*, vol. 222, p. 119812, Jul. 2023, doi: 10.1016/j.eswa.2023.119812.
[47] H. Bem, S. Janiak, and B. Przybył, “Survey of indoor radon (Rn-222) entry and concentrations in different types of building in Kalisz, Poland,” *Journal of Radioanalytical and Nuclear Chemistry*, vol. 326, no. 2, pp. 1299–1306, 2020, doi: 10.1007/s10967-020-07394-0.
[48] R. Yang, J. Wang, X. Zhang, J. Li, and M. Chen, “Radon exhalation from cement-based materials under accelerated carbonation,” *Environmental Science and Pollution Research*, vol. 30, no. 17, pp. 50610–50619, 2023, doi: 10.1007/s11356-023-25831-x.
[49] S. Antignani *et al.*, “A 10-year follow-up study of yearly indoor radon measurements in homes, review of other studies and implications on lung cancer risk estimates,” *Science of The Total Environment*, vol. 762, p. 144150, Mar. 2021, doi: 10.1016/j.scitotenv.2020.144150.
[50] G. Kropat *et al.*, “Major influencing factors of indoor radon concentrations in Switzerland,” *Journal of Environmental Radioactivity*, vol. 129, pp. 7–22, 2014, doi: 10.1016/j.jenvrad.2013.11.010.
[51] Z. Stojanovska, J. Januseski, P. Bossew, Z. S. Zunic, T. Tollefsen, and M. Ristova, “Seasonal indoor radon concentration in FYR of Macedonia,” *Radiation Measurements*, vol. 46, no. 6–7, pp. 602–610, Jun. 2011, doi: 10.1016/j.radmeas.2011.04.022.
[52] C. K. Man and H. S. Yeung, “Modeling and measuring the indoor radon concentrations in high-rise buildings in Hong Kong,” *Applied Radiation and Isotopes*, vol. 50, no. 6, pp. 1131–1135, Jun. 1999, doi: 10.1016/S0969-8043(98)00128-6.
[53] S. M. Khan, J. Gomes, and D. R. Krewski, “Radon interventions around the globe: A systematic review,” *Heliyon*, vol. 5, no. 5, 2019, doi: 10.1016/j.heliyon.2019.e01737.
[54] J. Chen, N. M. Rahman, and I. A. Atiya, “Radon exhalation from building materials for decorative use,” *Journal of Environmental Radioactivity*, vol. 101, no. 4, pp. 317–322, Apr. 2010, doi: 10.1016/j.jenvrad.2010.01.005.
[55] I. Finne *et al.*, “Overview of radon management in the Nordic countries,” Swedish Radiation Safety Authority SSM, Stockholm, Nordic Working Group on Natural Ionizing Radiation (Nordic-Nat) 01:2024, 2024. Accessed: Jan. 09, 2025. [Online]. Available: https://www.stralsakerhetsmyndigheten.se/en/publications/reports/nordic-series/012024/

[56] L. Mjönes, H. Arvela, I. Finne, T. Strand, and K. Ulbak, “Recommendations for radon in dwellings in the Nordic countries.” Accessed: Jan. 09, 2025. [Online]. Available: https://dsa.no/en/publications/recommendations-for-radon-in-dwellings-in-the-nordic-countries/Recommendations%20for%20radon%20in%20dwellings%20in%20the%20Nordic%20countries.pdf
[57] R. Borgoni, V. Tritto, C. Bigliotto, and D. De Bartolo, “A Geostatistical Approach to Assess the Spatial Association between Indoor Radon Concentration, Geological Features and Building Characteristics: The Case of Lombardy, Northern Italy,” *International Journal of Environmental Research and Public Health*, vol. 8, no. 5, Art. no. 5, May 2011, doi: 10.3390/ijerph8051420.
[58] J. Elío *et al.*, “The first version of the Pan-European Indoor Radon Map,” *Natural Hazards and Earth System Sciences*, vol. 19, no. 11, pp. 2451–2464, Nov. 2019, doi: 10.5194/nhess-19-2451-2019.
[59] B. Olsthoorn *et al.*, “Indoor radon exposure and its correlation with the radiometric map of uranium in Sweden,” *Science of The Total Environment*, vol. 811, p. 151406, Mar. 2022, doi: 10.1016/j.scitotenv.2021.151406.
[60] F. Rezaie *et al.*, “Application of Machine Learning Algorithms for Geogenic Radon Potential Mapping in Danyang-Gun, South Korea,” *Front. Environ. Sci.*, vol. 9, Sep. 2021, doi: 10.3389/fenvs.2021.753028.
[61] R. J. Watson, M. A. Smethurst, G. V. Ganerød, I. Finne, and A. L. Rudjord, “The use of mapped geology as a predictor of radon potential in Norway,” *J Environ Radioact*, vol. 166, no. Pt 2, pp. 341–354, Jan. 2017, doi: 10.1016/j.jenvrad.2016.05.031.
[62] H. A. P. Smit and J. Bezuidenhout, “Influence of climate and weather on the mitigation of radon exposure in two towns of the Western Cape, South Africa,” *Journal of Radiation Research and Applied Sciences*, vol. 14, no. 1, pp. 236–245, Dec. 2021, doi: 10.1080/16878507.2021.1940750.
[63] E. Algin, C. Asici, H. Sogukpinar, and N. Akkurt, “A CASE STUDY ON THE USE OF SEASONAL CORRECTION FACTORS FOR INDOOR RADON MEASUREMENTS,” *Radiation Protection Dosimetry*, vol. 183, no. 4, pp. 423–431, Jun. 2019, doi: 10.1093/rpd/ncy161.
[64] P. Baltrėnas, R. Grubliauskas, and V. Danila, “Seasonal Variation of Indoor Radon Concentration Levels in Different Premises of a University Building,” *Sustainability*, vol. 12, no. 15, Art. no. 15, Jan. 2020, doi: 10.3390/su12156174.
[65] Ó. Burke, S. Long, P. Murphy, C. Organo, D. Fenton, and P. A. Colgan, “Estimation of seasonal correction factors through Fourier decomposition analysis—a new model for indoor radon levels in Irish homes,” *J. Radiol. Prot.*, vol. 30, no. 3, pp. 433–443, Sep. 2010, doi: 10.1088/0952-4746/30/3/002.
[66] A. R. Denman, R. G. M. Crockett, C. J. Groves-Kirkby, P. S. Phillips, G. K. Gillmore, and A. C. Woolridge, “The value of Seasonal Correction Factors in assessing the health risk from domestic radon—A case study in Northamptonshire, UK,” *Environment International*, vol. 33, no. 1, pp. 34–44, Jan. 2007, doi: 10.1016/j.envint.2006.06.021.
[67] E. A. Merrill and F. Akbar-Khanzadeh, “Diurnal and Seasonal Variations of Radon Levels, Effects of Climatic Conditions, and Radon Exposure Assessment in a Former Uranium Metal Production Facility,” *Health Physics*, vol. 74, no. 5, p. 568, May 1998.

[68] J. H. Park, C. M. Lee, H. Y. Lee, and D. R. Kang, “Estimation of Seasonal Correction Factors for Indoor Radon Concentrations in Korea,” *Int J Environ Res Public Health*, vol. 15, no. 10, p. 2251, Oct. 2018, doi: 10.3390/ijerph15102251.
[69] J. Porstendorfer, G. Butterweck, and A. Reineking, “Daily Variation of the Radon Concentration Indoors and Outdoors and the Influence of Meteorological Parameters,” *Health Physics*, vol. 67, no. 3, p. 283, Sep. 1994.
[70] E. G. Vogiannis and D. Nikolopoulos, “Radon Sources and Associated Risk in Terms of Exposure and Dose,” *Front. Public Health*, vol. 2, Jan. 2015, doi: 10.3389/fpubh.2014.00207.
[71] I. Seftelis, G. Nicolaou, S. Trassanidis, and F. N. Tsagas, “Diurnal variation of radon progeny,” *Journal of Environmental Radioactivity*, vol. 97, no. 2, pp. 116–123, Oct. 2007, doi: 10.1016/j.jenvrad.2007.03.007.
[72] S. L. M. F. Kamgang, M. M. Monti, and A. Salame-Alfie, “Temporal Variation in Indoor Radon Concentrations Using Environmental Public Health Tracking Data,” *Health Phys*, vol. 124, no. 4, pp. 342–347, Apr. 2023, doi: 10.1097/HP.0000000000001671.
[73] J. Pinel, T. Fearn, S. C. Darby, and J. C. H. Miles, “Seasonal Correction Factors for Indoor Radon Measurements in the United Kingdom,” *Radiation Protection Dosimetry*, vol. 58, no. 2, pp. 127–132, Feb. 1995, doi: 10.1093/oxfordjournals.rpd.a082606.
[74] C. Di Carlo *et al.*, “Extreme reverse seasonal variations of indoor radon concentration and possible implications on some measurement protocols and remedial strategies,” *Environmental Pollution*, vol. 327, p. 121480, Jun. 2023, doi: 10.1016/j.envpol.2023.121480.
[75] D. Spasić and L. Gulan, “High Indoor Radon Case Study: Influence of Meteorological Parameters and Indication of Radon Prone Area,” *Atmosphere*, vol. 13, no. 12, Art. no. 12, Dec. 2022, doi: 10.3390/atmos13122120.
[76] B. Levesque *et al.*, “Radon in Residences: Influences of Geological and Housing Characteristics,” *Health Physics*, vol. 72, no. 6, p. 907, Jun. 1997.
[77] J. Milner *et al.*, “Home energy efficiency and radon related risk of lung cancer: modelling study,” *BMJ*, vol. 348, p. f7493, Jan. 2014, doi: 10.1136/bmj.f7493.
[78] W. Meyer, “Impact of constructional energy-saving measures on radon levels indoors,” *Indoor Air*, vol. 29, no. 4, pp. 680–685, 2019, doi: 10.1111/ina.12553.
[79] L. Du, V. Leivo, T. Prasauskas, M. Täubel, D. Martuzevicius, and U. Haverinen-Shaughnessy, “Effects of energy retrofits on Indoor Air Quality in multifamily buildings,” *Indoor Air*, vol. 29, no. 4, pp. 686–697, 2019, doi: 10.1111/ina.12555.
[80] A. V. Vasilyev, I. V. Yarmoshenko, and M. V. Zhukovsky, “Low air exchange rate causes high indoor radon concentration in energy-efficient buildings,” *Radiation Protection Dosimetry*, vol. 164, no. 4, pp. 601–605, Jun. 2015, doi: 10.1093/rpd/ncv319.
[81] M. Kolovou, C. Potiriadis, and N. Kallithrakas-Kontos, “A study on the correlation between indoor radon concentrations and the construction year of the dwellings,” *Eur. Phys. J. Spec. Top.*, vol. 232, no. 10, pp. 1625–1629, Aug. 2023, doi: 10.1140/epjs/s11734-023-00888-4.
[82] J. A. McGrath, R. Aghamolaei, J. O’Donnell, and M. A. Byrne, “Factors influencing radon concentration during energy retrofitting in domestic buildings: A computational

evaluation," *Building and Environment*, vol. 194, p. 107712, May 2021, doi: 10.1016/j.buildenv.2021.107712.
[83] N. V. Bakaeva and A. V. Kalaydo, "Prediction of radon concentrations in above-ground apartments," *Journal of Applied Engineering Science*, vol. 15, no. 3, pp. 280–285, 2017, doi: 10.5937/jaes15-14656.
[84] S. Jeong and H.-T. Chon, "Indoor radon measurements of the multi-storey buildings in Seoul, Korea," *Geosystem Engineering*, vol. 16, no. 4, pp. 289–295, 2013, doi: 10.1080/12269328.2013.861642.
[85] J. Jeong and K. Cho, "Experimental Study on CO2 and Radon Mitigations in an Apartment Using a Mechanical Ventilation System," *Buildings*, vol. 13, no. 6, 2023, doi: 10.3390/buildings13061439.
[86] J. Dehnert *et al.*, "Radon protection in apartments using a ventilation system wireless-controlled by radon activity concentration," *J. Radiol. Prot.*, vol. 41, no. 3, p. S109, Aug. 2021, doi: 10.1088/1361-6498/abfc97.
[87] M. V. Zhukovsky, I. V. Yarmoshenko, A. D. Onishchenko, G. P. Malinovsky, A. V. Vasilyev, and E. I. Nazarov, "Assessment of radon levels in multistory buildings on example of eight Russian cities," *Radiatsionnaya Gygiena*, vol. 15, no. 1, pp. 47–58, 2022, doi: 10.21514/1998-426X-2022-15-1-47-58.
[88] V. Gruber, S. Baumann, G. Wurm, W. Ringer, and O. Alber, "The new Austrian indoor radon survey (ÖNRAP 2, 2013–2019): Design, implementation, results," *Journal of Environmental Radioactivity*, vol. 233, p. 106618, Jul. 2021, doi: 10.1016/j.jenvrad.2021.106618.
[89] S. Yang, J. Goyette Pernot, C. Hager Jörin, H. Niculita-Hirzel, V. Perret, and D. Licina, "Radon Investigation in 650 Energy Efficient Dwellings in Western Switzerland: Impact of Energy Renovation and Building Characteristics," *Atmosphere*, vol. 10, no. 12, Art. no. 12, Dec. 2019, doi: 10.3390/atmos10120777.
[90] H. Arvela, O. Holmgren, and H. Reisbacka, "Radon prevention in new construction in Finland: a nationwide sample survey in 2009," *Radiation Protection Dosimetry*, vol. 148, no. 4, pp. 465–474, Mar. 2012, doi: 10.1093/rpd/ncr192.
[91] R. Tianshan, L. Lianqing, C. Zhipeng, L. Guiyuan, and C. Amin, "Indoor 222Rn measurements in the region of beijing, people's Republic of China," *Health Physics*, vol. 53, no. 3, pp. 219–225, 1987, doi: 10.1097/00004032-198709000-00001.
[92] V. Udovicic *et al.*, "Radon variability due to floor level in two typical residential buildings in Serbia," *Nukleonika*, vol. 65, no. 2, pp. 121–125, May 2020, doi: 10.2478/nuka-2020-0019.
[93] G. Gallelli, D. Panatto, P. Lai, P. Orlando, and D. Risso, "Relevance of main factors affecting radon concentration in multi-storey buildings in Liguria (Northern Italy)," *Journal of Environmental Radioactivity*, vol. 39, no. 2, pp. 117–128, Feb. 1998, doi: 10.1016/S0265-931X(97)00056-8.
[94] J. Choi *et al.*, "Comparison of Indoor Radon Reduction Effects Based on Apartment Housing Ventilation Methods," *Atmosphere*, vol. 13, no. 2, 2022, doi: 10.3390/atmos13020204.
[95] T. Rönnqvist and R. L. Ab, "2021-28 Analysis of Radon Levels in Swedish Dwellings and Workplaces," 2021.

[96] K. Kojo, T. Turtiainen, O. Holmgren, and P. Kurttio, “Radon Exposure Concentrations in Finnish Workplaces,” *Health Physics*, vol. 125, no. 2, p. 92, Aug. 2023, doi: 10.1097/HP.0000000000001692.
[97] C. Su *et al.*, “Indoor exposure levels of radon in dwellings, schools, and offices in China from 2000 to 2020: A systematic review,” *Indoor Air*, vol. 32, no. 1, p. e12920, 2022, doi: 10.1111/ina.12920.
[98] L. X. Yang, T. L. Kirkham, L. Boksman, A.-M. Nicol, and P. A. Demers, “Characterizing Radon Among Public Buildings and Small/Medium-Sized Businesses in a Canadian Province,” *Atmosphere*, vol. 16, no. 1, Art. no. 1, Jan. 2025, doi: 10.3390/atmos16010021.
[99] J. Vaupotič, “Radon in kindergartens and schools-a review,” in *Handbook of Radon: Properties, Applications and Health*, 2012, pp. 447–494. [Online]. Available: https://www.scopus.com/inward/record.uri?eid=2-s2.0-84876287261&partnerID=40&md5=a8e38e85ddb6b2b8a859c6b98b9345f6
[100] S. H. Hwang and W. M. Park, “Radon and PM10 concentrations in underground parking lots and subway stations with health risks in South Korea,” *Environ Sci Pollut Res*, vol. 25, no. 35, pp. 35242–35248, Dec. 2018, doi: 10.1007/s11356-018-3428-6.
[101] E. Petermann, P. Bossew, J. Kemski, V. Gruber, N. Suhr, and B. Hoffmann, “Development of a High-Resolution Indoor Radon Map Using a New Machine Learning-Based Probabilistic Model and German Radon Survey Data,” *Environmental Health Perspectives*, vol. 132, no. 9, p. 097009, Sep. 2024, doi: 10.1289/EHP14171.
[102] E. Benà *et al.*, “A new perspective in radon risk assessment: Mapping the geological hazard as a first step to define the collective radon risk exposure,” *Science of The Total Environment*, vol. 912, p. 169569, Feb. 2024, doi: 10.1016/j.scitotenv.2023.169569.
[103] L. Li, B. A. Coull, C. L. Zilli Vieira, and P. Koutrakis, “High-resolution national radon maps based on massive indoor measurements in the United States,” *Proceedings of the National Academy of Sciences*, vol. 122, no. 3, p. e2408084121, Jan. 2025, doi: 10.1073/pnas.2408084121.
[104] UK Health Security Agency, “UKradon - UK maps of radon,” UKradon. Accessed: Jun. 01, 2025. [Online]. Available: https://www.ukradon.org/information/ukmaps
[105] F. Ambrosino, G. La Verde, G. Della Peruta, R. Mottareale, and M. Pugliese, “Italian National Radon Action Plan: The state of the Art in Campania Region,” in *2024 IEEE International Workshop on Metrology for Living Environment (MetroLivEnv)*, Jun. 2024, pp. 307–311. doi: 10.1109/MetroLivEnv60384.2024.10615884.
[106] J. Trieu, C. Young, P. D. M. Nguyen, A.-M. Nicol, S. B. Henderson, and D. McVea, “The BC Radon Data Repository (BCRDR) and BC Radon Map: Integrating disparate data sources for improved public health communication,” *Canadian Journal of Public Health*, vol. 115, no. 4, pp. 680–687, Aug. 2024, doi: 10.17269/s41997-024-00895-5.
[107] P.-Y. Wu, T. Johansson, C. Sandels, M. Mangold, and K. Mjörnell, “Indoor radon interval prediction in the Swedish building stock using machine learning,” *Building and Environment*, vol. 245, p. 110879, Nov. 2023, doi: 10.1016/j.buildenv.2023.110879.
[108] J. Elío, E. Petermann, P. Bossew, and M. Janik, “Machine learning in environmental radon science,” *Applied Radiation and Isotopes*, vol. 194, p. 110684, Apr. 2023, doi: 10.1016/j.apradiso.2023.110684.

[109] T. Dicu *et al.*, “Exploring statistical and machine learning techniques to identify factors influencing indoor radon concentration,” *Science of The Total Environment*, vol. 905, p. 167024, Dec. 2023, doi: 10.1016/j.scitotenv.2023.167024.
[110] L. Li, R. A. Stern, E. Garshick, C. L. Zilli Vieira, B. Coull, and P. Koutrakis, “Predicting Monthly Community-Level Radon Concentrations with Spatial Random Forest in the Northeastern and Midwestern United States,” *Environ. Sci. Technol.*, vol. 57, no. 46, pp. 18001–18012, Nov. 2023, doi: 10.1021/acs.est.2c08840.
[111] E. Petermann, H. Meyer, M. Nussbaum, and P. Bossew, “Mapping the geogenic radon potential for Germany by machine learning,” *Science of The Total Environment*, vol. 754, p. 142291, Feb. 2021, doi: 10.1016/j.scitotenv.2020.142291.
[112] E. Petermann, P. Bossew, J. Kemski, V. Gruber, N. Suhr, and B. Hoffmann, “Development of a High-Resolution Indoor Radon Map Using a New Machine Learning-Based Probabilistic Model and German Radon Survey Data,” *Environmental Health Perspectives*, vol. 132, no. 9, p. 097009, Sep. 2024, doi: 10.1289/EHP14171.
[113] P.-Y. Wu, T. Johansson, M. Mangold, C. Sandels, and K. Mjörnell, “Evaluating the indoor radon concentrations in the Swedish building stock using statistical and machine learning,” *J. Phys.: Conf. Ser.*, vol. 2654, no. 1, p. 012086, Dec. 2023, doi: 10.1088/1742-6596/2654/1/012086.
[114] S. Baumann *et al.*, “Radon hazard mapping: usability of environmental predictors including atmospheric radon and radon flux and knowledge transfer between regions (Belgium and Germany),” *Environ Earth Sci*, vol. 84, no. 7, p. 196, Apr. 2025, doi: 10.1007/s12665-025-12126-2.
[115] C. Lee and D. Lee, “Review of domestic and international methods of measuring radon in residential buildings,” *Ann Occup Environ Med*, vol. 28, p. 14, Mar. 2016, doi: 10.1186/s40557-016-0097-0.
[116] N. Celebi, B. Ataksor, H. Taskın, and N. A. Bingoldag, “Indoor radon measurements in Turkey dwellings,” *Radiation Protection Dosimetry*, vol. 167, no. 4, pp. 626–632, Dec. 2015, doi: 10.1093/rpd/ncu329.
[117] J. Park, Y.-J. Kim, B.-U. Chang, J.-Y. Kim, and K. P. Kim, “Assessment of indoor radon exposure in South Korea,” *J. Radiol. Prot.*, vol. 43, no. 2, p. 021506, Jun. 2023, doi: 10.1088/1361-6498/acc8e0.
[118] H. Synnott, O. Hanley, D. Fenton, and P. A. Colgan, “Radon in Irish schools: the results of a national survey,” *J Radiol Prot*, vol. 26, no. 1, pp. 85–96, Mar. 2006, doi: 10.1088/0952-4746/26/1/005.
[119] H. Wang, L. Zhang, P. Gao, and Q. Guo, “A pilot survey on indoor radon concentration in Beijing,” *Radiation Medicine and Protection*, vol. 3, no. 1, pp. 22–25, Mar. 2022, doi: 10.1016/j.radmp.2022.01.003.
[120] Bertin Technologies, “AlphaGUARD – Radon monitor,” Bertin Technologies. Accessed: Jan. 16, 2025. [Online]. Available: https://www.bertin-technologies.com/product/radon-professional-monitoring/radon-alphaguard/
[121] DURRIDGE, “RAD7 Radon Detector - DURRIDGE Scientific Research radon detectors,” DURRIDGE. Accessed: Jan. 16, 2025. [Online]. Available: https://durridge.com/products/rad7-radon-detector/

[122] A. Bahadori and B. Hanson, “Evaluation of consumer digital radon measurement devices: a comparative analysis,” *J. Radiol. Prot.*, vol. 44, no. 2, p. 021514, Jun. 2024, doi: 10.1088/1361-6498/ad4bf1.
[123] H. C. Government of Canada, “Air Steward Portable Radon Monitor recalled due to Inaccurate Radon Detection - Recalls, advisories and safety alerts – Canada.ca.” Accessed: Jan. 16, 2025. [Online]. Available: https://recalls-rappels.canada.ca/en/alert-recall/air-steward-portable-radon-monitor-recalled-due-inaccurate-radon-detection
[124] Z. Daraktchieva, C. B. Howarth, J. M. Wasikiewicz, C. A. Miller, and D. A. Wright, “Long-term comparison and performance study of consumer grade electronic radon integrating monitors,” *J Radiol Prot*, vol. 44, no. 3, Aug. 2024, doi: 10.1088/1361-6498/ad66db.
[125] I. Dimitrova, S. Georgiev, K. Mitev, V. Todorov, C. Dutsov, and B. Sabot, “Study of the performance and time response of the RadonEye Plus2 continuous radon monitor,” *Measurement*, vol. 207, p. 112409, Feb. 2023, doi: 10.1016/j.measurement.2022.112409.
[126] I. Dimitrova *et al.*, “Coherent long-term average indoor radon concentration estimates obtained by electronic and solid state nuclear track detectors,” *Radiation Physics and Chemistry*, vol. 226, p. 112212, Jan. 2025, doi: 10.1016/j.radphyschem.2024.112212.
[127] M. Fuente *et al.*, “Performance of radon monitors in a purpose-built radon chamber,” *J. Radiol. Prot.*, vol. 38, no. 3, p. 1111, Aug. 2018, doi: 10.1088/1361-6498/aad969.
[128] G. A. Gunning, M. Murray, S. C. Long, M. J. Foley, and E. C. Finch, “Inter-comparison of radon detectors for one to four week measurement periods,” *J. Radiol. Prot.*, vol. 36, no. 1, p. 104, Jan. 2016, doi: 10.1088/0952-4746/36/1/104.
[129] J. A. McGrath, S. Long, P. Murphy, A. Dowdall, and M. A. Byrne, “Assessing the accuracy of consumer-grade digital radon monitors under ‘real world’ conditions,” presented at the 17th International Conference on Indoor Air Quality and Climate, INDOOR AIR 2022, 2022.
[130] J. F. Rey, N. Meisser, D. Licina, and J. Goyette Pernot, “Evaluating the impact of indoor aerosols on the performance of real-time radon sensors,” *Front. Built Environ.*, vol. 10, p. 1407499, May 2024, doi: 10.3389/fbuil.2024.1407499.
[131] R. A. Stern, J. Lawrence, J. M. Wolfson, L. Li, and P. Koutrakis, “Radon sampling methodologies: A case for accurate, accessible measurements using household instruments,” *Journal of the Air & Waste Management Association*, vol. 73, no. 7, pp. 519–524, Jul. 2023, doi: 10.1080/10962247.2023.2223149.
[132] P. Warkentin, E. Curry, O. Michael, and B. Bjorndal, “A comparison of consumer-grade electronic radon monitors,” *J. Radiol. Prot.*, vol. 40, no. 4, p. 1258, Oct. 2020, doi: 10.1088/1361-6498/ab96d6.
[133] National Collaborating Centre for Environmental Health, *Effective Interventions to Reduce Indoor Radon Levels*. Vancouver, BC: Public Health Agency of Canada, 2008. Accessed: Apr. 08, 2025. [Online]. Available: https://ncceh.ca/sites/default/files/Radon_Interventions_Dec_2008.pdf
[134] Statistics Canada, “Table 36-10-0688-01 Housing stock in units included in the gross domestic product by income and expenditure.” Accessed: Apr. 08, 2025. [Online]. Available: https://doi.org/10.25318/3610068801-eng
[135] N. M. Rahman and B. L. Tracy, “Radon control systems in existing and new construction: a review,” *Radiation Protection Dosimetry*, vol. 135, no. 4, pp. 243–255, Aug. 2009, doi: 10.1093/rpd/ncp112.

[136] H. Canada, “Radon action guide for municipalities: Building codes, bylaws and provisions.” Accessed: Jan. 23, 2025. [Online]. Available: https://www.canada.ca/en/health-canada/services/health-risks-safety/radiation/radon/action-guides/municipalities/building-codes-bylaws-provisions.html
[137] H. Haanes, T. Kolstad, I. E. Finne, and B. Olsen, “The effect of new building regulations on indoor radon in radonprone municipalities,” *Journal of the European Radon Association*, Jan. 2022, doi: 10.35815/radon.v3.7886.
[138] D. Moir, K. Bush, J. Chen, K. Ford, and J. Whyte, “The national radon program: A continuing success story in Canada,” in *Handbook of Radon: Properties, Applications and Health*, 2012, pp. 265–283. [Online]. Available: https://www.scopus.com/inward/record.uri?eid=2-s2.0-84902558729&partnerID=40&md5=ed1426ba16e4680f00f6aed12e192609
[139] C. R. Boardman and S. V. Glass, “Basement radon entry and stack driven moisture infiltration reduced by active soil depressurization,” *Building and Environment*, vol. 85, pp. 220–232, Feb. 2015, doi: 10.1016/j.buildenv.2014.12.008.
[140] L. (Grace) Zhou *et al.*, “Passive soil depressurization in Canadian homes for radon control,” *Building and Environment*, vol. 188, p. 107487, Jan. 2021, doi: 10.1016/j.buildenv.2020.107487.
[141] H. Arvela, O. Holmgren, H. Reisbacka, and J. Vinha, “Review of low-energy construction, air tightness, ventilation strategies and indoor radon: results from Finnish houses and apartments,” *Radiation Protection Dosimetry*, vol. 162, no. 3, pp. 351–363, Dec. 2014, doi: 10.1093/rpd/nct278.
[142] I. E. Finne, T. Kolstad, M. Larsson, B. Olsen, J. Prendergast, and A. L. Rudjord, “Significant reduction in indoor radon in newly built houses,” *Journal of Environmental Radioactivity*, vol. 196, pp. 259–263, Jan. 2019, doi: 10.1016/j.jenvrad.2018.01.013.
[143] I.-C. Mareș *et al.*, “Research on best solution for improving indoor air quality and reducing energy consumption in a high-risk radon dwelling from romania,” *International Journal of Environmental Research and Public Health*, vol. 18, no. 23, 2021, doi: 10.3390/ijerph182312482.
[144] D. B. Henschel, “Analysis of Radon Mitigation Techniques Used in Existing US Houses,” *Radiation Protection Dosimetry*, vol. 56, no. 1–4, pp. 21–27, Dec. 1994, doi: 10.1093/oxfordjournals.rpd.a082416.
[145] S. P. Naismith, J. C. H. Miles, and C. R. Scivyer, “The Influence of House Characteristics on the Effectiveness of Radon Remedial Measures,” *Health Physics*, vol. 75, no. 4, p. 410, Oct. 1998.
[146] H. Arvela, “Radon mitigation in blocks of flats,” *Science of The Total Environment*, vol. 272, no. 1, p. 137, May 2001, doi: 10.1016/S0048-9697(01)00677-5.
[147] J. Wang, O. Meisenberg, Y. Chen, E. Karg, and J. Tschiersch, “Mitigation of radon and thoron decay products by filtration,” *Science of The Total Environment*, vol. 409, no. 19, pp. 3613–3619, Sep. 2011, doi: 10.1016/j.scitotenv.2011.06.030.
[148] K. Iwaoka, S. Tokonami, T. Ishikawa, and H. Yonehara, “Mitigation effects of radon decay products by air cleaner,” *J Radioanal Nucl Chem*, vol. 295, no. 1, pp. 639–642, Jan. 2013, doi: 10.1007/s10967-012-1813-z.

[149] C. Kranrod *et al.*, “Mitigation of the effective dose of radon decay products through the use of an air cleaner in a dwelling in Okinawa, Japan,” *Applied Radiation and Isotopes*, vol. 67, no. 6, pp. 1127–1132, Jun. 2009, doi: 10.1016/j.apradiso.2009.02.087.
[150] Y. Yasuoka, T. Ishikawa, S. Tokonami, H. Takahashi, A. Sorimachi, and M. Shinogi, “Radon mitigation using an air cleaner,” Mar. 2009, doi: 10.1007/s10967-008-7379-0.
[151] J. D. Harrison and J. W. Marsh, “ICRP recommendations on radon,” *Ann ICRP*, vol. 49, no. 1_suppl, pp. 68–76, Dec. 2020, doi: 10.1177/0146645320931974.
[152] T. Valmari, Ed., *Suomen radonkartasto 2010: = Radonatlas över Finland 2010 = Radon atlas of Finland 2010*. in STUK A, no. 245. Helsinki: STUK, 2010.
[153] European Society of Radiology, “Summary of the European Directive 2013/59/Euratom: essentials for health professionals in radiology,” *Insights Imaging*, vol. 6, no. 4, pp. 411–417, May 2015, doi: 10.1007/s13244-015-0410-4.
[154] G. Cinelli, M. De Cort, and T. Tollefsen, *European Atlas of Natural Radiation*. Luxembourg: Publication Office of the European Union, 2019. Accessed: Sep. 03, 2024. [Online]. Available: https://data.europa.eu/doi/10.2760/46388
[155] M. Janik, P. Bossew, M. M. Hasan, and G. Cinelli, “Indoor Radon Research in the Asia-Pacific Region,” *Atmosphere*, vol. 14, no. 6, Art. no. 6, Jun. 2023, doi: 10.3390/atmos14060948.
[156] A. R. Denman, J. Sinclair, P. S. Phillips, R. G. M. Crockett, and C. J. Groves-Kirkby, “The cost effectiveness of radon reduction programmes in domestic housing in England and Wales: The impact of improved radon mapping and housing trends,” *Environment International*, vol. 59, pp. 73–85, Sep. 2013, doi: 10.1016/j.envint.2013.05.012.
[157] N. McColl *et al.*, “Limitation of Human Exposure to Radon,” Health Protection Agency, RCE-15, Jul. 2010.
[158] O. US EPA, “Health Risk of Radon.” Accessed: Jan. 07, 2025. [Online]. Available: https://www.epa.gov/radon/health-risk-radon
[159] E. A. G. Geltman, “State Radon Laws,” The Policy Surveillance Program. Accessed: Apr. 23, 2025. [Online]. Available: https://legacy.lawatlas.org/datasets/state-radon-laws?_gl=1*1nd239q*_ga*ODA0Mzc3NjE5LjE3NDU0NDYxNDQ.*_ga_HH1EXGKQJ0*MTc0NTQ0NjE0My4xLjAuMTc0NTQ0NjE0My42MC4wLjA.
[160] M. E. Kitto, C. Murphy, S. L. Dixon, D. E. Jacobs, J. Wilson, and J. Malone, “Evaluating and Assessing Radon Testing in Multifamily Housing,” *Journal of Public Health Management and Practice*, vol. 28, no. 2, p. E525, Apr. 2022, doi: 10.1097/PHH.0000000000001392.
[161] J. Gaskin, J. Whyte, L. G. Zhou, and D. Coyle, “Regional cost effectiveness analyses for increasing radon protection strategies in housing in Canada,” *Journal of Environmental Radioactivity*, vol. 240, p. 106752, Dec. 2021, doi: 10.1016/j.jenvrad.2021.106752.
[162] Government of British Columbia, “Radon Rough-in Requirements,” British Columbia Government. Accessed: Apr. 23, 2025. [Online]. Available: https://www2.gov.bc.ca/assets/gov/farming-natural-resources-and-industry/construction-industry/building-codes-and-standards/bulletins/2024-code/b24-03_radon.pdf
[163] National Research Council of Canada, “Proposed changes.” Accessed: Apr. 23, 2025. [Online]. Available: https://codes.nrc-cnrc.gc.ca/en/certifications-evaluations-standards/codes-canada/codes-development-process/proposed_changes.html

[164] Y. Yao, B. Chen, and W. Zhuo, “Reanalysis of residential radon surveys in China from 1980 to 2019,” *Science of The Total Environment*, vol. 757, p. 143767, Feb. 2021, doi: 10.1016/j.scitotenv.2020.143767.
[165] J. Chen, “A Summary of Residential Radon Surveys and the Influence of Housing Characteristics on Indoor Radon Levels in Canada,” *Health Physics*, vol. 121, no. 6, p. 574, Dec. 2021, doi: 10.1097/HP.0000000000001469.
[166] R. Liza *et al.*, “Application of Statistical Methods for the Characterization of Radon Distribution in Indoor Environments: A Case Study in Lima, Peru,” *Eng*, vol. 6, no. 1, Art. no. 1, Jan. 2025, doi: 10.3390/eng6010014.
[167] J. Miles, “Mapping Radon-prone Areas by Lognormal Modeling of House Radon Data,” *Health Physics*, vol. 74, no. 3, p. 370, Mar. 1998.
[168] J. A. Casey *et al.*, “Predictors of Indoor Radon Concentrations in Pennsylvania, 1989–2013,” *Environmental Health Perspectives*, vol. 123, no. 11, pp. 1130–1137, Nov. 2015, doi: 10.1289/ehp.1409014.
[169] T. Zhu, “Analysis on the Applicability of the Random Forest,” *J. Phys.: Conf. Ser.*, vol. 1607, no. 1, p. 012123, Aug. 2020, doi: 10.1088/1742-6596/1607/1/012123.
[170] F. Pargent, F. Pfisterer, J. Thomas, and B. Bischl, “Regularized target encoding outperforms traditional methods in supervised machine learning with high cardinality features,” *Comput Stat*, vol. 37, no. 5, pp. 2671–2692, Nov. 2022, doi: 10.1007/s00180-022-01207-6.
[171] L. Yu, L. Liu, and K. E. Peace, “Regression multiple imputation for missing data analysis,” *Statistical Methods in Medical Research*, vol. 29, no. 9, pp. 2647–2664, 2020, doi: 10.1177/0962280220908613.
[172] I. Yarmoshenko *et al.*, “Variance of indoor radon concentration: Major influencing factors,” *Science of The Total Environment*, vol. 541, pp. 155–160, Jan. 2016, doi: 10.1016/j.scitotenv.2015.09.077.
[173] Health Canada, “Guide for radon measurements in homes.” Accessed: May 16, 2025. [Online]. Available: https://www.canada.ca/en/health-canada/services/publications/health-risks-safety/guide-radon-measurements-residential-dwellings.html
[174] US EPA, “ANSI/AARST MAH 2023 Protocol for Conducting Measurements of Radon and Radon Decay Products in Homes,” Radon Standards of Practice. Accessed: Jun. 21, 2024. [Online]. Available: https://standards.aarst.org/MAH-2023/8/index.html#zoom=z
[175] P. Warkentin, E. Curry, O. Michael, and B. Bjorndal, “A comparison of consumer-grade electronic radon monitors,” *J. Radiol. Prot.*, vol. 40, no. 4, p. 1258, Oct. 2020, doi: 10.1088/1361-6498/ab96d6.
[176] C. A. Miller and C. B. Howarth, “Results of the 2018 PHE intercomparison of passive radon detectors,” Public Health England, Chilton, Didcot, Oxfordshire, Apr. 2020.
[177] S. Sousan *et al.*, “Inter-comparison of low-cost sensors for measuring the mass concentration of occupational aerosols,” *Aerosol Science and Technology*, vol. 50, no. 5, pp. 462–473, May 2016, doi: 10.1080/02786826.2016.1162901.
[178] US EPA, “40 CFR Parts 58- Ambient Air Quality Surveillance (Subchapter C).” Environmental Protection Agency, Washington, DC., 2016. Accessed: Apr. 03, 2025. [Online]. Available: https://www.ecfr.gov/current/title-40/part-58

[179] Government of Canada, “Hourly Data Report - Environment and Climate Change Canada,” Environment and Natural Resources. Accessed: Jul. 11, 2025. [Online]. Available: https://climate.weather.gc.ca/climate_data/hourly_data_e.html?timeframe=1&Year=2010&Month=4&Day=8&hlyRange=2002-10-03%7C2010-04-08&dlyRange=2002-10-03%7C2011-05-16&mlyRange=2002-11-01%7C2006-12-01&StationID=32008&Prov=ON&urlExtension=_e.html&searchType=stnName&optLimit=yearRange&StartYear=1840&EndYear=2025&selRowPerPage=25&Line=1&searchMethod=contains&txtStationName=waterloo

[180] B. Du *et al.*, “Estimating Air Change Rate in Mechanically Ventilated Classrooms Using a Single CO2 Sensor and Automated Data Segmentation,” *Environ Sci Technol*, vol. 58, no. 42, pp. 18788–18799, Oct. 2024, doi: 10.1021/acs.est.4c02797.

[181] Ontario Building Code, *O. Reg. 332/24, s. 3.1.13.7*.

[182] T. Valmari, H. Arvela, and H. Reisbacka, “Radon in Finnish apartment buildings,” *Radiation Protection Dosimetry*, vol. 152, no. 1–3, pp. 146–149, Nov. 2012, doi: 10.1093/rpd/ncs211.

[183] M. Kolovou, C. Potiriadis, and N. Kallithrakas-Kontos, “A study on the correlation between indoor radon concentrations and the construction year of the dwellings,” *Eur. Phys. J. Spec. Top.*, vol. 232, no. 10, pp. 1625–1629, Aug. 2023, doi: 10.1140/epjs/s11734-023-00888-4.

[184] T. Dicu *et al.*, “Exploring statistical and machine learning techniques to identify factors influencing indoor radon concentration,” *Science of The Total Environment*, vol. 905, p. 167024, Dec. 2023, doi: 10.1016/j.scitotenv.2023.167024.

[185] D. Vienneau *et al.*, “Residential radon – Comparative analysis of exposure models in Switzerland,” *Environmental Pollution*, vol. 271, p. 116356, Feb. 2021, doi: 10.1016/j.envpol.2020.116356.

[186] P.-Y. Wu, T. Johansson, M. Mangold, C. Sandels, and K. Mjörnell, “Evaluating the indoor radon concentrations in the Swedish building stock using statistical and machine learning,” *J. Phys.: Conf. Ser.*, vol. 2654, no. 1, p. 012086, Dec. 2023, doi: 10.1088/1742-6596/2654/1/012086.

[187] S. Baumann *et al.*, “Radon hazard mapping: usability of environmental predictors including atmospheric radon and radon flux and knowledge transfer between regions (Belgium and Germany),” *Environ Earth Sci*, vol. 84, no. 7, p. 196, Apr. 2025, doi: 10.1007/s12665-025-12126-2.

[188] A. Giang and T. Li, “Collocation Testing of Consumer-Grade Electronic Radon Sensors in Canadian Homes,” in *Proceedings of Healthy Buildings 2025 Europe*, Reykjavík, Iceland: ISIAQ, 2025.

[189] M. Schubert, A. Musolff, and H. Weiss, “Influences of meteorological parameters on indoor radon concentrations (222Rn) excluding the effects of forced ventilation and radon exhalation from soil and building materials,” *Journal of Environmental Radioactivity*, vol. 192, pp. 81–85, Dec. 2018, doi: 10.1016/j.jenvrad.2018.06.011.

[190] I. Dimitrova *et al.*, “Coherent long-term average indoor radon concentration estimates obtained by electronic and solid state nuclear track detectors,” *Radiation Physics and Chemistry*, vol. 226, p. 112212, Jan. 2025, doi: 10.1016/j.radphyschem.2024.112212.

[191] H. C. Government of Canada, “InkBird Wifi Radon Detector model RD-2 recalled due to inaccurate radon detection - Recalls, advisories and safety alerts – Canada.ca.” Accessed: Jul. 13, 2025. [Online]. Available: https://recalls-rappels.canada.ca/en/alert-recall/inkbird-wifi-radon-detector-model-rd-2-recalled-due-inaccurate-radon-detection
[192] I. V. Yarmoshenko, A. D. Onishchenko, G. P. Malinovsky, A. V. Vasilyev, and M. V. Zhukovsky, “MODELING and justification of indoor radon prevention and remediation measures in multi-storey apartment buildings,” *Results in Engineering*, vol. 16, p. 100754, Dec. 2022, doi: 10.1016/j.rineng.2022.100754.
[193] E. Petermann, H. Meyer, M. Nussbaum, and P. Bossew, “Mapping the geogenic radon potential for Germany by machine learning,” *Science of The Total Environment*, vol. 754, p. 142291, Feb. 2021, doi: 10.1016/j.scitotenv.2020.142291.
[194] G. Kropat *et al.*, “Improved predictive mapping of indoor radon concentrations using ensemble regression trees based on automatic clustering of geological units,” *Journal of Environmental Radioactivity*, vol. 147, pp. 51–62, Sep. 2015, doi: 10.1016/j.jenvrad.2015.05.006.
[195] P. Warkentin, “Canadian National Radon Proficiency Program,” 2023.
[196] E. S. Ford, A. E. Kelly, S. M. Teutsch, S. B. Thacker, and P. L. Garbe, “Radon and lung cancer: a cost-effectiveness analysis.,” *Am J Public Health*, vol. 89, no. 3, pp. 351–357, Mar. 1999, doi: 10.2105/AJPH.89.3.351.
[197] J. T. Hancock and T. M. Khoshgoftaar, “CatBoost for big data: an interdisciplinary review,” *Journal of Big Data*, vol. 7, no. 1, p. 94, Nov. 2020, doi: 10.1186/s40537-020-00369-8.

Appendix A

Table A1: Summary of Health Canada (HC) Dataset Variables

Category	Categorical Variables	Variable used in the RF model
Province/ Territory	The province or territory the measurement was recorded.	Excluded – postal codes are already unique to the province or territory.
Postal Code/ Forward Sorting Area	Only the first half of the postal code was recorded, also known as the forward sorting area code (FSA).	Included
Season	The season that predominates the test period. • Winter • Spring • Summer • Fall	Included – sorted the seasons into 'Heating', 'Cooling', or 'All Year' based on the test period. Winter and fall were counted towards 'Heating', whereas summer and spring were counted towards 'Cooling'. 'All Year' was used if the testing period spanned all seasons.
Floor	The floor the radon detector was placed. • Basement (underground) • Main (first) floor (on the ground) • Second floor (above ground) • Main (first) floor (above ground) • Basement - bi-level / walkout • Third floor (above ground) • Basement and main floor • Main and second floor • Mobile home/trailer • Other • No response	Included – simplified to reduce the number of variables within a category. • Floor above • Basement • Main floor (on ground) • Basement and main floor • Main and second floor • Mobile home/trailer
Building Type	The residential building type the detector was placed. • Single-detached home: bungalow • Single-detached home: two-story • Single-detached home: three-story • Single-detached home: split-level / bi-level • Semi-detached home: side-by-side • Semi-detached home: row house • Semi-detached home: duplex • Semi-detached home: townhouse • Trailer / mobile home • Pre-fabricated home • Single-detached home: 1-1/2 story • Condo/apartment • Ranch, raised ranch	Included – simplified to reduce the number of variables within a category. • Single-detached • Semi-detached • Condo/Apartment • Trailer • Pre-Fabrication

	• Other • No response • Bungalow • Two-story • Three-story • Split-level / 4-level • Side-by-side • Row house • Duplex/triplex • Townhouse • Trailer / mobile home • Pre-fabricated home • Bi-level / 1-1/2 story • Condo/apartment (basement or main floor) • Other	
Year of Construction	The year the building was constructed. • 1920 or before • 1921 to 1945 • 1946 to 1960 • 1961 to 1970 • 1971 to 1980 • 1981 to 1990 • 1991 to 2000 • 2001 to 2010 • Not sure	Included – All years' variables were retained.
Basement Type	The presence and type of basement corresponding to each building. • Yes, a full basement (underneath the entire building) • Yes, a partial basement (underneath part of the building) • There is a crawl space under all or part of the building • The house sits directly on the ground, with no basement • No response • Finished • Partially finished • Unfinished • No response	Included – simplified to reduce the number of variables within a category. • Yes, a full basement • Yes, a partial basement • Crawl space • No basement
Foundation Type	The type of foundation material corresponds to each building. • Poured concrete	Included – simplified to reduce the number of variables within a category.

	• Cinder block • Brick • Stone • Wood/wood blocks • Cement block (ICF/concrete) • Pilings (concrete/steel)/pillars/pier) • Gravel/rock • Other • Don't know • No response	• Concrete-based • Masonry • Wood • Other
Heating Fuel Type	The type of fuel used for heating each building. • Natural gas • Electric • Oil/fuel oil • Propane • Geothermal • Wood • Solar • Pellet stove • Outdoor furnace/stove / hydronic heater • Coal • Diesel • Hot water / radiant hot water • Heat pump • Other • No response	Included – simplified to reduce the number of variables within a category. • Fossil Fuel • Electric • Renewable • Wood-based • Radiant System • Other
Heating System	The type of heating system used for each building. • Forced air • Radiant (water) • Baseboard • Pellet/wood stove / radiant wood stove • Fireplace/wood fireplace/foyer • Gas/propane fireplace • Space heaters (gas, electric, oil) • Radiant (electric – ceiling, floor) • Electric fireplace • Heat pump/exchanger • Gas/propane stove • Convection / convective • Slow combustion • Furnace	Included – All variables were retained.

	• Fan related • Stove, other • Wood • Other • No response	
Presence of Air Conditioning	If the building has air conditioning. • No • Yes • No Response	Included – All variables were retained.
Air Conditioning System	If the building has air conditioning, the type of system it uses is. • Central air • Window unit • Both • No response	Included – All variables were retained.

Table A2: Summary of BCRDR Dataset Variables

Category	Categorical Variables	Variable used in the RF model
FSA	Only the first half of the postal code was recorded, also known as the forward sorting area code (FSA).	Included – All variables were retained.
Floor	The floor the radon detector was placed. • Basement • Crawl Space • Lowest Floor • Upper Floor • Main Floor	Included – All variables were retained.
Device	The type of radon detector used during the testing period. • AccuStar alpha track detector • AccuStar AT-100 alpha track detector • AccuStar Liquid Scintillation CLS100 • Airthings Corentium Home • Airthings Corentium Pro • Alpha track detector • Landauer alpha track detector • Lex Scientific Alpha Track Detector • Radonova alpha track detector • Radtrak Alpha Track Detector • Radtrak2 alpha track detector • Radtrak2 alpha track detector • Radtrak3 alpha track detector • Rapidos short-term detector • Saskatchewan Research Council alpha track detector • Sun Nuclear 1030 Continuous Radon Monitor • Rad Elec Recon CRM	Excluded – This category was excluded as most of the data points used alpha-track detectors. To avoid confounding variables, this category was also excluded to ensure the variables examined were either related to geology, season, or building-specific characteristics.
Building Type	The residential building type the detector was placed. • Detached • Semi-Detached • Attached • Condo • Apartment • Other • Unknown	Included – simplified to reduce the number of variables within a category. • Apartment • Semi-detached • Single-detached

Year Built	The year the building was constructed. • 1920 or before • 1921 to 1945 • 1946 to 1960 • 1961 to 1970 • 1971 to 1980 • 1981 to 1990 • 1991 to 2000 • 2001 to 2010 • 2011 or after • Unknown	Included – All variables were retained.
Presence of Air Conditioning	If the building has air conditioning. • Yes • No	Included – All variables were retained.
Heating System	The type of heating system used for each building. • Baseboard • Forced air • Radiant water • Multiple systems • Other • Unknown	Included – All variables were retained.
Start Date/ End Date	The start and end dates were recorded corresponding to the measurement period.	Included – simplified based on the start and end date by categorizing into 'Heating' or 'Cooling' season.

Table A3: Summary of Bland-Altman results from long-term collocation test

Sensor	Mean Difference	Upper Limit	Lower Limit
CH-5	35.72	96.79	-25.35
CH-6	21.63	80.96	-37.70
CH-7	24.50	85.91	-36.91
CRAD-4	56.12	139.11	-26.86
CRAD-5	52.65	117.18	-11.89
CRAD-6	47.64	127.45	-32.16
EB-4	17.96	65.32	-29.40
EB-5	18.00	60.36	-24.37
EB-6	7.06	46.12	-32.01
EQ-4	29.20	66.66	-8.26
EQ-5	27.38	64.74	-9.97
EQ-6	28.37	65.35	-8.62
FK-4	-43.28	8.21	-94.78
FK-5	-42.61	10.23	-95.45
FK-6	-43.65	5.11	-92.41
HAN-4	29.95	85.99	-26.09
HAN-5	12.69	62.47	-37.08
HAN-6	39.24	111.66	-33.17
IBD-4	-74.07	9.20	-157.33
IBD-5	17.07	77.67	-43.52
IBD-6	11.41	68.67	-45.84
LB-4	144.00	297.54	-9.54
LB-5	53.22	137.94	-31.49
LB-6	36.92	131.38	-57.53
LCA-4	-35.17	-14.13	-56.21
LCA-5	-21.78	-0.15	-43.41
LCA-6	-21.51	0.27	-43.28
LU-5	11.90	47.51	-23.72
LU-6	16.35	45.66	-12.96
PS4-4	9.65	58.64	-39.33
PS4-5	19.75	67.36	-27.86
PS4-6	20.67	66.51	-25.18
RD2-2	-32.97	-12.62	-53.32
RD2-4	-36.85	-16.20	-57.50
RD2-5	-30.81	-9.14	-52.47
RE-4	2.78	34.82	-29.26
RE-5	3.78	36.15	-28.58

RE-6	5.12	38.00	-27.76
VP-4	15.53	55.90	-24.85
VP-5	17.11	61.77	-27.56
VP-6	23.86	68.08	-20.36
WP-5	29.34	76.35	-17.67
WP-6	17.89	61.93	-26.14
WP-7	12.32	53.67	-29.04

Table A4: Summary of Spearman Rank Correlations for Outdoor Environmental Parameters vs. Radon Concentration by Floor with Statistically Significant Values Bolded

Floor	Parameter	Correlation Coefficient
1	*Temperature (°C)*	**0.092**
	Relative Humidity (%)	0.004
	Precipitation Amount (mm)	-0.013
	Outdoor Pressure (kPa)	-0.013
2	*Temperature (°C)*	-0.022
	Relative Humidity (%)	0.039
	Precipitation Amount (mm)	0.011
	Outdoor Pressure (kPa)	0.027
3	*Temperature (°C)*	**0.065**
	Relative Humidity (%)	**0.056**
	Precipitation Amount (mm)	0.004
	Outdoor Pressure (kPa)	0.012
4	*Temperature (°C)*	0.034
	Relative Humidity (%)	**0.074**
	Precipitation Amount (mm)	-0.008
	Outdoor Pressure (kPa)	**-0.049**
5	*Temperature (°C)*	0.019
	Relative Humidity (%)	**0.073**
	Precipitation Amount (mm)	**0.044**
	Outdoor Pressure (kPa)	**-0.107**
6	*Temperature (°C)*	**0.090**
	Relative Humidity (%)	-0.013
	Precipitation Amount (mm)	-0.015
	Outdoor Pressure (kPa)	-0.023
7	*Temperature (°C)*	**0.097**
	Relative Humidity (%)	0.010
	Precipitation Amount (mm)	-0.014
	Outdoor Pressure (kPa)	-0.022
8	*Temperature (°C)*	**0.064**
	Relative Humidity (%)	**0.049**
	Precipitation Amount (mm)	-0.007
	Outdoor Pressure (kPa)	**-0.068**
9	*Temperature (°C)*	**0.079**
	Relative Humidity (%)	0.026
	Precipitation Amount (mm)	-0.011
	Outdoor Pressure (kPa)	-0.048

10	*Temperature (°C)*	-0.005
	Relative Humidity (%)	0.009
	Precipitation Amount (mm)	-0.015
	Outdoor Pressure (kPa)	0.029
11	*Temperature (°C)*	0.026
	Relative Humidity (%)	-0.037
	Precipitation Amount (mm)	-0.055
	Outdoor Pressure (kPa)	-0.084
12	*Temperature (°C)*	0.035
	Relative Humidity (%)	-0.003
	Precipitation Amount (mm)	0.007
	Outdoor Pressure (kPa)	-0.129